

2018

# Improving Detection And Prediction Of Bridge Scour Damage And Vulnerability Under Extreme Flood Events Using Geomorphic And Watershed Data

Ian Anderson  
*University of Vermont*

Follow this and additional works at: <https://scholarworks.uvm.edu/graddis>



Part of the [Civil Engineering Commons](#)

---

## Recommended Citation

Anderson, Ian, "Improving Detection And Prediction Of Bridge Scour Damage And Vulnerability Under Extreme Flood Events Using Geomorphic And Watershed Data" (2018). *Graduate College Dissertations and Theses*. 823.  
<https://scholarworks.uvm.edu/graddis/823>

This Dissertation is brought to you for free and open access by the Dissertations and Theses at ScholarWorks @ UVM. It has been accepted for inclusion in Graduate College Dissertations and Theses by an authorized administrator of ScholarWorks @ UVM. For more information, please contact [donna.omalley@uvm.edu](mailto:donna.omalley@uvm.edu).

IMPROVING DETECTION AND PREDICTION OF BRIDGE SCOUR DAMAGE  
AND VULNERABILITY UNDER EXTREME FLOOD EVENTS USING  
GEOMORPHIC AND WATERSHED DATA

A Dissertation Presented

by

Ian Anderson

to

The Faculty of the Graduate College

of

The University of Vermont

In Partial Fulfillment of the Requirements  
for the Degree of Doctor of Philosophy  
Specializing in Civil and Environmental Engineering

January, 2018

Defense Date: 10-31-17  
Dissertation Examination Committee:

Mandar Dewoolkar, Ph.D., Advisor  
Donna M. Rizzo, Ph.D., Co-advisor  
Dryver Huston, Ph.D., Chairperson  
Arne Bomblies, Ph.D.  
Ehsan Ghazanfari, Ph.D.  
Cynthia J. Forehand, Ph.D., Dean of the Graduate College

## ABSTRACT

Bridge scour is the leading cause of bridge damage nationwide. Successfully mitigating bridge scour problems depends on our ability to reliably estimate scour potential, design safe and economical foundation elements that account for scour potential, identify vulnerabilities related to extreme events, and recognize changes to the environmental setting that increase risk at existing bridges.

This study leverages available information, gathered from several statewide resources, and adds watershed metrics to create a comprehensive, georeferenced dataset to identify parameters that correlate to bridges damaged in an extreme flood event. Understanding the underlying relationships between existing bridge condition, fluvial stresses, and geomorphological changes is key to identifying vulnerabilities in both existing and future bridge infrastructure. In creating this comprehensive database of bridge inspection records and associated damage characterization, features were identified that correlate to and discriminate between levels of bridge damage.

Stream geomorphic assessment features were spatially joined to every bridge, marking the first time that geomorphic assessments have been broadly used for estimating bridge vulnerability. Stream power assessments and watershed delineations for every bridge and stream reach were generated to supplement the comprehensive database. Individual features were tested for their significance to discriminate bridge damage, and then used to create empirical fragility curves and probabilistic predictions maps to aid in future bridge vulnerability detection. Damage to over 300 Vermont bridges from a single extreme flood event, the August 28, 2011 Tropical Storm Irene, was used as the basis for this study. Damage to historic bridges was also summarized and tabulated. In some areas of Vermont, the storm rainfall recurrence interval exceeded 500 years, causing widespread flooding and damaging over 300 bridges. With a dataset of over 330 features for more than 2,000 observations to bridges that were damaged as well as not damaged in the storm, an advanced evolutionary algorithm performed multivariate feature selection to overcome the shortfalls of traditional logistic regression analysis. The analysis identified distinct combinations of variables that correlate to the observed bridge damage under extreme food events.

## CITATIONS

Material from this dissertation has been published in the following form:

Anderson, I., Rizzo, D. M., Huston, D. R., and Dewoolkar, M. M.. (2017). “Analysis of bridge and stream conditions of over 300 Vermont bridges damaged in Tropical Storm Irene.” *Structure and Infrastructure Engineering*, 1-14.

AND

Anderson, I., Rizzo, D. M., Huston, D. R., and Dewoolkar, M. M.. (2017). “Stream Power Application for Bridge-Damage Probability Mapping Based on Empirical Evidence from Tropical Storm Irene.” *Journal of Bridge Engineering*, 22(5), 05017001.



## ACKNOWLEDGEMENTS

This work was funded by the Vermont Agency of Transportation (VTrans) and the United States Department of Transportation through the University of Vermont Transportation Research Center (UVM TRC). Partial support from Vermont EPSCoR with funds from the National Science Foundation Grant EPS-1101317 is acknowledged.

Special thank must be given to my co-advisors, for their time, their knowledge, and their contributions to this work. Thank you to Dr. Mandar Dewoolkar for the years of support, encouragement, and aid to my education, engineering development, and personal growth. Without you none of this would have been possible. Thank you also to Dr. Donna Rizzo, for helping me remain engaged in my work over these many years, for the of instruction and inspiration, and for teaching me so much.

Thanks to Bill Ahearn, Christopher Benda, Carolyn Carlson, George Colgrove, Callie Ewald, Jeff Wayne Symonds, Pam Thurber, Jason Tremblay, and Nick Wark of Vermont Agency of Transportation for their guidance and feedback during this work. Thank you to the staff at Vermont Agency of Natural Resources for their help and data.

Professors Arne Bomblies, Richard Downer and Eric Hernandez and Alan Howard of the University of Vermont provided valuable guidance in this work. A number of individuals including: Evan Fitzgerald, Scott Hamshaw, John Lens, Jessica Louisos, Roy Schiff and Kristen Underwood provided resources and input for this work. Thank you to my fellow graduate student co-authors for the contributions and assistance in the works we accomplished together, including: Lucas Howard, John Hanley, and Matt Brand. Thank you to my family, my friends, and Colleen Hertz. There is value in hard work, and I am thankful you were there to support me through it.

## TABLE OF CONTENT

CHAPTER 1 INTRODUCTION .....	1
1.1 Motivation .....	1
1.2 Objectives and Research Questions .....	4
1.3 Organization of the Thesis .....	5
CHAPTER 2 BACKGROUND LITERATURE.....	8
2.1 Bridge Scour and Regional Context.....	8
2.2 Bridge Scour Types .....	11
2.3 Methods to Compute Scour Depth .....	15
2.4 Scour Rating System .....	19
2.5 Stream Power .....	22
CHAPTER 3 ANALYSIS OF BRIDGE AND STREAM CONDITIONS OF OVER 300 VERMONT BRIDGES DAMAGED IN TROPICAL STORM IRENE.....	24
3.1 Introduction .....	25
3.1.1 Bridge Data .....	28
3.1.2 Rainfall Data .....	29
3.1.3 Stream Geomorphic Data.....	30
3.2 Geospatial Analysis and Data Processing .....	31
3.2.1 Selection of Variables and Analysis Method.....	32
3.3 Results and Discussion.....	38
3.3.1 Damage Classification and Cost Analysis .....	38

3.3.2	Rainfall.....	43
3.3.3	Bridge Characteristics.....	44
3.3.4	Bridge Ratings .....	46
3.3.5	Stream Characteristics .....	49
3.3.6	Logistic Regression and Empirical Fragility Estimate .....	53
3.4	Conclusions .....	56
CHAPTER 4 WATERSHED ASSESSMENT .....		59
4.1	Introduction .....	59
4.2	Watershed delineation .....	60
4.3	Rainfall .....	62
4.4	Land Cover .....	63
4.5	Hydrologic Soil Type .....	65
4.6	Stream Power Computation.....	66
4.7	Gradients .....	69
CHAPTER 5 STREAM POWER APPLICATION FOR BRIDGE DAMAGE PROBABILITY MAPPING BASED ON EMPIRICAL EVIDENCE FROM TROPICAL STORM IRENE .....		71
5.1	Introduction .....	72
5.2	Methods.....	76
5.2.1	Data Collection .....	76
5.2.2	Bridge Damage Classification .....	79
5.2.3	Stream Power Computation .....	82

5.3	Results and Discussion .....	84
5.3.1	Damage Distribution .....	84
5.3.2	Empirical Fragility Curves .....	88
5.3.3	Probability Mapping .....	90
5.4	Conclusions .....	93
CHAPTER 6 MULTIVARIATE FEATURE SELECTION.....		96
6.1	Introduction .....	96
6.2	Background and Research Objectives .....	99
6.2.1	Data Collection and Initial Statistical Analysis .....	101
6.2.2	Motivation.....	102
6.3	Watershed Analysis .....	104
6.4	Feature Selection Analysis .....	106
6.4.1	Conjunctive Clause Evolutionary Algorithm Complex Interaction Identification.....	106
6.4.2	Multiple Logistic Regression.....	108
6.5	Results and Discussion .....	108
6.5.1	EA and Logistic Regression.....	108
6.5.2	Disjunctive Normal Form Analysis .....	112
6.5.3	Geographic Prediction .....	116
6.6	Conclusions .....	117
6.7	Supplementary Material .....	121
CHAPTER 7 HISTORIC BRIDGE DAMAGE IN TROPICAL STORM IRENE ...		123
7.1	Introduction .....	123

7.2	Analysis .....	125
7.3	Conclusions .....	130
CHAPTER 8 CONCLUSIONS AND RECOMMENDATIONS .....		132
8.1	Work Performed .....	132
8.2	Overall Conclusions .....	135
8.3	Intellectual Merit/Contributions of the Research .....	137
8.4	Broader Impacts of the Research.....	139
8.5	Recommendations for Future Work .....	140
CHAPTER 9 COMPREHENSIVE BIBLIOGRAPHY .....		142

## LIST OF TABLES

Table 2.1. Scour Ratings Used by VTrans (FHWA, 1995) .....	21
Table 3.1. Variables considered in statistical Kruskal-Wallis analysis .....	36
Table 6.1. Description of damage categories used in analysis (Anderson et al., 2017a). .....	100
Table 6.2. Feature Combination Confusion Matrices, EA and Logistic Regression .....	110
Table 7.1. Damaged Historic Bridges.....	128

## LIST OF FIGURES

Figure 1.1. Examples of scour-related damage to Vermont bridges in Tropical Storm Irene (VAOT, 2014).....	4
Figure 2.1. Short contraction at a bridge (Ettema et al. 2010).....	12
Figure 2.2. Example of the flow patterns and vortices which result in abutment scour (Ettema et al. 2010).....	13
Figure 2.3. Vortices from a pier obstructing flow, resulting in local pier scour at (a) narrow, (b) transitional, and (c) wide pier (Ettema et al. 2011).....	14
Figure 2.4. Abutment scour conditions: (a) A – hydraulic scour of the main bed; (b) B – scour of the floodplain; and (c) C – scour of the approach, exposing the abutment as a pier (Ettema et al., 2010).....	19
Figure 3.1. Tropical Storm Irene impact on Vermont bridges – (a) Estimated rainfall totals and locations of damaged bridges, (b) Estimated annual recurrence interval, locations of damaged and reach-scale non-damaged bridges, (c) Estimated annual recurrence interval, and locations of damaged and watershed-scale non-damaged bridges .....	34
Figure 3.2. Bridge database process chart (the data identified in the boxes without background highlight were not used in the statistical analysis, n denotes sample size).....	35
Figure 3.3. Damage Type (VTrans, 2014) - (a) Scour damage, Dummerston VT30-B9: scour beneath the concrete spread footing, (b) Channel flanking damage, Jamaica VT30-B40: flanking behind the abutment, (c) Debris damage, Wallingford VT140-B10: debris buildup on a pier, reducing the flow area, (d) Superstructure damage, Montgomery C2001-B5: damage to the sideboards of a covered bridge.....	40
Figure 3.4. Damage Level (VTrans, 2014) – (a) and (b) Slight Damage, Northfield VT12-B61: conditions before and after the storm, (c) and (d) Moderate Damage, Bridgewater C3005-B37: conditions before and after the storm, (e) and (f) Extensive Damage, Halifax C2001-B17: conditions before and after the storm, (g) and (h) Complete Damage, Rochester VT73-B19: conditions before and after the storm.....	42
Figure 3.5. Repair cost and cost per deck area for various levels and type of damage: (a) Estimated cost of repair versus damage level, (b) Estimated cost of repair per deck area versus damage level, (c) Estimated cost of repair per deck area versus damage type, (d) Actual cost of repair per deck area of state-owned bridges (n denotes sample size) .....	43
Figure 3.6. Analysis of the rainfall data – (a) rainfall (mm), (b) ARI (yr) (n denotes sample size, m is the mean, and p is the significance value).....	44
Figure 3.7. Analysis of bridge characteristic variables – (a) vertical clearance (m), (b) year built (n denotes sample size, m is the mean, and p is the significance value).....	46
Figure 3.8. Analysis of bridge ratings – (a) scour rating, (b) substructure rating, (c) channel rating, (d) waterway adequacy rating (n denotes sample size, m is the mean, and p is the significance value) .....	48

Figure 3.9. Analysis of bridge ratings – (a) structural adequacy rating, (b) state sufficiency rating (n denotes sample size, m is the mean, and p is the significance value) .....	49
Figure 3.10. Analysis of variables related to stream characteristics - (a) sinuosity, (b) straightening percentage (n denotes sample size, m is the mean, and p is the significance value) .....	51
Figure 3.11. Analysis of variables related to stream characteristics ratios - (a) width to depth, (b) entrenchment ratio, (c) incision ratio (n denotes sample size, m is the mean, and p is the significance value).....	52
Figure 3.12. Fragility curve for bridge damage given the (a) channel rating, and (b) waterway adequacy rating. The best possible rating in these two categories is 9; therefore, the ratings are subtracted from 9 to reflect that the probability of damage increases with lower channel or waterway adequacy ratings.....	55
Figure 4.1. Watershed Delineation .....	60
Figure 4.2. Flow Direction.....	61
Figure 4.3. (a) Rainfall (in) with observation stations, (b) ARI (yr) interpolations .....	63
Figure 4.4. Watershed Sampling: (a) Irene Rainfall, (b) Annual Precipitation, (c) Land Cover, (d) Hydrologic Soil Group .....	64
Figure 4.5. Stream Power determination .....	70
Figure 5.1. Locations of damaged and non-damaged bridges in Tropical Storm Irene (a) state-wide superimposed on rainfall data, and (b) in watersheds where bridge damage was observed superimposed over recurrence interval estimates.....	73
Figure 5.2. Bridge damage Level (VTrans, 2014) before (left panel) and after (right panels) the storm - (a) and (b) Slight Damage, Wallingford VT140-B10, (c) and (d) Moderate Damage, Bridgewater C3005-B37, (e) and (f) Extensive Damage, Cavendish C3045-B35, (g) and (h) Major Damage, Rochester VT73-B19. ....	81
Figure 5.3. Stream power calculation: (a) catchment delineation, (b) slope calculation, (c) stream power, (d) specific stream power .....	86
Figure 5.4. Histogram distributions of SSP for (a) Damaged and (b) Non-Damaged bridges, and (c) Kruskal-Wallis (non-parametric) One-way Analysis of Variance on SSP .....	87
Figure 5.5. Histogram distributions of ISSP for (a) Damaged and (b) Non-Damaged bridges, and (c) Kruskal-Wallis (non-parametric) One-way Analysis of Variance on ISSP. ....	88
Figure 5.6. Fragility curves of the conditional exceedance probability generated from (a) SSP and (b) ISSP for each of four bridge damage classifications.....	90
Figure 5.7. Probability map for the state of Vermont generated from ISSP.....	91
Figure 5.8. Probability Map for the White River Watershed generated from (a) and (c) SSP and (b) and (d) ISSP.....	93
Figure 6.1. Damaged and Non-damaged bridges, over Irene Rainfall intensity.....	98
Figure 6.2. Bridge Damage Level and Type from Tropical Storm Irene .....	100
Figure 6.3. Accuracy and Coverage for Feature Combination .....	111
Figure 6.4. Accuracy and Coverage for DNF and FC .....	114



Figure 6.5. Spatial relationship of DNF 3313 results .....	117
Figure 7.1. Classic historic bridge types: (a) Kidder Hill Covered Bridge in Grafton, (b) York Hill Steel Pony Truss Bridge in Lincoln, (c) Battell Bridge in Middlebury.....	124
Figure 7.2. Damage to Historic bridges .....	127
Figure 7.3. Historic Bridge type, between population and damaged group .....	129
Figure 7.4. Distributions of Historic Bridge Features.....	130

## **CHAPTER 1 INTRODUCTION**

### **1.1 Motivation**

Bridge scour is the removal of streambed soil and sediments from the supports of bridge foundations caused by water induced-erosion. Scour is the leading cause of bridge failure in the United States and elsewhere. In the United States, 20,904 bridges are listed as scour critical (Gee, 2008). Recent estimates link hydraulic-caused damage to 52% of bridge failures, with the presumed primary cause being scour (Cook et al., 2015). Extreme weather events are expected to occur more frequently in certain parts of the world due to climate change (Melillo et al., 2014). For example, extreme rainfall events, those ranging in the 99<sup>th</sup> percentile of intensity, are happening more frequently, especially over the past three to five decades (e.g., Horton et al., 2014). The associated increase in magnitude and occurrence of flood events will likely result in greater instances of scour damage to bridges.

Current methods for rating and monitoring bridge scour typically rely on visual inspection, as well as the calculations performed at the time of bridge design to predict a bridge's vulnerability to scour. Hydraulic and scour calculations are typically conducted during the initial design and construction phase, and rarely updated. These initial scour calculations are then supplemented regularly with direct measurements and observations of scour during biannual inspections. For example, the Vermont Agency of Transportation (VAOT) inspection rating system is based on the Federal Highway Administration's National Bridge Inventory coding guide (FHWA, 2015). The National Bridge Inventory scour rating is based on the scour depth in relation to the bridge foundation and scour design calculations. As the scour depth approaches the bottom of the foundation, the bridge becomes at risk of failure and is rated as scour critical. In Vermont, only 815 of the over

4,000 hydraulic bridges have a hydraulic and scour report on file, with approximately 25% of the 2,249 bridges that are rated scour critical, or have an unknown foundation. The percentage of scour critical and unknown foundation bridges would likely increase if the uninspected local bridges were included.

Scour can occur in a variety of ways at a bridge, and at varying rates. Normal flow conditions can lead to continuous scour at a bridge, but often occurs slowly such that regular inspection can identify remedial measures and countermeasures that can prevent major damage. Flood flows have the potential to cause large amounts of scour over short amounts of time, faster than countermeasures/repairs can be made, possibly resulting in a bridge moving from a stable to failed state without much notice.

Changes in the stream stability and dynamics can result in a changing scour potential at the bridges below the affected reaches. Two scenarios can be hypothesized in which this could incorrectly predict scour vulnerability. The first is when design information on the bridge's foundation or hydraulic and scour calculations are not available, as is common on older and smaller local bridges. The second is when hydraulic conditions and scour calculations used in the initial design were never or are no longer valid.

Though current design measures may be able to produce a bridge that is robust to the scour produced by extreme events, thousands of existing bridges across the country are not adequately designed or maintained in relation to scour vulnerability under extreme flood events, and are at risk of premature end of service life. The hidden nature of foundation scour leaves the public unaware as a bridge becomes at risk of failure due to foundation undermining from scour.

Vermont, with its mountainous terrain, is prone to storm related scour risk, as the steeper slopes produce flash flood events, inundating bridges. In Vermont, 309 bridges were identified as scour critical in the VTrans bridge database. Infrequent, intense storm events, along with the increased frequency of lower magnitude storm events, put Vermont bridges at increased risk. In addition, the ability of Vermont bridges to resist scour is not well understood, as was evident from the damage caused to Vermont bridges by Tropical Storm Irene.

In August of 2011, Tropical Storm Irene brought 100-200 mm (4-8 inches) of precipitation, and floodwaters exceeding 100-yr flows, with select locations reaching the 500-yr flow. Examples of bridge damage from Irene can be seen in Figure 1.1. This research determined that of the 313 damaged structures, 269 bridges were assessed to be damaged because of scour or embankment erosion. Of the 91 extensive or complete damaged bridges, 59 had been considered non-scour critical, prior to the storm. Thus, structures throughout Vermont proved susceptible to scour damage, despite being considered non-scour critical per the current standard scour rating system based on the Federal Highway Administration's (FHWA) National Bridge Inventory guidelines (FHWA, 1995). This suggests that the current scour rating system is inadequate, at least under extreme events. It is envisioned that the existing scour rating system can perhaps be improved if additional larger scale geomorphic assessments were incorporated into the rating system. Climate data show that Vermont is experiencing more extreme events, and that this trend is predicted to continue with more significant floods and major flooding (Frumhoff et al., 2007; Stager and Thill, 2010; Betts, 2011) demanding more resilient approaches to scour and erosion mitigation for bridges.

Successfully mitigating scour-related problems associated with bridges depends on our ability to reliably estimate scour potential, design safe and economical foundation elements accounting for scour potential, identify vulnerabilities related to extreme events, and recognize changes to the environmental setting affecting risk at existing bridges, which served as the overarching goals for this study. Damage to Vermont bridges from Tropical Storm Irene served as case studies for much of the research included in this thesis. The developed methodologies and analyses however are applicable for studying and predicting bridge (or infrastructure) damage from extreme flood events in any geographic settings.



*Approach scour  
(Lundlow, VT).*

*Approach scour (Orleans,  
Vermont)*

*Foundation scour  
(Dummerston, VT)*

**Figure 1.1. Examples of scour-related damage to Vermont bridges in Tropical Storm Irene (VAOT, 2014)**

## **1.2 Objectives and Research Questions**

The main research question addressed in this study is: given the uncertainty of existing bridge scour design and all available information, what features best predict damage and understanding of bridge vulnerability under extreme events.

The specific objectives of this research were to: (1) collect and geo-reference all available bridge records and stream geomorphic assessment data and information into a comprehensive database for identifying features that best represent damage to Vermont bridges attributed to Tropical Storm Irene; (2) conduct watershed analysis on all hydraulic bridges, including delineating the watershed for every stream reach, and creating stream

power data to assess whether watershed stream power improves the prediction of bridge scour damage; (3) conduct a multivariate feature selection analysis to determine which variable groupings best correlated to bridge damage; and (4) analyze damage and cost of repair of historic bridges damaged in the storm.

### **1.3 Organization of the Thesis**

Chapter 2 presents a concise literature review on bridge scour case studies, methods to compute scour depth and scour rating system. Additionally, literature on geomorphology, stream stability, watershed analysis, and stream power is also included.

Chapter 3 presents network-level analysis of Vermont bridges damaged in 2011 Tropical Storm Irene, with focus on scour-related damage. A comparable analysis of damaged and non-damaged bridges identifies significant factors of bridge vulnerability under extreme flood events. Descriptions of the damage appear as case studies that include pre-storm bridge and stream geomorphology conditions. The georeferenced data include rainfall amounts, damage type and extent, estimated repair costs, bridge characteristics, bridge ratings, and stream geomorphic assessments from a number of sources: Vermont Agency of Transportation Bridge Inventory System, the State Short Structure Inventory Lists, Regional Planning Commission's Vermont Online Bridge and Culvert Inventory Tool, the Vermont Department of Emergency Management's records of town-owned bridges, and the Vermont Agency of Natural Resources' stream RGA (rapid geomorphic assessment) data.

Chapter 4 lays out the methodology used to conduct the watershed delineation and assessment, as well as the calculation of stream power. Numerous data sources were included in the delineation of watersheds at each Vermont bridge, as well as for each stream

reach segment. A series of automated scripts were created to conduct complete processing of all bridges and reaches in Vermont, allowing for broad, spatially referenced display of watershed features and power measures.

Chapter 5 links watershed stream power to the bridge damage from Tropical Storm Irene, develops a process to quantify the hazard at bridges both as a case study and for future storms, and uses stream power as a hazard metric to produce probabilistic predictions of bridge vulnerability. The analysis also offers comparison between damaged bridges and bridges that were not damaged in Tropical Storm Irene. For this purpose, Specific Stream Power (SSP) and the *event-based* Irene Specific Stream Power (ISSP) were computed for all bridges in the state.

Chapter 6 uses an advanced computational algorithm to conduct multivariate feature selection, to identify combinations of features that best correlate to bridge damage. The evolutionary algorithm conducts rapid search of the possible solutions and iteratively improves the possible combinations to create sets of feature combinations that improve upon common feature selection techniques and identify solutions from a “Big Data” perspective. The identified critical combinations of features show correlations between existing and new watershed metrics to bridge damage, aiding in the prediction of bridge vulnerability.

Chapter 7 uses the subset of Vermont historic bridges to investigate their response to the extreme flooding seen in Tropical Storm Irene. Historic covered bridges are of additional importance in Vermont, and represent a cultural and aesthetic resource. Understanding vulnerabilities to historic bridges, and how to best prevent, or minimize

their damage, as well as reduce repair expenses is key to sustainably preserving them into the future.

Chapter 8 concludes this thesis with overall conclusions and recommendations for future work.



## **CHAPTER 2 BACKGROUND LITERATURE**

This chapter presents a concise literature review on bridge scour case studies, methods to compute scour depth and scour rating system. Additionally, literature on geomorphology, stream stability, watershed analysis, and stream power is also included.

### **2.1 Bridge Scour and Regional Context**

On August 28, 2011 Tropical Storm Irene hit the state of Vermont with a severity that caused major damage throughout the state and impacted 225 of the state's 251 towns and cities (State of Vermont, 2012). Tropical Storm Irene entered with sustained winds of 80 km/h and deposited 100-200 mm (4-8 inches) of rain across the state (NWS, 2011). The greatest rainfall totals were along the higher elevations of the state's mountain ranges (State of Vermont, 2012). At these higher elevations, intense rain caused flash flooding, and progressed to widespread flooding throughout Central and Southern Vermont. The rainfall recurrence interval for a twelve-hour storm exceeded 500 years in some areas, with widespread rainfall in excess of the 100-year recurrence interval where damage was reported. It caused record flows in nine streams. Nine other streams had peak flows among the top four on record (USGS, 2011). This was the second worst state-wide flooding event on record, after the storm of November 1927, which dropped 150 mm (6 inches) or more of rain over a three-day period (State of Vermont, 2012). Both storms were preceded by a series of higher than average rainfall events, resulting in saturated ground conditions that exacerbated flood conditions. The flooding and high stream flows resulting from Tropical Storm Irene reportedly caused damage or failure to 389 Vermont bridges per Thomas, et al. (2013).

Other recent extreme events have caused damage to numerous bridges in other parts of the United States. For example, studies from Hurricane Katrina in 2005 indicate that uplifting and hydrodynamic forces on the superstructure caused the majority of the damage to short and medium span coastal bridges (Okeil and Cai, 2008). An economic analysis of 44 bridges damaged from Hurricane Katrina showed a relationship between surge elevation, damage level and repair costs (Padgett et al., 2008). Subsequent analysis of 262 bridges, of which 36 were damaged, identified surge elevation as a key factor in determining damage level from Hurricane Katrina, and related it to the estimated likelihood of damage through empirical fragility curves (Padgett et al., 2012). Both of these studies leveraged the National Bridge Inventory (NBI) as the primary source of bridge data. Similar bridge infrastructure vulnerabilities have been witnessed at Escambia Bay, Florida during the 2004 Hurricane Ivan (Douglass et al., 2004) and in Hokkaido, Japan during the 2004 Songda Typhoon (Okada et al., 2006). More recently, severe flooding in September 2013 caused the collapse of 30 highway bridges, and damage to an additional 20 bridges in Colorado (Kim et al., 2014).

For some time now, scour has been recognized as the primary cause of bridge failures in the United States (Kattell and Eriksson, 1998) and in other parts of the world providing case studies on bridge damage. For example, Wardhana and Hadipriono (2003) analyzed 503 cases of bridge failures in the United States from 1989 to 2000, and found that flood and scour caused nearly 50% of all failures. Melville and Coleman (1973) report 31 case studies of scour damage to bridges in New Zealand, of which 13, 8, 4 and 6 cases were primarily attributed to pier failure, erosion of the approach or abutment, general degradation, and debris flow or aggradation, respectively. The HEC-18 document

(Arneson et al., 2012) mentions numerous examples of scour related bridge damage and failure. During the spring floods of 1987, 17 bridges in New York and New England were damaged or destroyed by scour. The collapse of the I-90 Bridge over the Schoharie Creek near Amsterdam, NY, resulted in the loss of 10 lives and millions of dollars in bridge repair and replacement costs (FHWA, 2015). In 1985, floods in Pennsylvania, Virginia, and West Virginia destroyed 73 bridges. A 1973 national study (FHWA 1973) of 383 bridge failures caused by catastrophic flooding showed that 25 percent involved pier damage and 75 percent involved abutment damage. A second more extensive study in 1978 indicated local scour at bridge piers to be a problem about equal to abutment scour problems (FHWA, 1978; Arneson et al., 2012). The 1993 flood in the upper Mississippi basin caused damage to 2,400 bridge crossings (FHWA, 2015) including 23 bridge failures. The modes of bridge failure included 14 from abutment scour, 3 from pier and abutment scour, 2 from pier scour only, 2 from lateral bank migration, 1 from debris load, and 1 from unknown cause (Arneson et al., 2012). Arneson et al. (2012) also report that the 1994 flooding from storm Alberto in Georgia affected over 500 state and locally owned bridges with damage attributed to scour.

The above case history summary of bridge damage, both coastal and inland, illustrates the vulnerability of existing bridge infrastructure to extreme flooding events. The occurrence of such severe events is expected to increase because of climate change in many parts of the world (Melillo et al., 2014). For example, extreme rainfall events, those ranging in the 99<sup>th</sup> percentile of intensity, are happening more frequently, especially over the past three to five decades (e.g., Horton et al., 2014). The effects of Tropical Storm Irene

on Vermont bridges therefore provide a uniquely large dataset, where a single hurricane-related extreme flood event caused widespread damage to over 300 bridges in a single state.

## **2.2 Bridge Scour Types**

The literature suggests that total bridge scour can be divided into various components that are considered independent and additive, including general scour and local scour. The latter is further subdivided into contraction scour, abutment scour, and pier scour (Briaud et al., 2011). Most research has focused on the three components of local scour, so this section provides an overview of the local scour evaluation process for contraction scour, pier and abutment scour.

Contraction scour is the erosion of material from the bed and banks across all or most of the channel width, resulting from the contraction of flow area imposed by the bridge abutments and piers, as depicted in Figure 2.1 (Arneson et al., 2012). As flow increases, filling the channel and spilling water onto the flood plains, it often meets an obstruction at the bridge. Bridge abutments and embankments used to elevate the bridge deck over the river to an appropriate freeboard, creates obstructions to the flow in the floodplain (Ettema et al. 2010). Common forms used are wing-wall abutments, vertical-wall abutments, and spill through abutments commonly embedded in earthen embankments. Many smaller span bridges also have abutments placed within the channel, causing constriction even in low flows. The blockages caused by abutments in the channel or floodplain force the flow through a smaller section, creating higher velocities and shear stresses (Arneson et al., 2012). At severely contracted sections, backwater occurs upstream, and large-scale turbulences dominate the flow field. Contraction scour has traditionally been classified as live-bed or clear-water, which reflects the bed material sediment-

transport conditions of approaching flows (Arneson et al., 2012). In the case of live-bed scour, the common assumption is that scour will cease when the load of sediment transported into the contraction is equal to or greater than the load of sediment transported from the contraction. Clear-water scour is the case when no upstream bed movement is occurring.

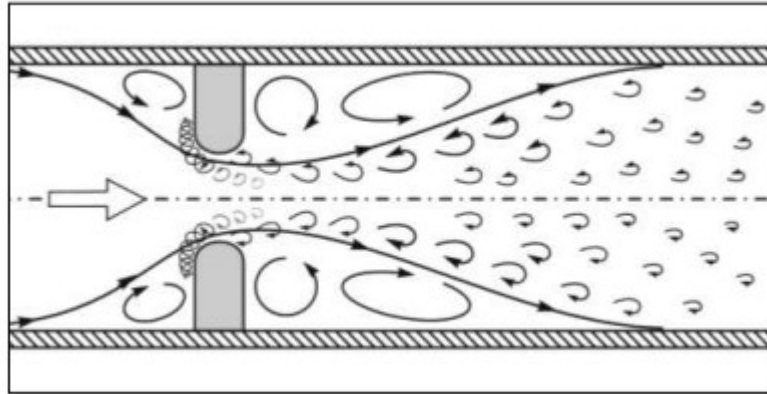


**Figure 2.1. Short contraction at a bridge (source: Ettema et al. 2010)**

Local pier or abutment scour is the removal of bed material from around flow obstructions such as piers, abutments, spurs, and embankments caused by the local flow field induced by a pier or abutment, as depicted in Figures 2.2 and 2.3 (Arneson et al., 2012). Abutments are essentially erodible short contractions. High flow velocities and large-scale turbulences around abutments erode the boundary soils (Ettema et al., 2010). Scour holes typically develop near the end of the abutments, where the wake vortices are the greatest. Geotechnical stability of the embankment is also a key component to abutment scour, if the scour causes geotechnical failure, then the abutment can be treated as a pier.

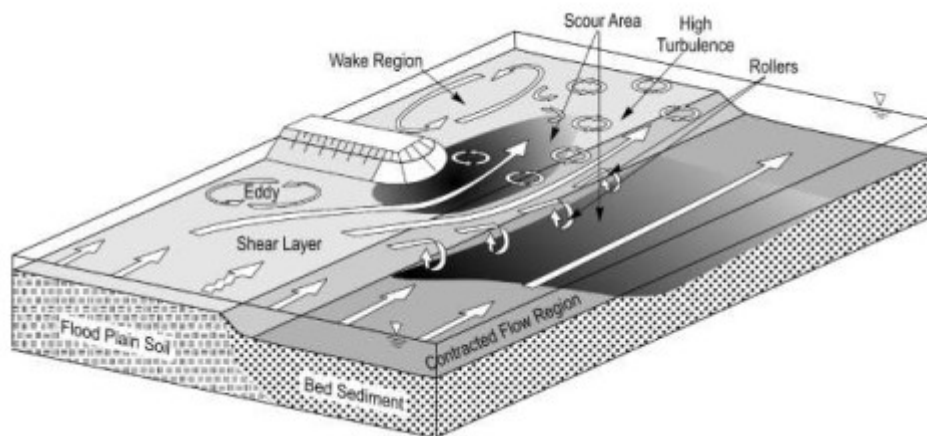


**Figure 2.2. Example of the flow patterns and vortices which result in abutment scour (source: Ettema et al. 2010)**

Local scour at piers has been studied extensively in the laboratory in single soil layers; however, there are limited field data. The common inverted-frustum scour hole has been seen in single layer sediments. The laboratory studies have been mostly of simple piers, but there have been some laboratory studies of complex piers (Richardson and Davis 2001; Sheppard et al., 2011). Often the studies of complex piers are model studies of actual or proposed pier configurations. To understand pier scour, it is necessary to understand the flow field at a pier, and how it changes with pier size and form. Notably, it is an unsteady three-dimensional flow field, interacting with a turbulence structure. The scour forces on the soil are generated by flow contraction around the pier, with a downward flow at the pier's face, and vary with pier width and form, and flow depth (Figure 2.3). For narrow piers, (depth/width >1.4) the scour is deepest at the pier face, as downward forces create a scour hole, while lateral contraction forces cause an increase in velocity and shear stress around the piers' sides, causing scour (Arneson et al., 2012). As the scour develops to a hole fully around the pier, the horseshoe vortices strengthen. Transition piers (depth/width >0.2) function much the same as narrow piers, though they result in shallower scour depths

(Arneson et al., 2012). The reduction in depth lowers the potential for down flow, and increases bed friction in the shallower flow. Wide piers (depth/width < 0.2) have very little down-flow, with most of the scour occurring as the flow turns laterally along the face, and causes contraction on the sides (Arneson et al., 2012). The deepest scour occurs at the pier flanks.

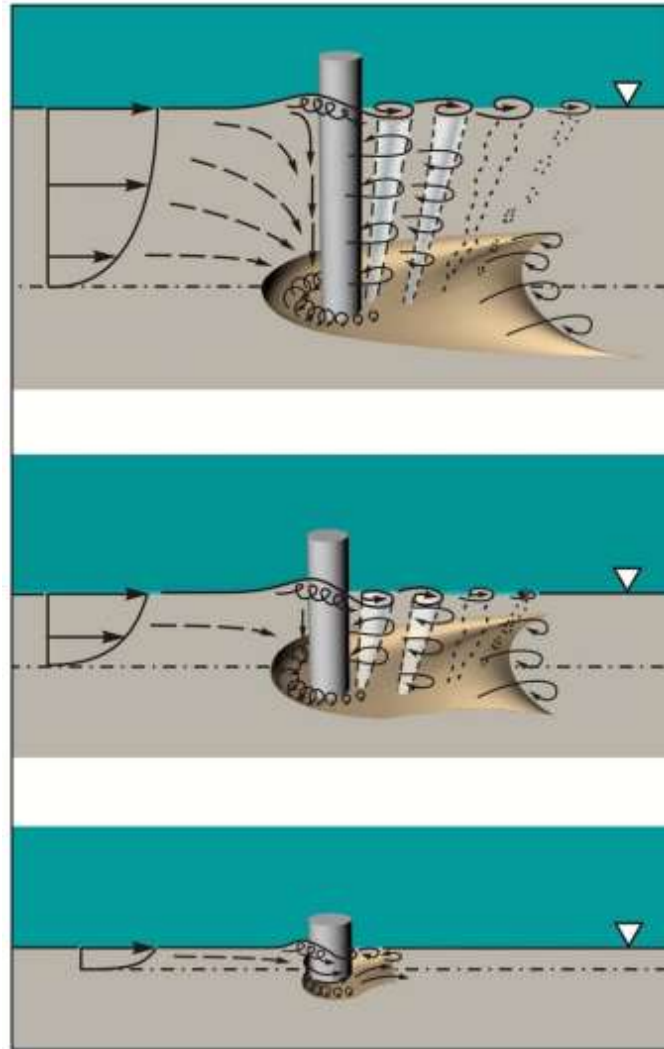


**Figure 2.3. Vortices from a pier obstructing flow, resulting in local pier scour at (a) narrow, (b) transitional, and (c) wide pier (source: Ettema et al. 2011)**

### **2.3 Methods to Compute Scour Depth**

Traditional scour equations are generally considered to not reflect the present knowledge about scour processes, but rather use the primary dimensions of the foundation width and lengths, flow depth, and sediment size to define the structure and geometric scale of the flow field, and thereby scour depth. Total scour depths at a bridge cross-section are the function of stream hydraulic conditions, sediment transport by flowing water, streambed sediment properties, and bridge structure dimensions. The complex interactions among those variables also complicate the scour development. A large number of studies have been conducted on various bridge scour topics and resulted in several physical and numerical models/equations. Scour calculations are often done as the summation of the multiple scour types, with ultimate scour being the combination of contraction, and local scour, from piers and/or abutments. The state of the art in bridge scour prediction is outlined in the FHWA HEC-18, updated most recently in 2012 (Arneson et al., 2012).

Contraction scour is a major component of the ultimate scour depth, caused by flow accelerations due to narrowing of the channel cross section, either by natural reductions in the main channel width, or by the blockage in the floodplain, returning flow back to the channel. The literature describes a number of semi-empirical contraction-scour equations that were developed by the use of conservation of flow and sediment in a control volume in conjunction with laboratory-derived concepts of sediment transport (Straub 1934; Laursen 1963; Melville 1997; Sheppard and Miller 2006). Researchers through laboratory studies (Froehlich 1989; Laursen 1980; Liu et al. 1961; Melville 1992; and Mueller and Wagner 2005) have found that the transport or lack of transport of sediment in the flow approaching an obstruction or contraction is critical in assessing scour at bridges.



Floodplain contraction scour is usually treated separately from main channel contraction scour in compound channels. In this case, one of the difficulties in applying a contraction scour formula is the determination of the discharge distribution between the floodplain and the main channel in the bridge section. Both live-bed and clear-water contraction scour can occur in the field. The former commonly occurs in the main channel of a sand-bed river, while the latter is more likely to be found in a floodplain contraction or a relief bridge located on the floodplain. Contraction scour formulas have been developed analytically for an idealized long contraction as will be described subsequently. In the case of live-bed contraction scour, the limiting condition is the continuity of sediment transport between the approach-flow section and the contracted section. For clear-water scour, where no bed material is being transported upstream, it is the increase in shear stress at the contraction above the critical shear strength of the bed material that controls the scour process, which will continue degrading until enough material is removed to reduce contraction and reach equilibrium. Live bed contraction scour is estimated based on Laursen (1960) equations for long contractions, while clear-water scour is based on Laursen (1963).

Some of the notable studies conducted with the purpose of predicting abutment scour include: Froehlich (1989); Melville (1992); Richardson and Davis (2001); Strum (2006); Ettema et al. (2010); and Chang and Davis (1999). Most of these empirical equations are based on laboratory results and field data, and they differ from each other with respect to the factors considered in constructing the scour model, parameters used in the equation, laboratory or site conditions, and so on.

Pier scour is the other possible component to the local scour calculation. The Colorado State University (CSU) equation established by Richardson and Davis (2001) has

been the dominant method for prediction of pier scour depth. More recent work by Sheppard et al. (2011) through the NCHRP Project 24-32 has established the Sheppard-Mellville method, and has begun to replace the CSU method for most designs. The newer method is believed to better reflect scour processes, while the CSU method is adapted empirically to scour data. Despite the recent advances in modeling the underlying scour processes at piers, determination of scour depths is made difficult due to factors affecting the flow field, complex pier shapes, arrangements and interactions, and difficulties identifying foundation materials.

The majority of the methods in HEC-18 (Arneson et al., 2012) were developed by assuming uniform, non-cohesive sediments that are representative of the most severe scour condition, but the erosional resistance of typical soils found at a bridge site is a combination of stratified soils with varying degrees of cohesiveness. The hydraulic parameters used in HEC-18 models are estimated by a one-dimensional hydraulic model such as Water Surface Profile (WSPRO) or Hydraulic Engineering Center's River Analysis System (HEC-RAS) that distributes the flow across the approach and bridge opening by conveyance (combination of roughness and flow area). However, the flow distribution at a bridge or in its approach is non-uniform because of cross-stream flow caused by channel bed conditions, channel bends, irregular valley topography, and obstructions in the floodplain.

The live-bed abutment scour formula developed by Froehlich (1989) and the Highways in the River Environment (HIRE) equation (Richardson and Davis 2001) are suggested in HEC-18. (Richardson and Davis 2001). Froehlich's equation is derived from regression analysis applied to a list of dimensionless variables using laboratory data. The

HIRE equation is based on field scour data for spur dikes in the Mississippi River; the data were obtained by the U.S. Army Corps of Engineers.

Chang and Davis (1998, 1999) presented an abutment scour methodology called ABSCOUR, which has been further developed by the Maryland State Highway Administration (MSHA 2010). ABSCOUR treats abutment scour as an amplification of contraction scour. In addition, the methodology includes an adjustment/safety factor that is based on the user's assessment of risk and whether the floodplain is narrower or wider than 800 ft (244 m). The full ABSCOUR 9 computer program/methodology includes procedures to refine discharge, velocity distributions and channel setback distances under the bridge; evaluate scour in layered soils; consider the effect of pressure scour; evaluate the slope stability of the embankment; consider degradation and lateral channel movement and other specific concerns. The program is used to integrate contraction, abutment and pier scour, and to draw a scour cross-section under the bridge (MSHA 2010).

Work resulting from NCHRP24-20 (Ettema et al., 2010) established three scour conditions to describe the possible scenarios of abutment and contractions scour (Figure 2.4). This study also related abutment and contraction scour together, treating abutment scour as an amplification of contraction scour, and took into account geotechnical instability. The three scour conditions are: scour in the main channel leading to undercutting of the embankment and abutment resulting in local collapse, scour in the floodplain around the abutment occurring as clear-water scour, and failure of the approach embankment fully exposing the abutment and resulting in a pier flow field.

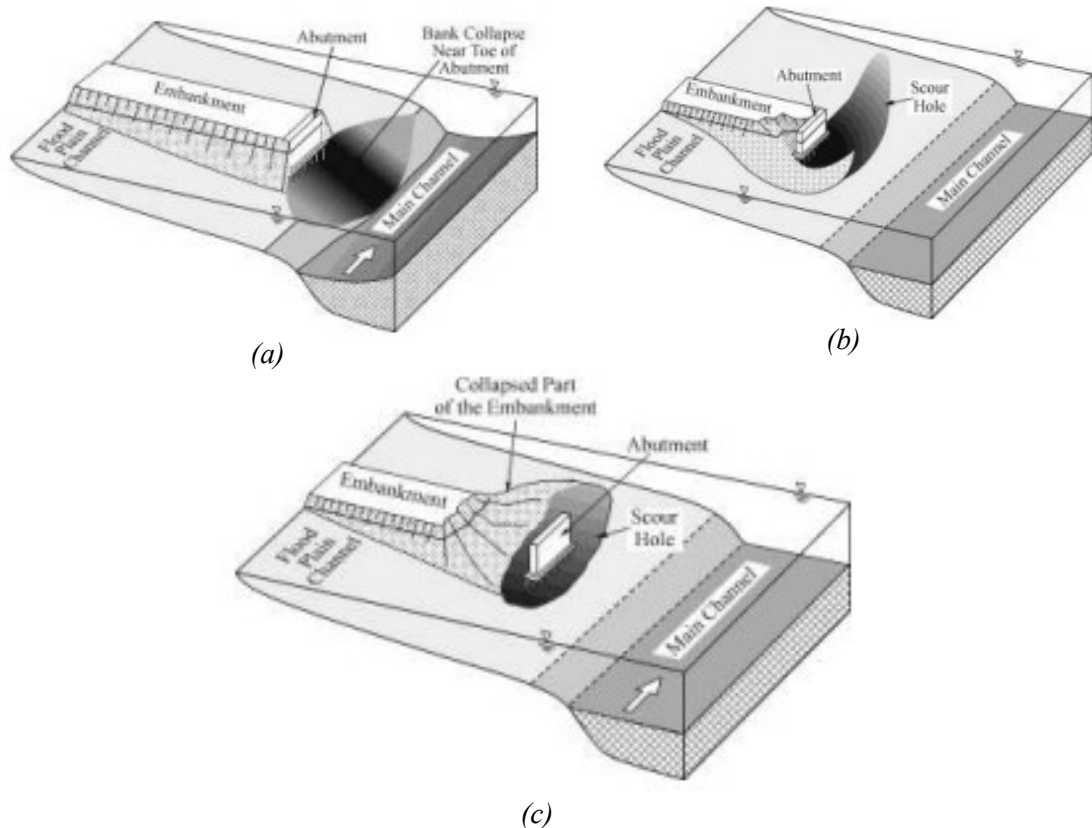


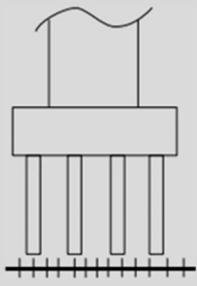
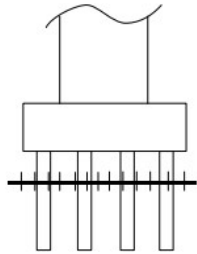
**Figure 2.4. Abutment scour conditions: (a) A – hydraulic scour of the main bed; (b) B – scour of the floodplain; and (c) C – scour of the approach, exposing the abutment as a pier (source: Ettema et al., 2010)**

## 2.4 Scour Rating System

The Vermont Agency of Transportation inspection rating system, and that of many other states, is based on the Federal Highway Administration’s National Bridge Inventory System (NBIS) (FHWA, 2015). Vermont’s bridge inspections occur on a 24-month basis, with a shorter inspection window for those bridges in need of more immediate attention. As part of the inspection, the scour depth at the bridge is observed. Scour is measured using a variety of techniques from rodding to full underwater inspection when needed. Item 113 of the National Bridge Inventory (NBI) is the Scour Critical Bridge rating, and it details the current status of the bridge regarding its vulnerability to scour. The Scour Critical

Bridge rating codes can be seen in Table 2.1 below. The system of scour rating relies on a combination of inspection observations as well as design calculations. The design aspect considers whether the foundation is constructed below the calculated depth of scour for a certain recurrence interval flow. In Vermont, the specific calculated scour depth is either determined during design and construction, or analyzed later as part of a review of scour at bridges. As of 2001, only 825 of the 2,317 hydraulic bridges have a hydraulic and scour report on file. Scour can present itself in a variety of ways at a bridge, and can act over vastly different temporal ranges. Normal flow condition can lead to continuous scour at a bridge, but often occurs slowly enough that observation and maintenance can prevent major damage. Flood flows have the potential to cause large amounts of scour in a short amount of time, faster than any repairs can be made, possibly resulting in a bridge going from a stable to failed condition without notice. As the scour depth approaches the bottom of the foundation, the bridge becomes at risk of failure and is rated as scour critical. Bridge ratings are categorical from 0-9 with an additional Unknown Foundations (U) category. The scale is not ordinal, instead each rating indicates a specific scenario, not a magnitude of risk. Scour critical bridges, rated 3 and below, are those found to be unstable through either observed scour or have a calculated scour potential greater than the design scour. Bridges with unknown foundations (U) could potentially be added to the scour critical lists. Scour critical bridges require a plan of action be created, outlining the steps needed to address the deficient bridges.

**Table 2.1. Scour Ratings Used by VTrans (FHWA, 1995)**

Rating	Description	Notes	example
U	No information on the foundation is available – Unknown foundation.	Bridges with U are expected to be added to those considered scour critical.	
0	Bridge is scour critical. Bridge has failed and is closed to traffic.	Bridges with ratings 0 through 3 are considered scour critical.	
1	Bridge is scour critical; field review indicates that failure of piers/abutments is imminent. Bridge is closed to traffic.		
2	Bridge is scour critical; field review indicates that extensive scour has occurred at bridge foundations. Immediate action is required to provide scour countermeasures.		
3	Bridge is scour critical; bridge foundations determined to be unstable for calculating scour conditions.		
4	Bridge foundations determined to be stable for calculated scour; field review indicates action required to protect foundations from additional erosion.	Bridges with ratings 4 through 9 are considered non-scour critical.	
5	Bridge foundations determined to be stable for calculated scour conditions; scour within limits of footing or piles.		
6	Scour calculation/evaluation has not been made.		
7	Countermeasures have been installed to correct previously existing scour. Bridge is no longer scour critical.		
8	Bridge foundations determined to be stable for calculated scour conditions; calculated scour is above top of footing. If bridge was screened or studied by experts and found to be low risk, it should fall into this category.		
9	Bridge foundations (including piles) well above flood water elevations.		

## 2.5 Stream Power

In this work, stream power is evaluated because it was thought to have a strong potential to be correlated to the hazard at bridges. Stream power is the rate of energy (i.e., power) of flowing water against the bed and banks of a river channel, and functionally controls stream dynamics and morphology. Stream power estimates from extreme events were shown to correlate positively with the instances of stream widening in the White River watershed of Vermont (Buraas et al., 2014). Also, Gartner et al. (2015) showed that in the Fourmile Canyon of Colorado, the erosion and deposition correlated with increased power gradients and decreased power gradients, respectively. Stream power generally has been shown to correlate positively to fluvial incision (Seidl and Dietrich, 1992; Anderson, 1994), channel size, mobility and pattern changes (Magilligan, 1992; Rosenbloom and Anderson, 1994; Lecce, 1997; Knighton, 1999), and as an estimate of flood power (Brooks and Lawrence, 1999).

Specific stream power (SSP) normalizes total stream power, which is the product of discharge, slope, and the specific weight of water, and normalizes it by the stream width (Bagnold, 1966). SSP allows for the expression of stream power at the unit bed area, rather than the cross-sectional area, as is the case in total stream power. Magilligan (1992) and Miller (1990) showed that  $300 \text{ W/m}^2$  provides a minimum SSP threshold to separate reaches with and without large-scale geomorphic change.

Stream power calculations have been conducted on multiple scales to support analysis of river systems for various objectives including risk to infrastructure, evaluation of channel stability, and assessment of instream habitats. At the finest scale, stream power has been used to conduct bridge scour analysis in erodible rock (Costa and O'Connor,

1995; FHWA 1999), and relate erodibility indices to local stream power measures. Point-location estimates have been prominent (e.g., Fonstad, 2003; Lecce, 1997; and Magilligan, 1992), with studies that sought to identify transitions in stream power along the longitudinal profile and better understand sediment storage dynamics within a basin. Longer reach-length profiles use continuous distributions of stream power to identify stream power functions through a single fluvial system (e.g. Fonstad, 2003; Reinfeld et al., 2004; and Knighton, 1999). Geographic information systems (GIS), leveraging digital elevation models (DEM), has been shown to effective in generating the progression from point- and reach-scale estimates of stream power to network or catchment scale modeling (Finlayson and Montgomery, 2003; Jain et al., 2006; Barker et al., 2008; and Vocal Ferencevic and Ashmore, 2012).



### **CHAPTER 3 ANALYSIS OF BRIDGE AND STREAM CONDITIONS OF OVER 300 VERMONT BRIDGES DAMAGED IN TROPICAL STORM IRENE**

This Chapter was published in the Structure and Infrastructure Journal, 2017

#### **Synopsis:**

The 2011 Tropical Storm Irene deposited 100-200 mm of rain in Vermont with a rainfall recurrence interval for a twelve-hour storm exceeding 500 years in some areas. This single hurricane-related event damaged over 300 bridges. The wide range of damage prompted a network-wide analysis of flood, scour, stream and structural conditions. A first step was the assembly of a unique dataset containing information on 326 damaged bridges, 1,936 undamaged bridges and the surrounding stream conditions. Descriptions of the damage appear as case studies that include pre-storm bridge and stream geomorphology conditions. The assembled and georeferenced data include rainfall, damage type and extent, estimated and actual repair costs, bridge characteristics, bridge ratings, and stream geomorphic assessments from a number of sources. The analyses identified significant features of bridge vulnerability under extreme floods. The bridge age and rating assessment characteristics, such as substructure, channel, and structural adequacy ratings, followed by scour, waterway adequacy, and sufficiency ratings, correlated strongly to damage. The stream geomorphic features have promise to supplement future bridge rating systems and in identifying hydraulic vulnerability of bridges. Empirical fragility curves relating probability of meeting or exceeding different bridge damage levels based on channel and waterway adequacy ratings are also presented.

### **3.1 Introduction**

On August 28, 2011 Tropical Storm Irene hit the state of Vermont with a severity that caused major damage throughout the state and impacted 225 of the state's 251 towns and cities (State of Vermont, 2012). Tropical Storm Irene entered with sustained winds of 80 km/h and deposited 100-200 mm (4-8 inches) of rain across the state (NWS, 2011). The greatest rainfall totals were along the higher elevations of the state's mountain ranges (State of Vermont, 2012). At these higher elevations, intense rain caused flash flooding, and progressed to widespread flooding throughout Central and Southern Vermont. The rainfall recurrence interval for a twelve-hour storm exceeded 500-years in some areas, with widespread rainfall in excess of the 100-year recurrence interval where damage was reported. It caused record flows in nine streams. Nine other streams had peak flows among the top four on record (USGS, 2011). This was the second worst state-wide flooding event on record, after the storm of November 1927, which dropped 150 mm (6 inches) or more of rain over a three-day period (State of Vermont, 2012). Both storms were preceded by a series of higher than average rainfall events, resulting in saturated ground conditions that exacerbated flood conditions. The flooding and high stream flows resulting from Tropical Storm Irene reportedly caused damage or failure to 389 Vermont bridges per Thomas et al. (2013).

Other recent extreme events have caused damage to numerous bridges in other parts of the United States. For example, studies from Hurricane Katrina in 2005 indicate that uplifting and hydrodynamic forces on the superstructure caused the majority of the damage to short and medium span coastal bridges (Okeil and Cai, 2008). An economic analysis of 44 bridges damaged from Hurricane Katrina shows a relationship between surge elevation,

damage level and repair costs (Padgett et al., 2008). Subsequent analysis of 262 bridges, of which 36 were damaged, identifies surge elevation as a key factor in determining damage levels from Katrina, and relates it to the estimated likelihood of damage through empirical fragility curves (Padgett et al., 2012). Both of these studies leverage the National Bridge Inventory (NBI) as the primary source of bridge data. Similar bridge infrastructure vulnerabilities have been witnessed at Escambia Bay, Florida during the 2004 Hurricane Ivan (Douglass et al., 2004) and in Hokkaido, Japan during the 2004 Songda Typhoon (Okada et al., 2006). More recently, severe flooding in September 2013 caused the collapse of 30 highway bridges, and damage to an additional 20 bridges in Colorado (Kim et al., 2014).

For some time now, scour has been recognized as the primary cause of bridge failures in the United States (Kattell and Eriksson, 1998) and in other parts of the world providing case studies on bridge damage. For example, Wardhana and Hadipriono (2003) analyzed 503 cases of bridge failures in the United States from 1989 to 2000, and found that flood and scour caused nearly 50% of all failures. Melville and Coleman (1973) report 31 case studies of scour damage to bridges in New Zealand, of which 13, 8, 4 and 6 cases were primarily attributed to pier failure, erosion of the approach or abutment, general degradation, and debris flow or aggradation, respectively. The HEC-18 document (Arneson et al., 2012) mentions numerous examples of scour related bridge damage and failure. During the spring floods of 1987, 17 bridges in New York and New England were damaged or destroyed by scour. The collapse of the I-90 Bridge over the Schoharie Creek near Amsterdam, NY, resulted in the loss of 10 lives and millions of dollars in bridge repair and replacement costs (FHWA, 2015). In 1985, floods in Pennsylvania, Virginia, and West

Virginia destroyed 73 bridges. A 1973 national study (FHWA 1973) of 383 bridge failures caused by catastrophic flooding showed that 25 percent involved pier damage and 75 percent involved abutment damage. A second more extensive study in 1978 indicated local scour at bridge piers to be a problem about equal to abutment scour problems (FHWA, 1978; Arneson et al., 2012). The 1993 flood in the upper Mississippi basin caused damage to 2,400 bridge crossings (FHWA, 2015) including 23 bridge failures. The modes of bridge failure included 14 from abutment scour, 3 from pier and abutment scour, 2 from pier scour only, 2 from lateral bank migration, 1 from debris load, and 1 from an unknown cause (Arneson et al., 2012). Arneson et al. (2012) also reported that the 1994 flooding from storm Alberto in Georgia affected over 500 state and locally owned bridges with damage attributed to scour.

The above case history summary of bridge damage, both coastal and inland, illustrates the vulnerability of existing bridge infrastructure to extreme flooding events. The occurrence of such severe events is expected to increase because of climate change in many parts of the world will shift precipitation patterns (Melillo et al., 2014). For example, extreme rainfall events, those ranging in the 99<sup>th</sup> percentile of intensity, are happening more frequently, especially over the past three to five decades (e.g., Horton et al., 2014). The effects of Tropical Storm Irene on Vermont bridges therefore provide a uniquely large dataset, where a single hurricane-related extreme flood event caused widespread damage to over 300 bridges in a single state. The network-wide analysis on damaged and statistically comparable non-damaged bridges on a dataset this large is believed to be not available in the literature. This paper presents example case studies including descriptions of the damage and corresponding estimated and actual repair/replacement costs, and

feature-based analysis of observed damage. A univariate statistical comparison between damaged and comparable non-damaged bridges identifies an initial set of significant features of bridge vulnerability under extreme events. An ordinal logistic regression further tests those features individually against damage level, revealing features that are correlated to increasing damage. The most significant features may be used to generate fragility curves showing probability for exceeding levels of damage under extreme events for a given feature; and examples are presented.

### **3.1.1 Bridge Data**

To study the effects of Tropical Storm Irene on Vermont's bridge infrastructure, a comprehensive database of all available records on bridges prior to the storm was compiled. The data collection and assembly identified geo-referenced locations and information for all river and stream crossing bridges, including all available inspection data and relevant photographic records. This encompassed 4,761 state- and town-owned bridges from the Vermont Agency of Transportation (VTrans) Bridge Inventory System (BIS). The BIS functions as a record for all bridge inspections conducted in accordance with the Federal Highway Administration's National Bridge Inventory (NBI) coding guide, and contains all bridges, both state- and town-owned over 6 m in span length. For the purposes of this study, we compiled a comprehensive list of all bridge structures, including traditional bridges, stone arches, and open bottom culverts, and applied the general term of "bridge" to all.

Information quantifying Tropical Storm Irene-related damage came from VTrans and the Vermont Department of Emergency Management (VDEM). The VTrans provided information on the damage to state-owned bridges. The VDEM collected damage to town-

owned bridges for the purpose of applying for Federal Emergency Management Agency (FEMA) repair funding. The damage records were linked to the comprehensive bridge list to locate and identify the damaged bridges. In some cases, database errors prevented finding a link between the two databases and required further geospatial analysis. This cross-referencing identified 153 bridges in the comprehensive bridge list as having been damaged during the storm. An additional 173 bridges were identified as damaged via a follow-up study of available VTrans online bridge inspection photograph archives, including supplemental inspection photos taken during the post-Tropical Storm Irene recovery. This process identified a total of 326 bridges as having been damaged, with damage ranging from minor streambank erosion to entire bridge collapse. The number of damaged bridges identified in the database (326 bridges) differs from that reported by the VDEM (Thomas et al. 2012, 389 bridges), and is thought to be due to the misclassification of certain culverts as bridges in the higher estimate, as well as rapid and unrecorded post storm bridge repair. Bridges with spans shorter than 6 m were removed from the list, as the analysis relies on inspection records, which are not available for bridges with spans shorter than 6 m. This resulted in 313 damaged bridges available for use in subsequent statistical analysis and feature extraction for comparison with the corresponding 1,950 non-damaged bridges from the comprehensive list of Vermont bridges.

### **3.1.2 Rainfall Data**

The analysis presented here used climate observations collected during Tropical Storm Irene throughout the state of Vermont and surrounding counties in New York, New Hampshire and Quebec (Springston et al., 2012). Ordinary Kriging was used to generate a spatial interpolation of the rainfall measurements over the entire state of Vermont, and

provided the average recurrence interval (ARI), using a 12-hr duration storm to match the duration of Tropical Storm Irene (Kiah et al., 2013).

### **3.1.3 Stream Geomorphic Data**

The Vermont Agency of Natural Resources (VTANR) has been quantitatively assessing the hydraulic stability and sensitivity of Vermont streams over the past 15+ years. The River Management Program developed and utilized a set of peer-reviewed stream assessment protocols to collect geomorphic information for over 3,200 km of Vermont streams to create the Rapid Geomorphic Assessment (RGA) database (Kline et al., 2007). The VTANR RGA protocol is a nationally recognized method to provide a measure of stream disequilibrium and stream sensitivity to indicate the likelihood of a stream responding via lateral and/or vertical adjustment to natural or human-induced watershed disturbances (Somerville and Pruitt, 2004; Besaw et al., 2009). The assessments consider each stream on a reach scale, designated as the length of channel considered to be consistent in slope, bed material, and distinguishable in some way from the upstream and downstream sections. The RGA protocols divide into three phases. Phase I compiles existing topographic maps, orthophotos, and local expert knowledge. Phase II comprises field survey results, and stream stability metrics performed at the reach scale. Phase III is an in-depth assessment on a sub-reach scale, including a detailed field survey and quantitative measurements of channel dimension, pattern, profile, and sediments, used when a specific concern requires greater detail than the Phase II. This analysis uses only the Phase I and II data. In addition to providing an overall RGA (stream reach disequilibrium) score, all information collected during the RGA protocols is available in Arc-GIS (ESRI 2011), including the geometry of the valley and channel reach, watershed and floodplain

characteristics, and classification of streambed materials. Additionally, the analysis of damaged bridges included widely available National (and Vermont) hydrography data (i.e., stream-reach characteristics and geomorphology data).

### **3.2 Geospatial Analysis and Data Processing**

The comparison between damaged and non-damaged bridges focuses on two subsets of non-damaged bridges that vary in scale. Selection of the non-damaged bridges began by geospatially indexing the bridge list in Arc-GIS, and identifying the damaged bridges within the state as presented in Figure 3.1a. The two sets of non-damaged bridges used in this analysis include (1) reach scale (Reach-ND), the nearest non-damaged bridge ( $n = 274$ ), (Figure 3.1b); and (2) watershed scale (Watershed-ND), non-damaged bridges located in subwatersheds that contain the damaged bridges ( $n = 954$ ), (Figure 3.1c). The Arc-GIS analysis identified the non-damaged bridges nearest to the damaged bridges (reach scale) as well as the subwatersheds with damaged bridges (watershed scale). The reach scale non-damaged bridges were selected using stream flow path distance, rather than Euclidean distance to create one-to-one pairings of damaged and non-damaged bridges that likely experienced equivalent storm-related streamflow impacts. Instances where two damaged bridges share the same nearest non-damaged bridges resulted in fewer non-damaged bridges being included in the Reach-ND set than the damaged bridges.

The watershed scale, which used the USGS (United States Geological Survey) Watershed Boundary Dataset (WBD) 6<sup>th</sup> level (12-digit) subwatershed for delineation, provides a comparison with non-damaged bridges that are located within similar geographic settings, and were generally exposed to similar storm impacts as the damaged bridges. The USGS WBD is a hierarchical hydrologic unit dataset based on topographic



and hydrologic features across the United States that defines the perimeters of drainage areas, including six levels of detailed nested hydrologic unit boundaries (USGS and USDA-NRCS, 2013). The motivation for using watershed and reach scales to identify comparable non-damaged bridges was to ensure that statistical comparisons were more discriminating by providing comparisons of bridges that for a particular scale experienced similar storm impacts and came from geographically and topologically similar settings. Storm impacts differ with location, and the closer a non-damaged bridge is to a damaged bridge, the more likely it is to experience similar storm impacts. The watershed scale was created to capture non-damaged bridges in the hardest hit regions in the state. The decreased non-damaged data sets also help to reduce the statistical power associated with such a high number of data points, as was the case in the statewide data. A flow chart of the process of collecting and analyzing the bridge database, and the reduction of the data for each dataset being analyzed appears in Figure 3.2.

### **3.2.1 Selection of Variables and Analysis Method**

A Kruskal–Wallis one-way analysis of variance (ANOVA) by ranks was used to compare the damaged and non-damaged bridge data at two scales (i.e., reach and watershed), using the programming environment MATLAB 2012. This non-parametric equivalent of the traditional one-way ANOVA test can accommodate the observed non-Gaussian distributions of some feature residuals that limit the application of a traditional ANOVA (Kruskal and Wallis, 1952; Siegel, 1956). Additionally, the presence of ordinal data types necessitated the use of a non-parametric test. Significant variables from the ANOVA were then tested for correlation to damage state with a multivariate logistic regression.

Table 3.1 summarizes the bridge and stream variable analysis of variance, and lists the resulting means and p-values. Testing was conducted between damaged bridges and each of the non-damaged bridges individually. A small p-value (e.g., less than or equal to some user-defined threshold of say,  $p < 0.05$ ), indicates that it is unlikely (i.e., less than a 5% chance) that the differences observed (i.e., means being tested) are due to random chance. Thus, we could reject the null hypothesis that damaged and non-damaged bridges have similar means. Statistical analysis was conducted on all variables available in the existing databases; however, only those with either intrinsic or statistical significance receive further discussion in the paper. The means for all individual features across all bridges in the state are included as well to assess if the damaged bridges represented typical bridges in the state. The variables in Table 1 separate into three categories: bridge characteristics, bridge rating assessments, and stream geomorphology assessments with the database source identified as VTrans-BIS or VANR-RGA in Table 1.

The variables selected for testing to represent the bridge characteristics from the VTrans IS include: approach road width, maximum span, span, deck width, vertical clearance, year built, and average daily traffic. The VTrans BIS additionally includes Bridge Ratings Assessments for the deck, superstructure, substructure, channel, scour, waterway adequacy, structural, and state sufficiency ratings. The deck, superstructure and substructure ratings are similar in their method of determining the current condition of the various bridge components, which is scored from 0-9 and U (unknown).

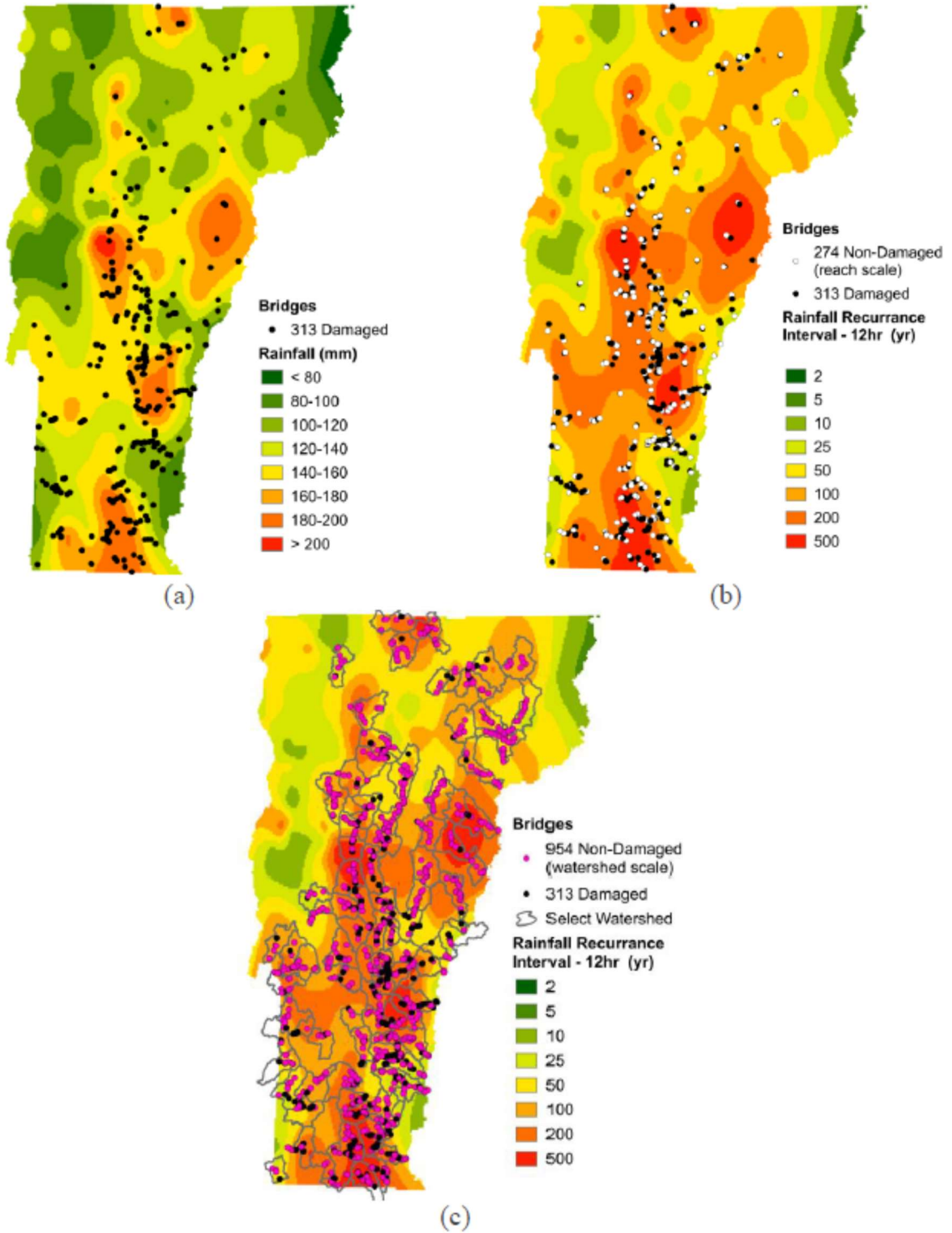


Figure 3.1. Tropical Storm Irene impact on Vermont bridges – (a) Estimated rainfall totals and locations of damaged bridges, (b) Estimated annual recurrence interval, locations of damaged and reach-scale non-damaged bridges, (c) Estimated annual recurrence interval, and locations of damaged and watershed-scale non-damaged bridges

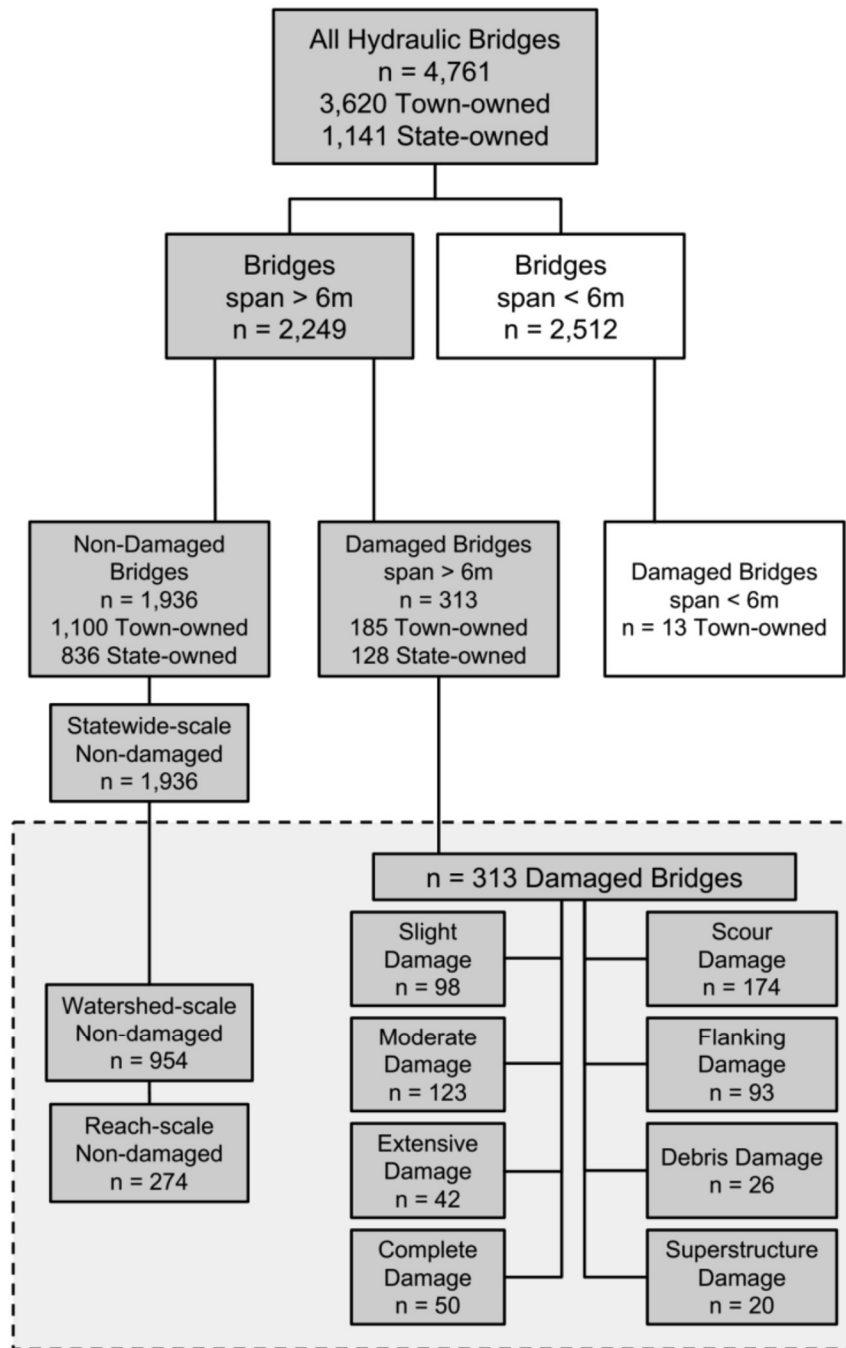


Figure 3.2. Bridge database process chart (the data identified in the boxes without background highlight were not used in the statistical analysis, n denotes sample size)

**Table 3.1. Variables considered in statistical Kruskal-Wallis analysis**

(significance indicated in bold, n denotes sample size)

Variable (unit)	Mean				Statistical Significance (p-value)	
	Damaged Bridges (n=313)	Non-Damaged Bridges			Non-Damaged Bridges	
		Reach (n=274)	Watershed (n=954)	Statewide (n=1,936)	Reach (n=274)	Watershed (n=954)
<i>Bridge Characteristics (VTrans-BIS)</i>						
Approach Width (m)	7.5	7.6	7.6	7.8	0.502	0.341
Max Span (m)	17.7	18.4	17.0	17.6	0.876	0.052
Structure Length (m)	23.9	23.8	22.7	24.7	0.496	0.004
Deck Width (m)	78.2	78.7	80.1	81.8	0.415	0.104
Vertical Clearance (m)	34.3	39.8	37.7	38.9	0.018	0.423
Year Built	1948.7	1955.9	1957.2	1957.1	0.010	<0.001
Average Daily Traffic	1392.9	1470.2	1467.1	1791.5	0.828	0.755
<i>Bridge Rating Assessments (VTrans-BIS)</i>						
Deck Rating	6.7	7.1	7.0	7.0	0.004	0.017
Superstructure Rating	6.6	7.1	7.0	7.0	<0.001	0.001
Substructure Rating	6.4	6.9	6.8	6.8	<0.001	<0.001
Channel Rating	6.4	6.9	6.9	7.0	<0.001	<0.001
Waterway Adequacy Rating	6.2	6.6	6.8	6.8	0.002	<0.001
Scour Rating	6.3	6.9	7.1	7.1	0.006	<0.001
Structural Adequacy Rating	39.3	45.3	45.8	45.9	<0.001	<0.001
State Sufficiency Rating	66.0	73.4	75.2	75.5	0.004	<0.001
<i>Stream Geomorphic Assessments (VTANR-RGA)</i>						
Stream Order	3.95	3.92	3.86	4.02	0.715	0.215
Channel Slope (%)	4.1	3.8	4.1	3.6	0.257	0.228
Sinuosity	1.11	1.12	1.16	1.17	0.103	<0.001
Straightening (%)	43.6	36.4	33.0	31.8	0.025	<0.001
Max Depth (m)	1.16	1.17	1.20	1.29	0.619	0.867
Mean Depth (m)	0.80	0.81	0.85	0.93	0.643	0.304
Flood Prone Width (m)	70.7	89.1	102.0	116.3	0.231	0.078
Abandoned Floodplain Height (m)	1.9	1.8	1.8	1.9	0.275	0.165
Width to Depth Ratio	26.5	31.7	24.2	22.3	0.116	0.005
Confinement Ratio	9.4	9.5	10.5	11.0	0.717	0.137
Entrenchment Ratio	3.7	4.1	6.2	7.1	0.701	0.007
Incision Ratio	1.71	1.65	1.58	1.54	0.479	0.038
RGA Degradation Score	9.0	8.8	9.9	10.5	0.901	0.065
RGA Aggradation Score	11.0	10.8	11.0	11.6	0.730	0.882
RGA Widening Score	11.2	10.9	11.6	11.8	0.618	0.197
RGA Planform Score	11.0	11.2	11.1	11.5	0.952	0.940
RGA Rating	0.53	0.52	0.55	0.57	0.788	0.257

The channel, waterway adequacy and scour ratings use descriptive cases of damage to assign values that are roughly ordinal, though the lack of a scale for damage would suggest the data is more likely to be considered nominal. The channel rating assesses the condition of the embankments and channel near the bridge for erosive damage, and rates the condition of any installed countermeasures. The scour rating evaluates the risk of bridge failure from scour, based on the observed scour compared to the design scour depths. The waterway adequacy rating combines the likelihood of the bridge being overtopped by a flow event with a weighting that depends on the road's level of significance, such that high traffic volume highways would be required to withstand greater storm flows than low volume rural roads. The state sufficiency rating determines the bridge fitness (i.e., sufficiency to remain in service) based on the service it performs using factors derived from over 20 NBI data fields. As a factor in the sufficiency rating, the structural adequacy rating combines the minima of the superstructure and substructure ratings with the reduction in load capacity to determine one component score included in the sufficiency rating.

Variables used to characterize the stream geomorphic assessment include: channel length, bankfull channel width, flood-prone width, maximum depth, mean depth, floodplain height, stream order, sinuosity, straightening percent, confinement ratio, span to channel ratio, width to depth ratio, entrenchment ratio, incision ratio, channel slope, watershed area, specific stream power, RGA degradation score, RGA aggradation score, RGA widening score, RGA planform score, and an overall RGA rating. Details on these parameters may be found in the RGA protocols of Kline et al. (2007). The stream geomorphology parameters apply to an entire stream reach. Therefore, when damaged and non-damaged bridges lie within the same stream reach, they would be assigned the same

stream geomorphic assessment values. The analysis uses width, length, depth and floodplain height parameters to determine whether there was a significant difference in stream size for bridges that were damaged. The ratios for sinuosity, confinement, span to channel, width to depth, entrenchment and incision, as well as percentage of the stream reach that was straightened help characterize the geomorphological condition of the stream reach; while the four RGA component scores (i.e., degradation, aggradation, widening and planform) are weighted and combined by experts to assess an overall RGA rating to assess stream reach disequilibrium (i.e., geomorphic stability).

A large number of possible variables from both the BIS and RGA were not included in this parametric analysis, as they are represented by categorical fields and ordinal data with sparse intervals. The most relevant of these variables include the bridge type, foundation type, stream type, bed material, and other fields that may aid in the future evaluation of bridge scour vulnerability.

The variables determined to be statistically significant on the reach scale were additionally tested using a multivariate logistic regression, using the damage level as the dependent variable, to determine which variables contributed to the observed level of damage. An empirical fragility curve was then developed for one of the resulting characteristics as a first step toward risk-based analysis of the bridges.

### **3.3 Results and Discussion**

#### **3.3.1 Damage Classification and Cost Analysis**

Bridge damage from Tropical Storm Irene was categorized based on photographic documentation and descriptions in available reports. Bridges damaged included 55% steel beam, 34% concrete slab or beam, and 11% historical steel or wood truss superstructures.

Single span bridges made up the vast majority (82%) of bridges damaged, with 12% double span, and the few remaining included 3 and 4 span structures. In cases where photographs were absent, available descriptions were used for damage categorization.

Bridge damage was grouped into four categories: scour, channel flanking, superstructure damage, and debris blockage, with the most prominent type of observed damage determining the category. The majority (55.6%) of bridge damage resulted from scour (e.g., Figure 3.3a). Channel flanking (e.g., Figure 3.3b), the erosion of the approach embankment behind the bridge abutments and specifically not within the channel, was responsible for 29.7% of the damaged bridges. Debris blockage (e.g., Figure 3.3c) was documented at 8.3% of the bridges, at which no other hydraulic damage was observed. Debris accumulation was commonly observed along with the other three types of bridge damage. Superstructure damage (Figure 3.3d) included damage to the deck, guardrails, and siding, and accounted for 6.4% of the reported damage. The majority ( $n = 198$ ) of the 313 damaged bridges were town-owned.

Bridge damage was further categorized into four levels: slight, moderate, extensive and complete. This damage ranking system was based on that proposed in HAZUS (Scawthorn, 2006), and later amended by Padgett et al. (2008). The ranking system descriptions were expanded to include the damage types observed in Tropical Storm Irene, particularly damage from flooded river flow. Slight damage includes: channel erosion not affecting the bridge foundation, superstructure and guardrail damage, and debris accumulation without scour present (Figures 3.4a and b). Moderate damage (Figure 3.4c and d) includes: scour affecting the foundation, but not to a critical state, bank and approach erosion, superstructure damage but not to a critical state, and heavy aggradation. Extensive



damage (Figure 3.4e and f) includes: critical scour, with some settlement to a single foundation, but not collapse, full flanking of both approaches, and damage to the superstructure making it structurally unsafe. Complete damage includes cases where the bridge was washed away, collapsed or has significant foundation damage requiring replacement (Figure 3.4g and f). Characterization of the level and type of damage was performed independent of any knowledge of the repair costs. Of the damaged bridges, 30% were categorized as having slight damage, 39% as moderate damage, 14.5% as extensive damage, and 16.5% as complete damage.

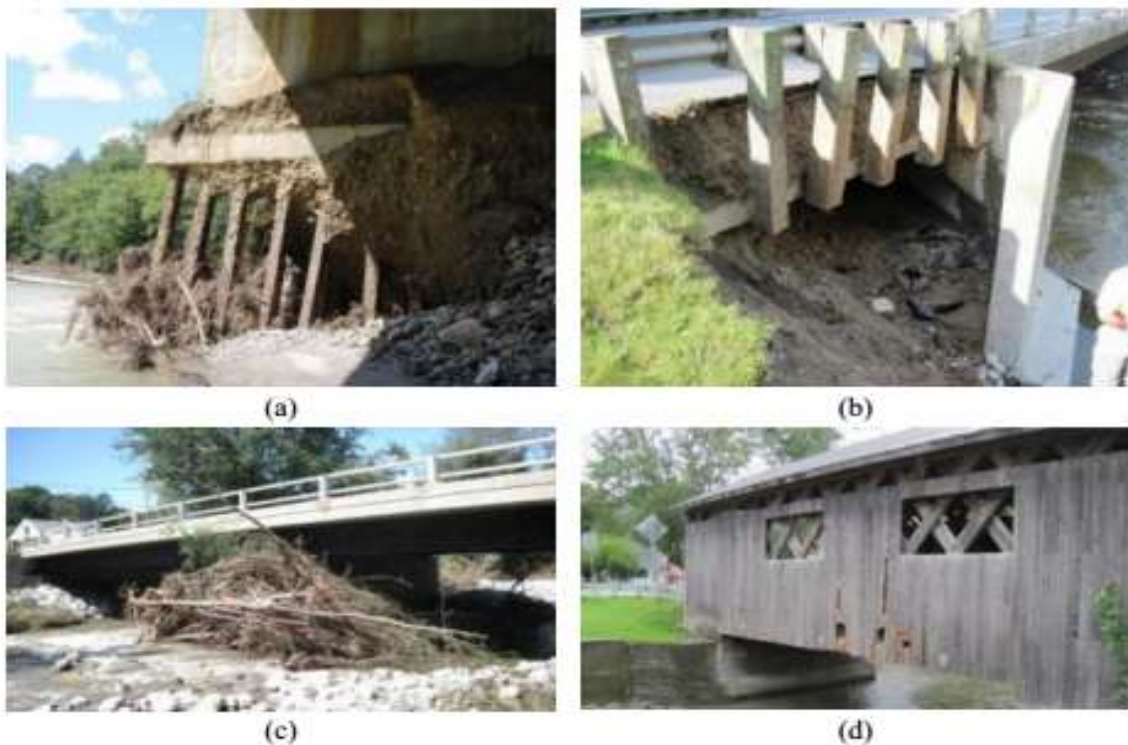


**Figure 3.3. Damage Type (VTrans, 2014) - (a) Scour damage, Dummerston VT30-B9: scour beneath the concrete spread footing, (b) Channel flanking damage, Jamaica VT30-B40: flanking behind the abutment, (c) Debris damage, Wallingford VT140-B10: debris buildup on a pier, reducing the flow area, (d) Superstructure damage, Montgomery C2001-B5: damage to the sideboards of a covered bridge**

Bridges, with their assigned damage level and estimated cost (when available) for repairing the bridge back to its pre-storm condition, are shown in millions of U.S. dollars and U.S. dollars per deck area in Figures 3.5a and b, respectively. The horizontal line and asterisk within each box plot represents the median and mean, respectively; the edges of the box are the 25<sup>th</sup> and 75<sup>th</sup> percentiles, and the whiskers extend to the most extreme data points not considered outliers. Outliers are plotted individually. The estimated cost of repair correlates well with damage levels, and when normalized by deck area, shows an increasing trend with average repair cost. When repair costs per deck area are categorized by damage type, the scour damage has significantly greater cost (Figure 3.5c). When a bridge showed only flanking damage, the associated estimated costs of repair were substantially smaller than those associated with scour damage. The average estimated cost of repair for scour, flanking, and superstructure damage were about \$260,000, \$108,000, and \$18,000 per bridge, or \$318, \$120, and \$30 per square meter of deck area, respectively. The completed construction costs for a select number of state-owned bridges rebuilt or remediated following Tropical Storm Irene (n = 12, all with extensive and complete damage) are plotted in Figure 3.5d. In general, the actual repair costs (per deck area) for state-owned bridges appear to be of similar range to the costs of repairs for town-owned bridges estimated for FEMA funding.

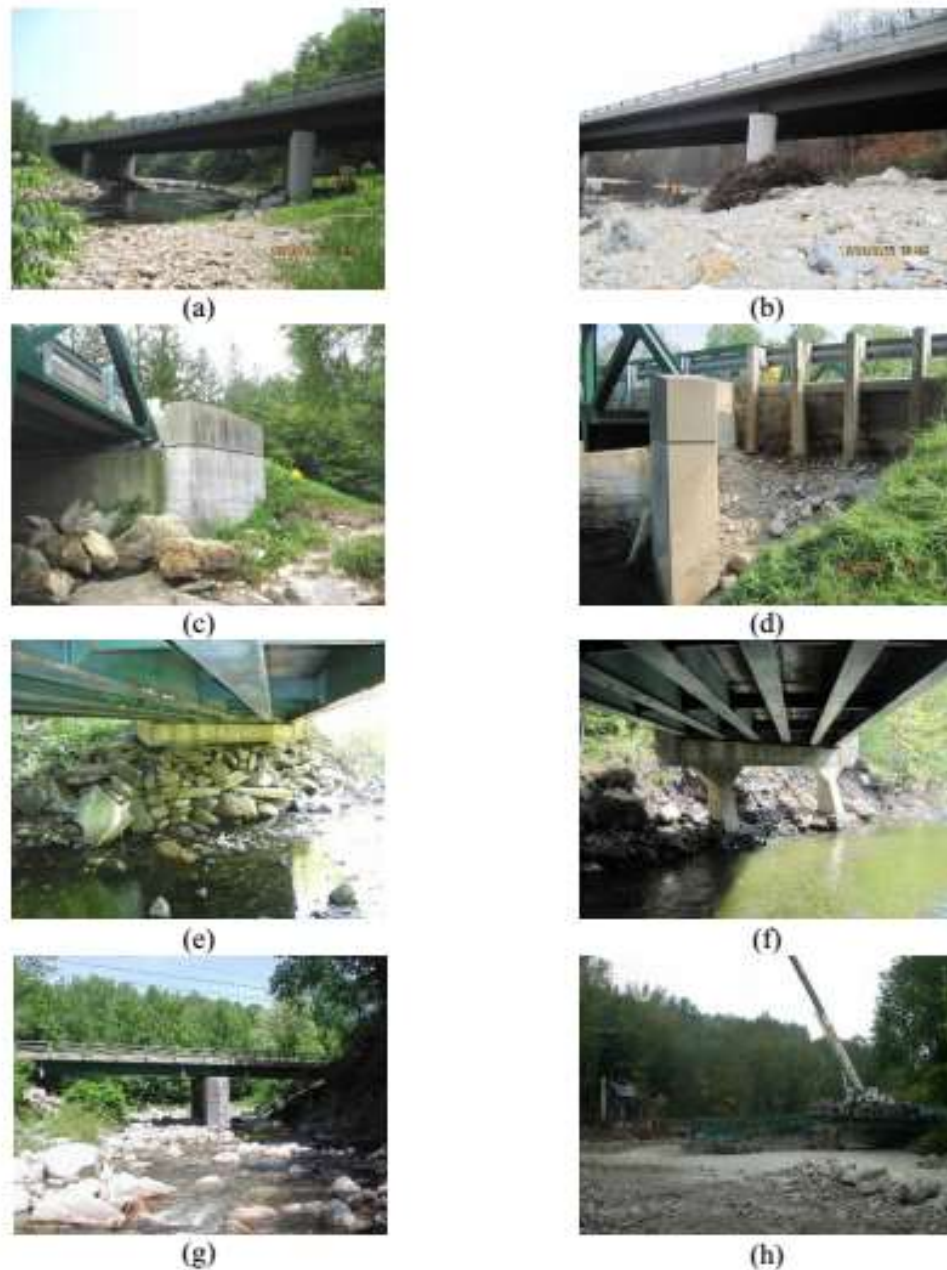


**Figure 3.4. Damage Level (VTrans, 2014) – (a) and (b) Slight Damage, Northfield VT12-B61: conditions before and after the storm, (c) and (d) Moderate Damage, Bridgewater C3005-B37: conditions before and after the storm, (e) and (f) Extensive Damage, Halifax C2001-B17: conditions before and after the storm, (g) and (h) Complete Damage, Rochester VT73-B19: conditions before and after the storm**

### 3.3.2 Rainfall

Figure 3.6 compares the distribution of rainfall and ARI (panels a and b, respectively), for the damaged bridges (n=313) and non-damaged bridges at two different scales – the reach scale (n=274) and watershed scale (n=954). The non-damaged bridges at the reach scale experienced similar storm impacts to the damaged bridges, and were not statistically different ( $p = 0.117$ , for both rainfall and ARI). The non-damaged bridges at the watershed scale however experienced a statistically lower storm impacts ( $p < 0.001$ , for both rainfall and ARI). The watershed scale captured a larger area with greater number of bridges likely bringing the watershed scale mean closer to the global (statewide scale) mean.

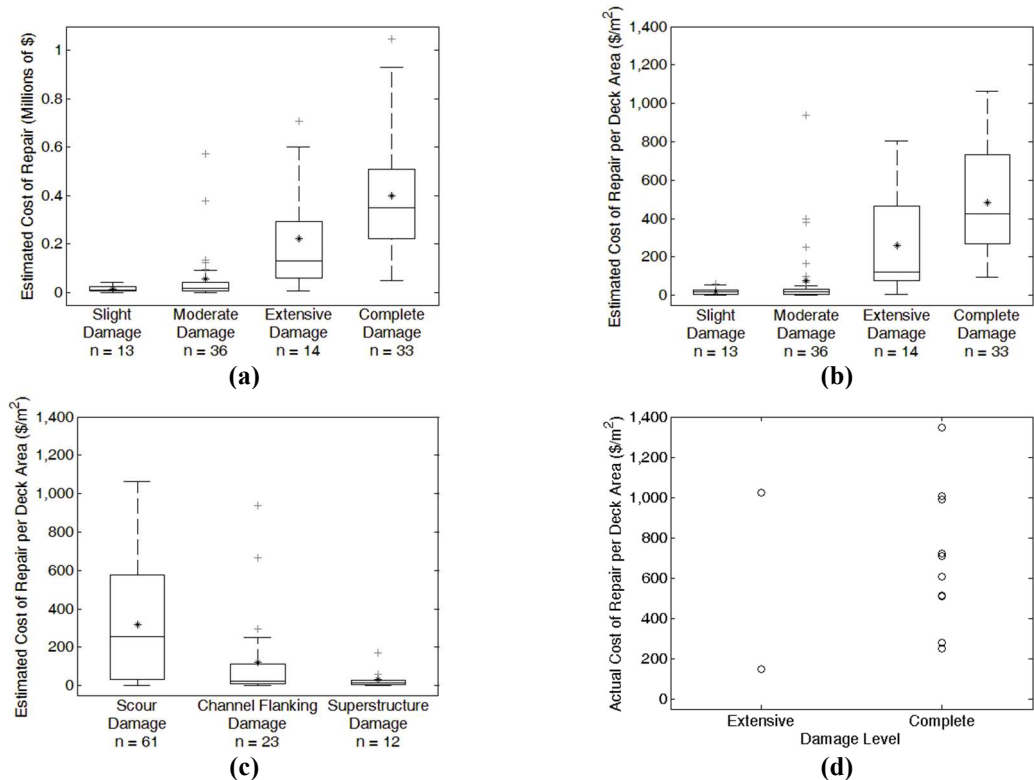


**Figure 3.5. Repair cost and cost per deck area for various levels and type of damage: (a) Estimated cost of repair versus damage level, (b) Estimated cost of repair per deck area versus damage level, (c) Estimated cost of repair per deck area versus damage type, (d) Actual cost of repair per deck area of state-owned bridges (n denotes sample size)**

### 3.3.3 Bridge Characteristics

An analysis of the bridges at the reach scale was performed to help identify features important in predicting bridge damage. The p-values in Table 3.1 indicate the probability that the null hypothesis is correct (with significance against the null set at  $p < 0.05$ ) for a given feature, and show that the span and structure length of damaged bridges to be greater when compared to the non-damaged bridges on the watershed scale. The vertical clearance, the distance from the bottom bridge member to the streambed, is significantly lower for the damaged bridges than the non-damaged reach scale (Figure 3.7a), where storm impacts are thought to be the most similar.

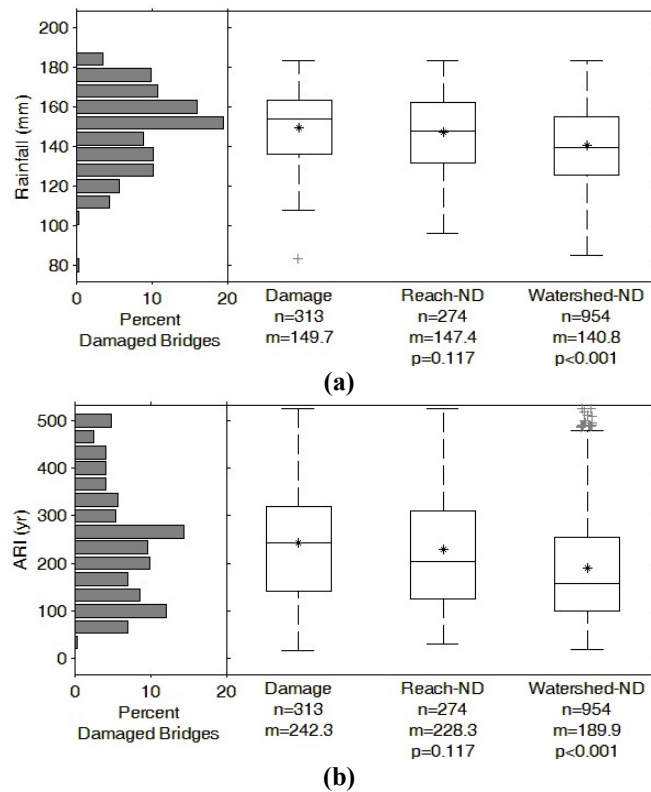


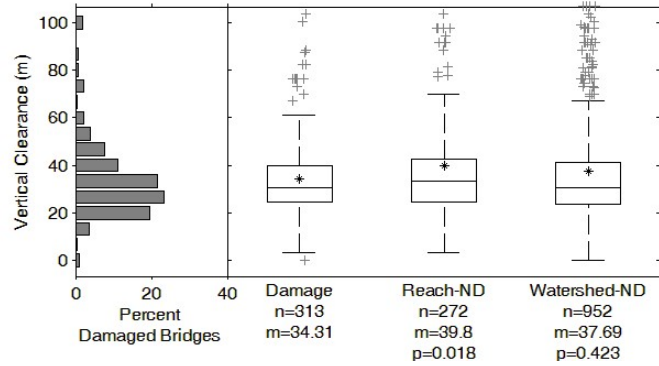
**Figure 3.6. Analysis of the rainfall data – (a) rainfall (mm), (b) ARI (yr) (n denotes sample size, m is the mean, and p is the significance value)**

Bridge geometry variables are important in that they determine the size and orientation of the bridge to the stream. Scour calculations often include bridge geometry in

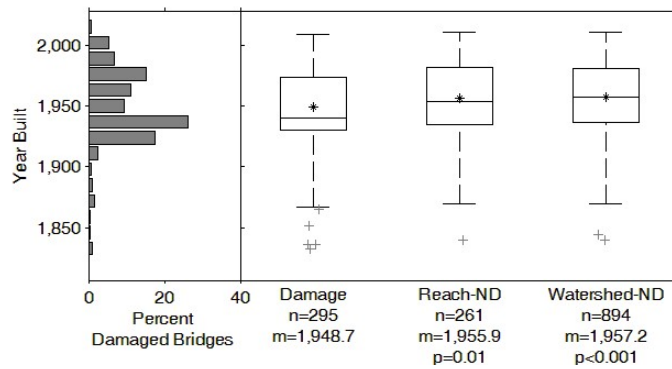
which the span, width, and clearance play direct roles. The span and clearance of the bridge determine the opening area, where a smaller opening would result in contraction. The width of the bridge indicates the length of contraction, or the length of contact with the stream, where longer widths lead to increased velocities in contraction. A hypothesis is that smaller and lower bridges are more likely to be damaged due to the high and intense flows, and are more prone to debris blockage. The data supports this with respect to vertical clearance, but shows that damaged bridges were longer (in span) than the corresponding non-damaged bridges from the same reach. Bridge geometry could play a more important role if combined and compared to stream size. Channel width is needed to determine if the span is undersized, but that data is not available in the NBI. Likewise, knowing the vertical under-clearance for the bridge would be more useful if it included the depth of flow, to determine freeboard. The current measurement only provides the distance from the low chord to the stream bottom.

A comparison of bridge age shows damaged bridges to be older than non-damaged bridges at both scales (Figure 3.7b). The year built, in which new bridges are generally viewed as more robustly designed, meets the expectation that older bridges were more vulnerable to damage. The significance of age in discriminating between damaged and non-damaged bridges may be due in part to the effort put into managing historic bridges. In particular, many covered bridges were more closely inspected and monitored after Tropical Storm Irene. Bridge age may only reflect regional bridge design and construction practices. Hazard return periods may vary from one region to another, yet bridge age may be a good, holistic parameter because it comprises inherent features (e.g., design standards,

storms, construction practices, history of success, major maintenance, etc.) that are not available in existing databases.



(a)



(b)

Figure 3.7. Analysis of bridge characteristic variables – (a) vertical clearance (m), (b) year built (n denotes sample size, m is the mean, and p is the significance value)

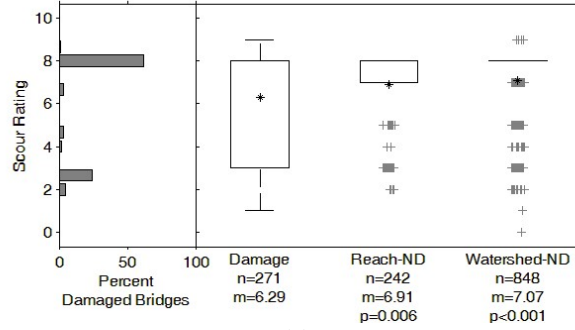
### 3.3.4 Bridge Ratings

The NBI bridge ratings for damaged bridges were significantly lower than those for both reach and watershed scale non-damaged bridges. The lower ratings prior to the storm show that several damaged bridges may have had preexisting issues, whether from structural deterioration, or prior hydrologic issues.

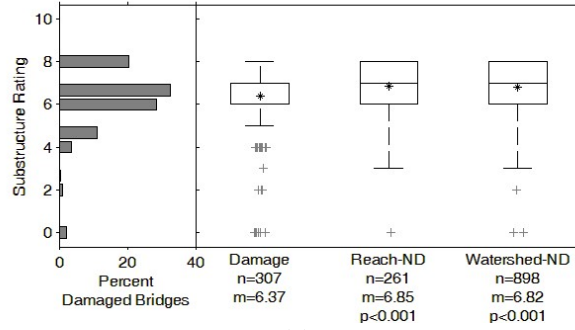
The scour ratings for bridges damaged in Tropical Storm Irene are compared to non-damaged bridges at the reach and watershed scales, both of which are significantly different and higher than the scour ratings of the damaged bridges as seen in Figure 3.8a. Surprisingly, the majority of damaged bridges (over 50%) had non-critical scour ratings prior to Tropical Storm Irene. Included in the bridge database, 42 damaged and 229 non-damaged bridges were listed as unknown foundation in the scour rating field. However, bridges rated as scour critical (rating of 3 or below) do have a larger proportion of bridges with damage compared to non-damaged bridges at the reach and watershed scales, indicating that a low scour rating may show vulnerability to scour, but a high rating does not necessarily show immunity, particularly during extreme flood events.

The substructure rating (Figure 3.8b), which rates the structural components of the bridge on an ordinal scale, shows worse ratings for damaged bridges. The channel rating (Figure 3.8c), which accounts for the condition of the embankments and channel protection, indicates that damaged bridges likely had prior occurrences of erosion. The waterway adequacy (Figure 3.8d) rates the likelihood of overtopping of the bridges. The data show that damaged bridges had an increased vulnerability to overtopping. The structural adequacy rating (Figure 3.9a), which takes a load rating reduction factor of the superstructure or substructure, and the state sufficiency rating (Figure 3.9b), which uses as formulated combination of 21 other available parameters in the BIS, shows the greatest difference between damaged and non-damaged bridges particularly at each end of the rating spectrum.

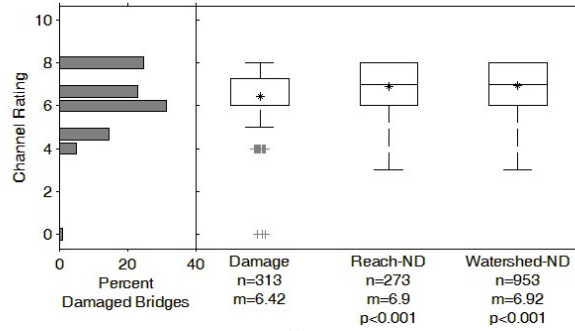




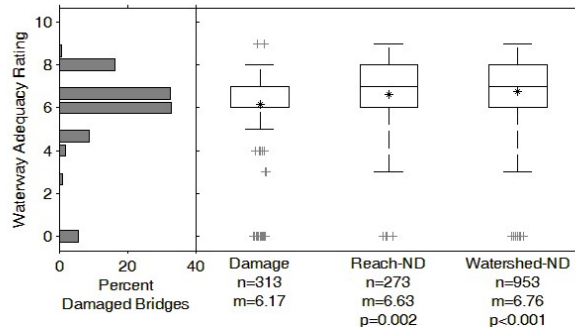
(a)



(b)

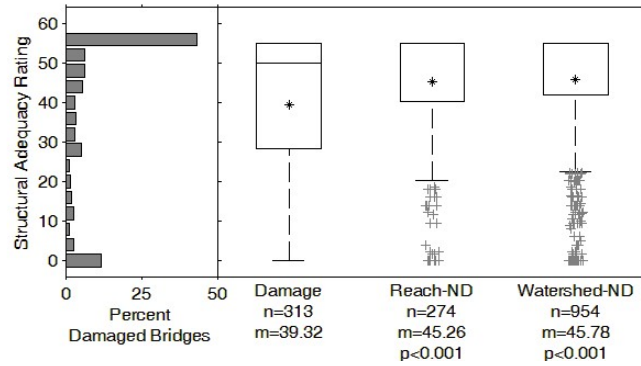


(c)

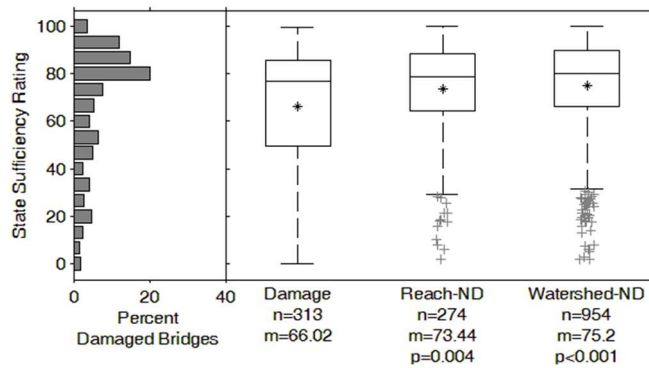


(d)

Figure 3.8. Analysis of bridge ratings – (a) scour rating, (b) substructure rating, (c) channel rating, (d) waterway adequacy rating (n denotes sample size, m is the mean, and p is the significance value)



(a)



(b)

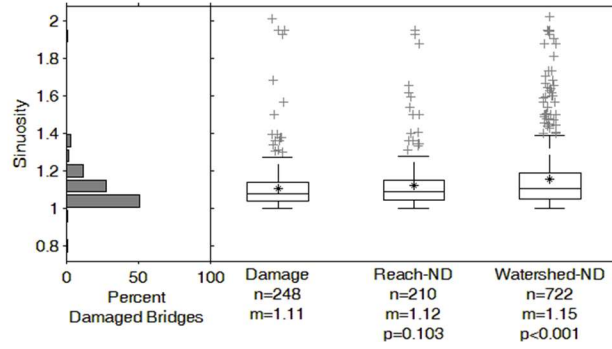
**Figure 3.9. Analysis of bridge ratings – (a) structural adequacy rating, (b) state sufficiency rating (n denotes sample size, m is the mean, and p is the significance value)**

### 3.3.5 Stream Characteristics

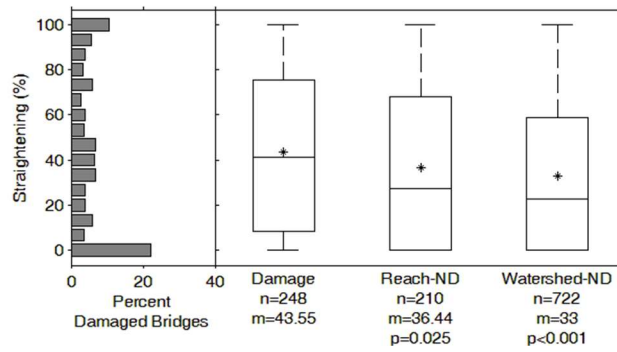
Stream geomorphic assessment information adds information and expert knowledge about the stream geomorphology that was previously missing from the bridge inventory. The geomorphic data, however, only applies at a stream-reach scale, which given the nearest-neighbor selection of non-damaged bridges at the reach scale, often results in the same stream parameters being applied to the pair of nearest neighbors. This lowers the statistical power of the data and the likelihood that the reach-scale non-damaged bridges will differ statistically from the damaged bridges without a larger sample size.

Geomorphic assessments have not been completed across all streams in the state, and so the data was applied only where available. Additionally, a number of geomorphic assessment variables help assess the stream for departure from a reference stream type. Individual reach assessments must take the dominant stream type into account when determining the current condition.

The sinuosity of the stream is significantly lower for damaged bridges than non-damaged bridges at the watershed scale (Figure 3.10a). Additionally, the percentage of straightening was significantly higher for damaged bridges than for both non-damaged bridges at both scales (Figure 3.10b). A stream with low sinuosity and high percentage straightening has fewer degrees of freedom for lateral adjustment, and would result in an increased velocity in a flood event. The width to depth ratio of damaged bridges was significantly lower than non-damaged bridges at the reach and watershed scales (Figure 3.11a). Lower width to depth ratios for a given stream type are indicative of incision and an associated increase in shear stress and stream power. The entrenchment and incision ratios are significantly different for damaged bridges when compared to the watershed scale non-damaged bridges (Figures 3.11b and c). Lower entrenchment ratios represents a disconnection from the floodplain and increased channelization during flood events. Higher incision ratios indicate bed degradation, as incised streams hold greater flood flows before accessing the floodplain.

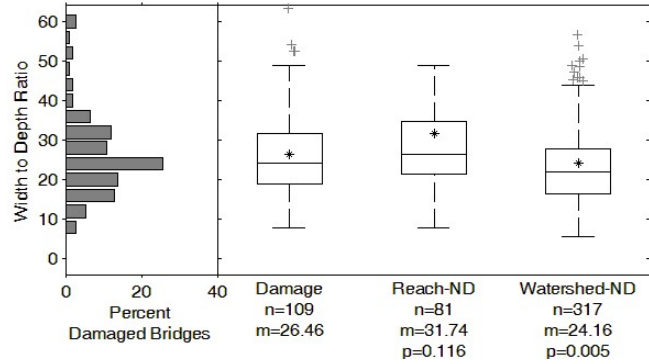


(a)

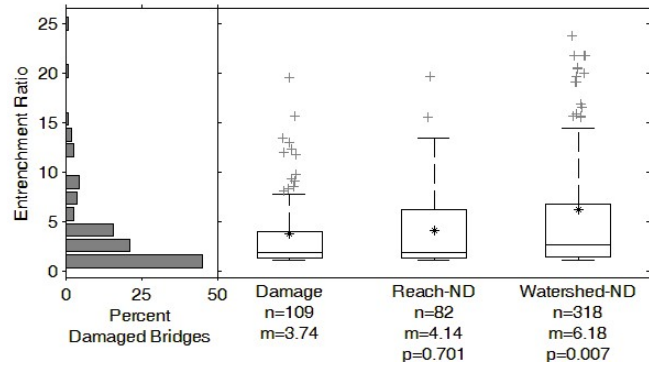


(b)

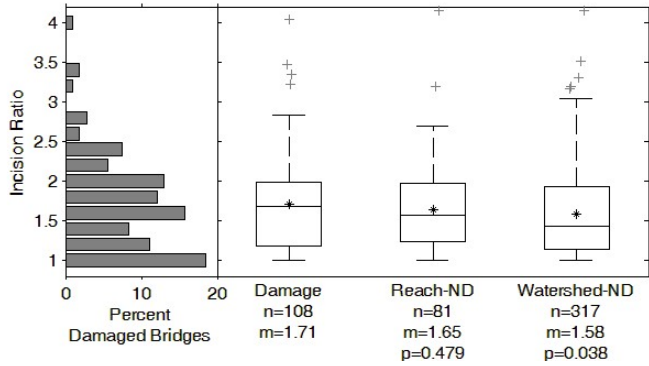
Figure 3.10. Analysis of variables related to stream characteristics - (a) sinuosity, (b) straightening percentage (n denotes sample size, m is the mean, and p is the significance value)



(a)



(b)



(c)

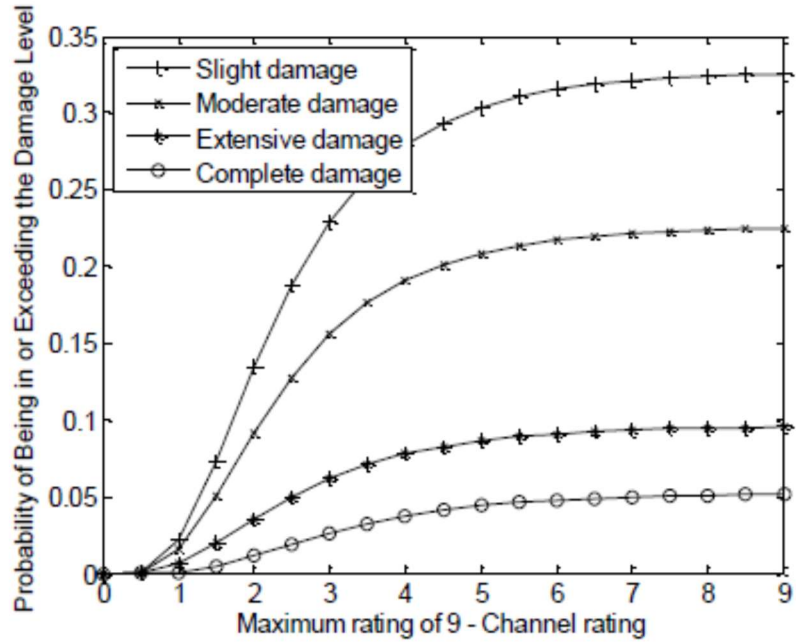
Figure 3.11. Analysis of variables related to stream characteristics ratios - (a) width to depth, (b) entrenchment ratio, (c) incision ratio (n denotes sample size, m is the mean, and p is the significance value)

### 3.3.6 Logistic Regression and Empirical Fragility Estimate

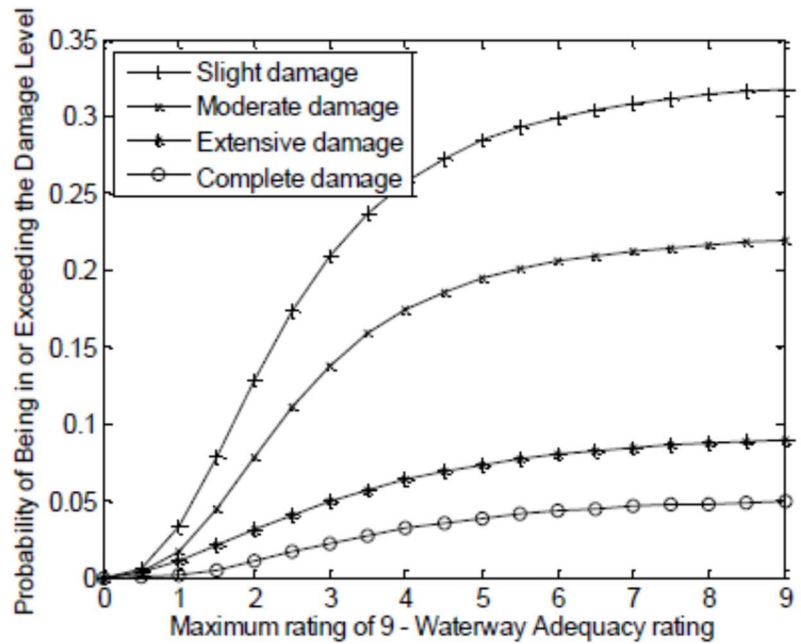
Ordinal logistic regression helped to identify features that discriminate between damage levels at the reach scale. The analysis was conducted on the variables that were identified to be significant in the univariate analysis and were of interest in relating bridge and stream interactions - channel rating and waterway adequacy. The results are consistent with the expectation that a bridge with a lower channel and waterway adequacy rating would be more susceptible to damage, as indicated by their history of channel stability, and flow passage.

Empirical fragility curves were created based on the channel rating and waterway adequacy rating on the watershed scale bridges. For each of these, the ratings are presented as the deduction from the maximum rating of 9. Channel and waterway adequacy ratings were selected because they assess the current bridge and stream interactions. While it would have been advantageous to use the scour rating for this purpose, the values used in the scour rating are not ordinal in nature, but rather are a ranked nominal system, without clear distinctions on the scale. Fragility curves have been applied to empirical bridge damage (Padgett et al., 2012), as well as comprehensively summarized in applications of water resource infrastructure (Schultz et al., 2010). Each damage level is expressed as an individual curve showing the probability of being damaged at or above that level. To create the fragility curves, bridges were separated by damage level, and distributed as a histogram according to the value of each feature. Each distribution is then fit with a lognormal curve. The cumulative distribution function (CDF) of the lognormal fit to each damage level set is estimated at regular intervals to produce the conditional probability curve. The conditional probability is then used to determine the exceedance probability curves, by

combining the probability of greater damage into each of the lower damage levels. The finalized fragility curves express the conditional probability of meeting or exceeding the given damage level, as a function of channel rating (Figure 3.12a) and waterway adequacy rating (Figure 3.12b) for the watershed bridges displayed in Figure 3.1c. The probability of damage is scaled depending on the ratio of damaged to non-damaged bridges in a given study area, with the maximum probability equivalent to the ratio of damage to non-damaged bridges being assessed. Probabilistic models of this sort can be the basis of a risk assessment of bridges under extreme flood events in the future. Stake holders would be able to determine the probability of damage exceeding a certain level for each bridge in their inventory under an extreme event similar to Tropical Storm Irene, to assist in determining the overall risk present in the network. In observing the pair of fragility curves, it appears the probability of damages plateaus beyond a rating of 6 (displayed as  $9 - 6 = 3$ ), and that this could be a worthy point of differentiation for at risk bridges in the future. Bridges with poor ratings (potentially below 6) for both channel and waterway adequacy rating would be good candidates for a hydraulic review, to evaluate their vulnerability in flood events.



(a)



(b)

Figure 3.12. Fragility curve for bridge damage given the (a) channel rating, and (b) waterway adequacy rating. The best possible rating in these two categories is 9; therefore, the ratings are subtracted from 9 to reflect that the probability of damage increases with lower channel or waterway adequacy ratings



### 3.4 Conclusions

The effects of Tropical Storm Irene on Vermont bridges provide a unique, large dataset, where a *single* extreme hurricane-related flood event caused widespread damage to more than 300 bridges across a single state. A total of 326 Vermont bridges were identified as damaged during Tropical Storm Irene, with damage ranging from minor streambank erosion to entire bridge collapse. Of these, 313 bridges with spans greater than 6 m had inspection records available and were considered further. The characteristics of damaged bridges ( $n = 313$ ) were compared statistically to those of non-damaged bridges at the reach scale ( $n = 274$ ) and the watershed scale ( $n = 954$ ).

The collection and georeferencing of hundreds of damaged and non-damaged bridges during a single extreme hurricane-related storm event, in combination with their inspection records and associated stream geomorphic assessments create a unique and significantly useful dataset. To the best of our knowledge such a database is not available in the literature. This database is made available in a spreadsheet format and can be downloaded from: <http://go.uvm.edu/vtbridges-irene-data>.

The damaged bridges included 55% steel beam, 34% concrete slab or beam, and the remaining 11% historical steel or wood truss superstructures. Single span bridges made up the vast majority, 82%, of bridges damaged, with 12% double span, and the few remaining including 3 and 4 span structures.

About 55.6% of the damaged bridges had scour damage, 29.7% had channel flanking, 8.3% had debris damage, and the remaining 6.3% had superstructure damage. When a bridge showed only flanking damage, the associated estimated costs of repair were substantially smaller than those associated with scour damage. The average estimated cost

of repair for scour, flanking, and superstructure damage were about \$260,000, \$108,000, and \$18,000 per bridge, or \$318, \$120, and \$30 per square meter of deck area, respectively.

The bridge rating assessment characteristics were all strongly correlated to damage. Channel rating and waterway adequacy rating had strong discriminating power between bridge damage levels.

The analysis indicated that stream geomorphic data have the potential to be used to supplement and enhance the bridge rating systems, and may aid in identifying hydraulic vulnerability. Ratios such as entrenchment, incision, width to depth and straightening show significance at the watershed scale, and indicate that relative measures of a stream's geomorphic condition (disequilibrium) are more important than specific measurements. Vermont was one of the first states to develop and implement a three-phase geomorphic assessment of streams, nationally recognized as one of the best overall protocols for assessing stream stability (Somerville and Pruitt, 2004). To the best of our knowledge, this is the first study that links hydrologic stream networks with performance of bridges. As geomorphic data becomes more widely available, the framework presented here could be applied elsewhere.

The analysis identified individual features of the bridge and stream that correlate with underlying damage vulnerability, through comparisons at the stream reach and watershed scales, and outlines a framework to leverage these features to aid in the prediction of bridge vulnerability. Logistic regression identified correlations in the key features and levels of bridge damage, as classified through inspection reports and visual observation by the authors. Empirical fragility curves were created to depict the exceedance

probability for a given damage level against the channel and waterway adequacy rating, creating insights that can aid in evaluating bridges vulnerability to extreme events.

## **CHAPTER 4 WATERSHED ASSESSMENT**

### **4.1 Introduction**

This chapter includes details on the computation of various additional parameters that were added to the comprehensive bridge dataset. Several statewide data sources were used to create a hydrologic watershed delineation model of each stream reach. A stream reach is a segment of the stream considered geomorphically consistent, and thus can be assigned a single metric (Kline et al., 2007). VTANR has been analyzing stream reaches in Vermont for the numerous features included in their rapid geomorphic assessments, and this same reach break convention was used in the watershed analysis. Each delineated watershed was then used in a number of applications to both characterize the watershed properties, and compute inputs for the stream power assessment. Four key features were sought through the watershed analysis:

- 1) Tropical Storm Irene (August 2011) rainfall,
- 2) land use characterization,
- 3) soil hydrologic grouping, and
- 4) stream power assessment.

The Tropical Storm Irene rainfall data were included in the comprehensive database, and utilized in the work presented in Chapters 3, 5 and 6. The land cover characterization and soil hydrologic grouping information are a part of the feature selection analysis presented in Chapter 6. The stream power assessment was used in the statistical and feature selection analysis presented in Chapters 5 and 6, respectively. Beyond the features sampled, the watershed analysis can be used to extract values of any data source available with statewide raster coverage.

## 4.2 Watershed delineation

The analysis included watershed delineation for a total of 15,123 stream reaches. Stream reaches were those delineated by VTANR in the RGA process, and supplemented in a few instances with stream order 3 segments from the National Hydrography Dataset. This combined group signifies every stream in Vermont used in the watershed analysis. A watershed delineation defines the boundary ridges of the catchment area to determine the contributing area of drainage to the target point. Any rainfall runoff within a watershed will eventually flow to the outlet point, as illustrated in Figure 4.1. In order to delineate the watershed for each stream reach, an automated ArcGIS script was created. A statewide 10 m hydrologically-corrected digital elevation model (HydroDEM) of Vermont was used as the base elevation raster, and separated into the main HUC8 basins to create manageable processing groups (VCGI, 2006). The HydroDEM was again tested for sinks and peaks, and removed through the fill process of Arc-GIS, to ensure a hydrologically continuous elevation model. For each of the major basins, flow direction and flow accumulation layers were created, as illustrated in Figure 4.2.

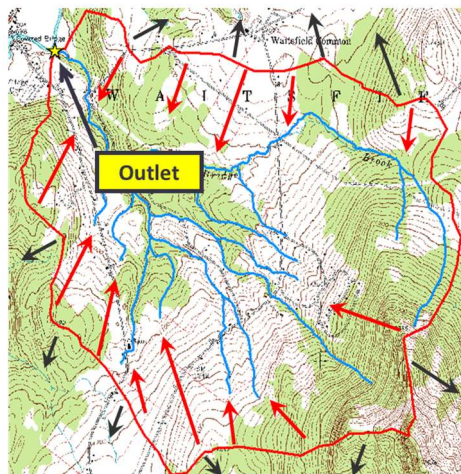
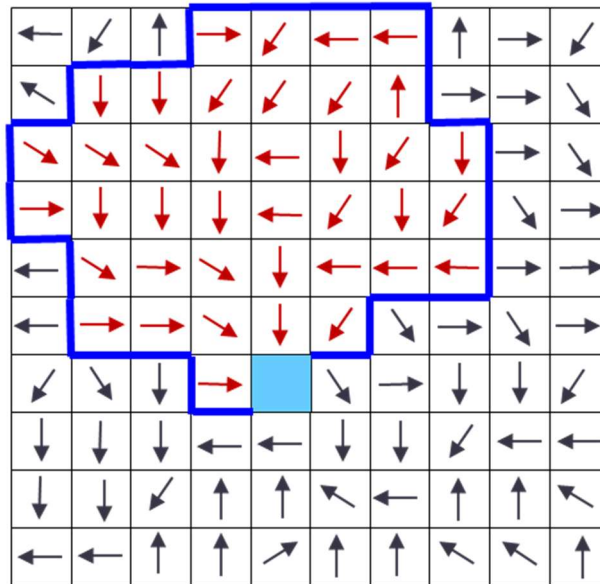


Figure 4.1. Watershed Delineation



**Figure 4.2. Flow Direction**

These raster layers are integral parts of the watershed delineation process, and detail the movement of water from each cell of the grid, creating a quantified flow path and directing the drainage. The down gradient end of each stream reach was used as the outlet pour point for the watershed analysis. For each stream reach, the complete upstream catchment was desired, so an iterative delineation scheme was created to overcome the limitations of the built-in watershed function, which does not allow for overlapping areas, and created adjacent partial watersheds. Each reach within the targeted basin had its watershed delineated, the total drainage area calculated, and saved as a polygon, to be used in further analysis. The collected watersheds were then used to sample various data layers by tabulating the area within each watershed for its percentage of each variable.

### **4.3 Rainfall**

Tropical Storm Irene of August 2011 hit the state of Vermont with severe rainfall and storm winds. Rainfall observations between 100-200 mm of precipitation caused flooding in 225 of 251 towns across the state. Prior to Tropical Storm Irene, only the devastating November 1927 flooding had such widespread damage, and the 2011 flood event remains the greatest natural disaster on record in Vermont (NWS, 2011; State of Vermont, 2012). Due to the path of the storm, the highest rainfall totals were located over the Green Mountains running through the center of the state, with estimates of rainfall recurrence intervals exceeding the 500-year storm in some areas, and 100 years through most of the affected areas. The rainfall resulted in extensive flash flooding, setting peak flow records in nine gauged streams, and reaching the top four for peak flows in nine others (USGS, 2011). Following the storm, the President declared a major disaster, FEMA-4022-DR for the State of Vermont.

The rainfall data used here included climate observations collected during Tropical Storm Irene throughout the state of Vermont and surrounding counties in New York, New Hampshire and Quebec (Springston et al., 2012). These observations were gathered from rain observation stations, and thus could be represented as point data. Using these rainfall observations, ordinary kriging was used to generate a spatial interpolation of the rainfall measurements in Arc-GIS. In addition to the rainfall interpolation map, the average recurrence interval (ARI) was mapped (Figure 3a and b), using a 12-hr duration storm to match the duration of Tropical Storm Irene (Kiah et al., 2013). Using the watershed delineated for each reach, the average rainfall and ARI for each watershed could be tabulated. In addition to the Tropical Storm Irene rainfall predictions, the average annual

expected precipitation was tabulated for each watershed, a parameter needed to determine the regression-based flow approximation (PRISM). Examples of the rainfall extraction can be seen in Figure 4.4a and b.

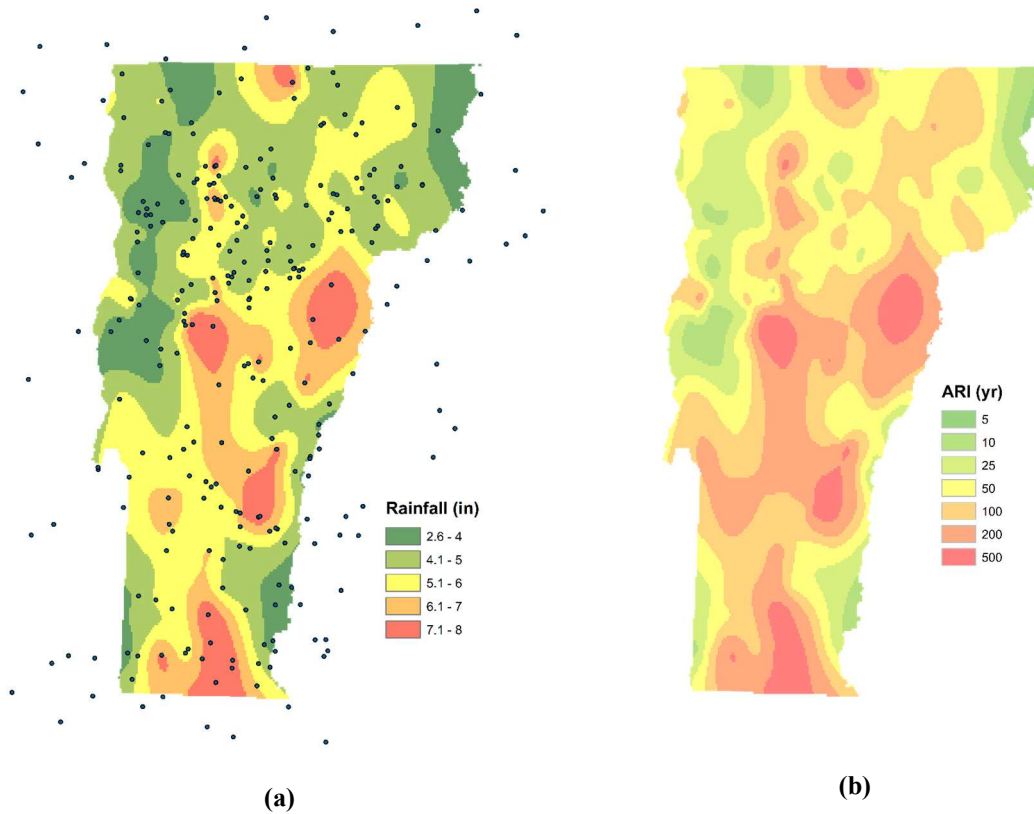


Figure 4.3. (a) Rainfall (in) with observation stations, (b) ARI (yr) interpolations

#### 4.4 Land Cover

Land cover is an important metric in determining watershed characterization and understanding the relationship between rainfall and streamflow. Developed land cover types generally contribute more stormwater runoff directly to surface water bodies, increasing flooding, while natural land cover and wetlands generally work to buffer flooding. Runoff reduction is a useful stormwater management technique to help reduce localized flooding. The National Land Cover Database (NLCD) provided land cover



classifications in 30 m spatial resolution, with 16 different land cover types that were simplified for five major types for this analysis (Homer et al., 2011). The categories used were (1) Developed, (2) Agriculture, (3) Water/Wetland, (4) Forest, and (5) Other. The land cover types were sampled using the delineated watersheds, providing the percentage of total area for each land cover type within the catchment area. An example watershed sampled for land cover type can be seen in Figure 4.4c.

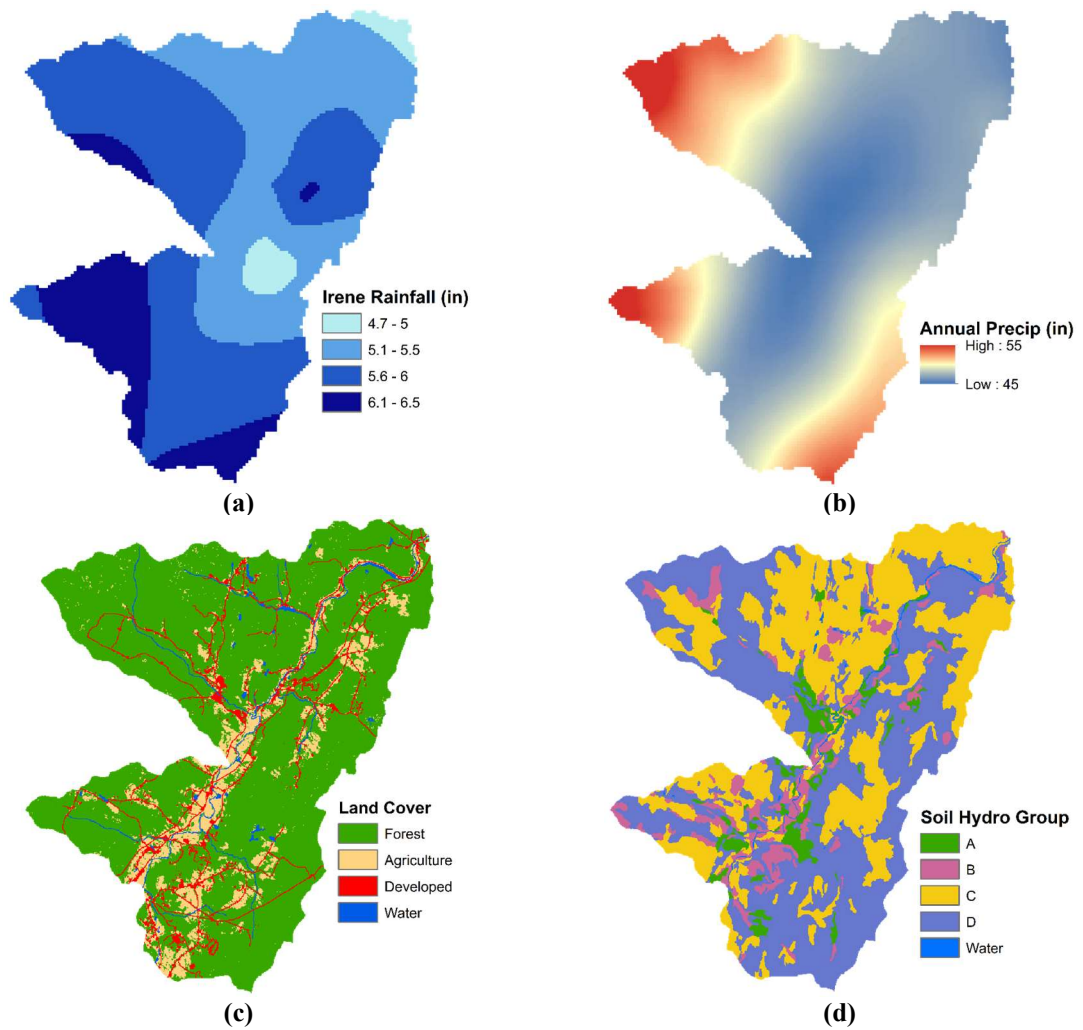


**Figure 4.4. Watershed Sampling: (a) Irene Rainfall, (b) Annual Precipitation, (c) Land Cover, (d) Hydrologic Soil Group**

#### 4.5 Hydrologic Soil Type

The hydrologic soil group (HSG) is a valuable variable in determining the runoff potential, and was established by the US Soil Conservation Service (USCS, 2009). The HSG is determined by the water transmitting soil layer with the lowest saturated hydraulic conductivity, and is categorized into four distinct groups. Group A included soil with low runoff potential, those soils with less than 10% clay and mostly comprised of sands and gravel, with a saturated hydraulic conductivity of greater than 40 micrometers per second ( $40 \times 10^{-6}$  m/s). Group B soils have moderately low runoff potential, between 10- 20% clay, with the remainder comprised of sand and loam, and saturated hydraulic conductivity between 10-40 micrometers per second ( $10-40 \times 10^{-6}$  m/s). Group C soils have moderately high runoff potential, between 20-40% clay, less than 50% sand, and have a saturated hydraulic conductivity of between 1-10 micrometers per second ( $1-10 \times 10^{-6}$  m/s). Group D soils have high runoff potential, over 40% clay, less than 50% sand, and a saturated hydraulic conductivity of less than 1 micrometer per second ( $< 1 \times 10^{-6}$  m/s), or if the water table is within 60 cm of the surface. Dual hydraulic soil groups are used when the soils are present in the full saturated condition, because of the presence of a high water table (within 60 cm), providing the soil classification of the soil if it were adequately drained. For this analysis, dual soil groups were considered group D, as Tropical Storm Irene came under nearly saturated antecedent soil conditions. The HSG was sampled to find the percentages of each soil type for every stream reach watershed, with an example shown in Figure 4.4d.

Soil coverage and land cover types with high runoff potential will contribute greater volumes of stormwater directly to rivers and streams, as less precipitation is infiltrated. Higher runoff potential leads to higher streamflow, increased occurrences of flash flooding,

shorter times to peak flow, and higher stream power than if the delineated area contains soils with lower runoff potential.

#### 4.6 Stream Power Computation

This work used stream power as a measure of the hazard. Stream power is the rate of energy (i.e., power) of flowing water against the bed and banks of a river channel, and functionally controls stream dynamics and morphology. Stream power is calculated as the product of flow, slope and specific weight of water, traditionally represented as watts per meter. The bankfull flow, typically a 2-year recurrence interval, is used for stream power calculations. Since stream power is a measure of stress against the bed and bank, the bankfull flow is seen to be the highest energy dissipation. This is because high flows will spill into the floodplain, thus reducing the total stress in channel.

The calculation of stream power used in this analysis occurs on a broad scale, using widely available data, rather than individual measured observations, to produce comprehensive estimates of stream power. A GIS script was developed to generate the stream power data, which automated the calculation of stream power at any desired point. Total stream power ( $\Omega$ ), also referred to as cross-sectional stream power (Fonstad, 2003) is defined as:

$$\Omega = \gamma \cdot Q \cdot s, \quad (1)$$

where  $\gamma$  is the specific weight of water,  $Q$  is the discharge, and  $s$  is the energy slope. SSP ( $\omega$ ) normalizes the total stream power by the width of the stream to estimate unit-bed-area stream power as:

$$\omega = \gamma \cdot Q \cdot s / b, \quad (2)$$

where  $b$  is the channel width. The script enables the calculation of stream power for any target point (e.g., bridge or endpoint of a stream reach) using commonly available GIS layers. The process follows those in the literature (Jain et al., 2006; Vocal Ferencevic and Ashmore, 2012; Biron et al., 2013), creating a script that leverages existing GIS tools to process the commonly available data into a stream power estimate. Channel width estimates using regression equations (Jaquith and Kline, 2001) were uniformly applied to calculate SSP for all streams.

The discharge values required for stream power were calculated using regional regression equations for flood discharge at various annual exceedance probability thresholds (Olson, 2014). The discharge used was the bankfull flow (estimated as the 2-year recurrence interval). The regression equations required the drainage area, the basin wetland percentage and the annual rainfall average. The wetland percentages and rainfall were found as part of the watershed assessment of land cover (National Land Cover Database, Homer et al., 2011) and rainfall tabulation (Daly et al., 2012). The U.S. Geological Survey (USGS) program StreamStats performs a similar function, though often having trouble with larger computations through its web interface, and thus would be incapable of running the required number of calculations, prompting the creation of a custom script.

With the discharge at each target reach estimated, the slope in this study was determined based on reach breaks established in the RGA. The RGA considers each stream on a reach scale, designated as the length of channel that is considered consistent in slope, valley confinement, sinuosity, and dominant bed material, and distinguishable in some way from the upstream and downstream sections. Streamlines were extracted from the National

Hydrography dataset (USGS, 2013), and the slope was determined by taking the inlet and outlet elevations of the selected reach, and dividing by the shape length (thalweg) to determine the channel slope of the target bridge. With the discharge and slope calculated at each target reach, the total stream power and SSP can be calculated according to equations 1 and 2, respectively. An example of the stream power computation for several reaches in a subwatershed can be seen in Figure 4.5, including (a) the watershed delineation, (b) slope determination, (c) stream power, and (d) specific stream power.

In addition to the conventional stream power, which is uniformly based on a 2-year recurrence interval discharge, an event based stream power was calculated using spatially dependent recurrence intervals based on Tropical Storm Irene rainfall totals, called Irene Stream Power (ISP), and Irene Specific Stream Power (ISSP). ISP and ISSP use the average rainfall ARI of the catchment area to select a scaled flow estimate, in lieu of measured stream flow estimates. The event-based ISSP provides a stream power measure scaled to the storm intensity, estimating the power present in Tropical Storm Irene. The scaled up versions of stream power is thought to represent a total power of water that would pass through the typically contracted bridge openings. During a flood, any floodplain flow is funneled back to the channel in order for flow conveyance to proceed downstream. In these cases, the scaled stream power measure captures the full potential force.

Together, SSP can be used as a measure for identifying the potential high power locations, while the event based ISSP extends upon this analysis, creating a framework of application in identifying high power in an actual storm event.

#### **4.7 Gradients**

The intersection between stream reaches is believed to be a major factor in determining geomorphic change. As each reach is considered a consistent slope, the reach breaks that separate segments are points of change or gradients in slope, and therefore power. To capture this potential change in power, the upstream and downstream changes in slope and stream power were tabulated for each reach, and added to the database of features. When a reach inflow point begins at the junction of two stream outflows (a junction of two reaches becoming one), the higher power reach was selected as the upstream value. A high power reach followed by a lower power reach will create an imbalance in energy, and likely result streambed and streambank instability.

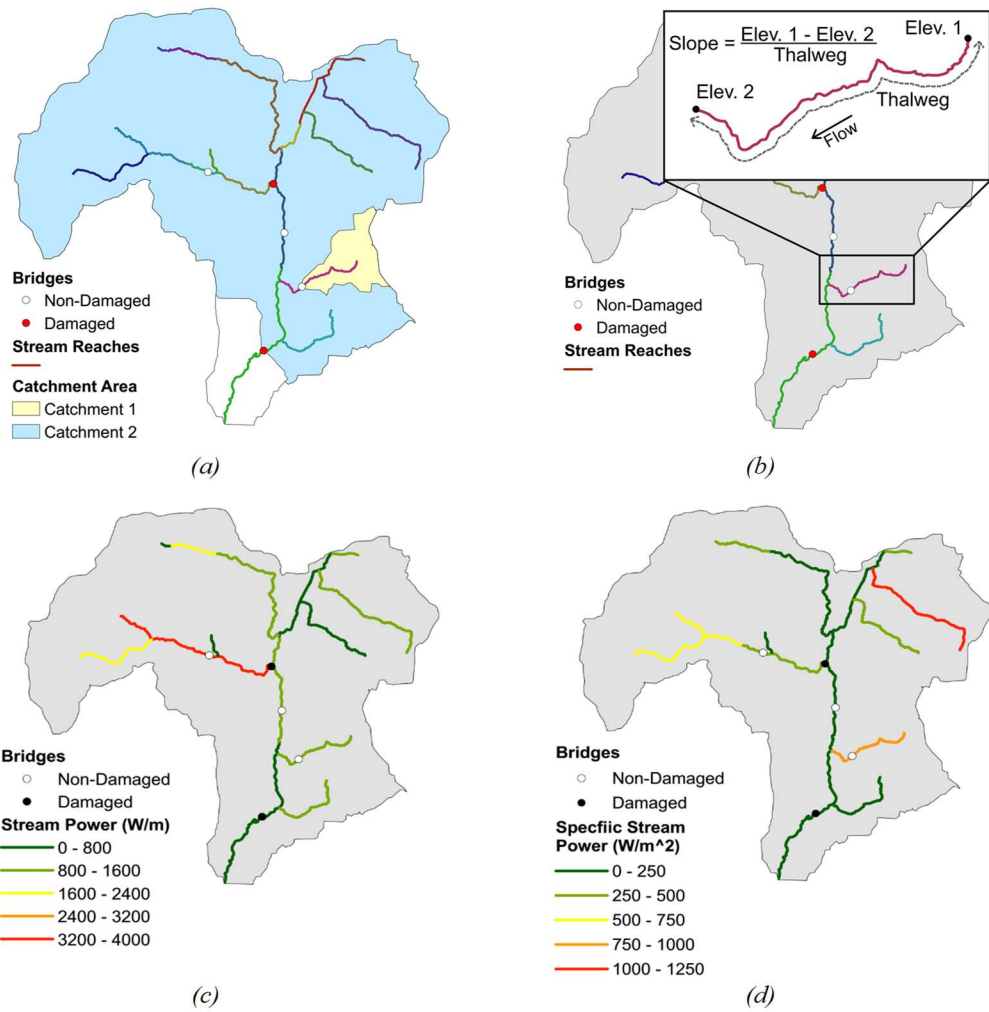


**Figure 4.5. Stream Power determination**

## CHAPTER 5 STREAM POWER APPLICATION FOR BRIDGE DAMAGE PROBABILITY MAPPING BASED ON EMPIRICAL EVIDENCE FROM TROPICAL STORM IRENE

This Chapter was published in the ASCE Journal of Bridge Engineering, 2017

### Synopsis:

On August 28, 2011 Tropical Storm Irene hit the state of Vermont with a severity that deposited 100-200 mm (4-8 inches) of rain across the state and resulted in damage or failure of over 300 bridges. The analysis of available datasets helped identify a set of 313 bridges (greater than 6 m in span) damaged in a single state from a *single* extreme flood event that caused a twelve-hour rainfall recurrence interval that exceeded 500 years in some areas, and 100 years throughout most of the affected areas. Based on available damage reports and photographs, the observed bridge damage was grouped into four levels of severity. This paper links watershed stream power to the observed bridge damage, develops a process to quantify the hazard at bridges both as a case study and for future storms, and uses stream power as a hazard metric to produce probabilistic predictions of bridge vulnerability. The analysis also offers comparisons between damaged bridges and bridges that were not damaged in Tropical Storm Irene. Specific Stream Power (SSP) and the *event-based* Irene Specific Stream Power (ISSP) were computed and found to be both statistically significant at discriminating between damaged and non-damaged bridges, as well as between damage levels. The application of empirical fragility curve analysis for SSP and ISSP produces a probability of damage generated from the results collected from Tropical Storm Irene. Spatially mapping the bridge damage probability from an extreme event like Tropical Storm Irene enables the hazard to be effectively displayed over a broad range of



scales (e.g., stream reaches, select watershed and statewide). This, in turn, helps identify problematic reaches, for which bridge placement would be at increased vulnerability. The methodology presented here can be applied to other geographic settings and storm events of interest, and to the best of the authors' knowledge, this is the first investigation comparing site-specific stream power to observed bridge damage at a system level.

## **5.1 Introduction**

Tropical Storm Irene of August 2011 hit the state of Vermont with a severity that caused major damage throughout the state altering the perception of extreme events and their impacts on Vermont's infrastructure. Dropping between 100-200 mm of rain, and causing flooding in 225 of 251 towns across the state, it follows only the devastating November 1927 flooding as the second greatest natural disaster on record in Vermont (NWS, 2011; State of Vermont, 2012). The highest rainfall totals were located over the Green Mountains running through the center of the state, with estimates of rainfall recurrence intervals exceeding the 500-year storm in some areas, and 100 years through most of the affected areas. The rainfall resulted in extensive flash flooding, setting peak flow records in nine gauged streams, and reaching the top four for peak flows in nine others (USGS, 2011). The flooding and high flows across many of Vermont's rivers and streams caused reports of damage to 389 bridges and hundreds of kilometers of roadway (Thomas et al. 2013). Figure 5.1a displays the location of damaged and non-damaged bridges in the state.

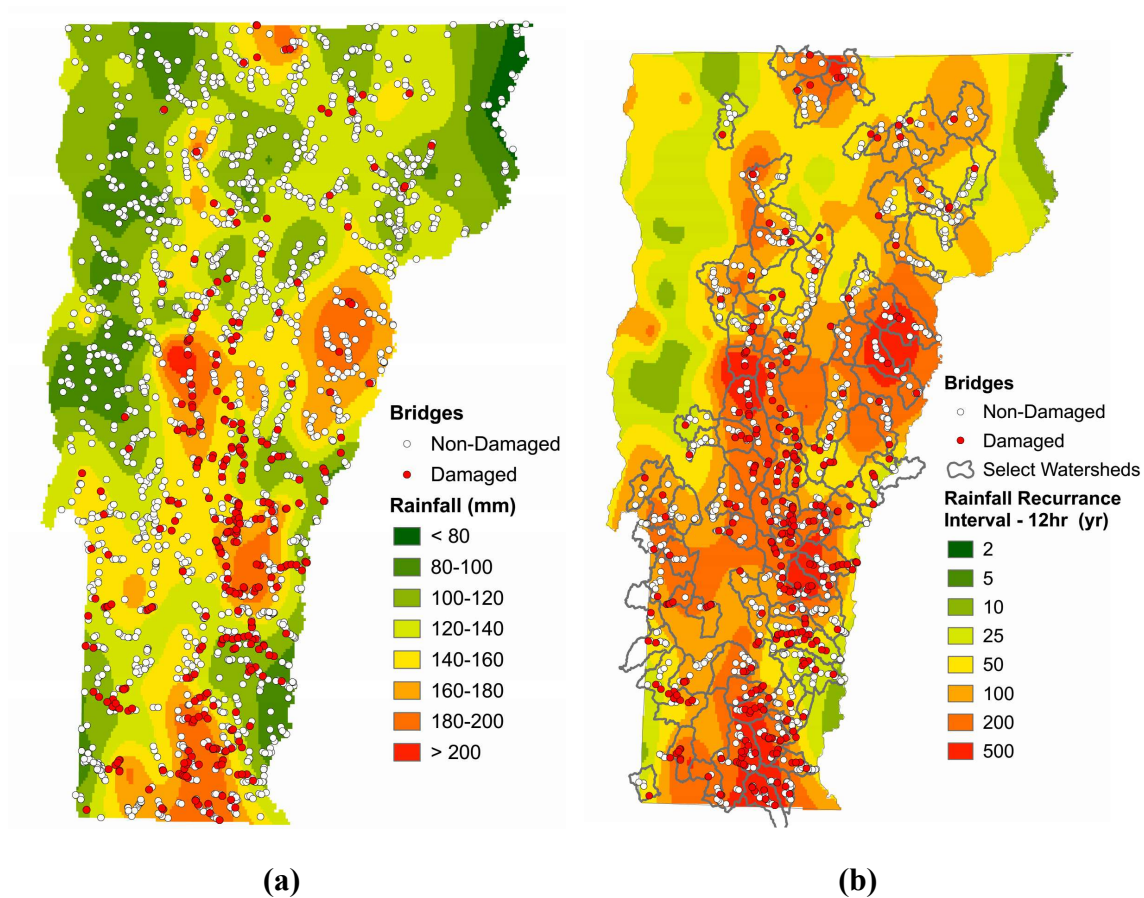


**Figure 5.1. Locations of damaged and non-damaged bridges in Tropical Storm Irene (a) state-wide superimposed on rainfall data, and (b) in watersheds where bridge damage was observed superimposed over recurrence interval estimates**

Other recent extreme events have caused damage to numerous bridges in other parts of the United States and other countries. For example, uplifting and hydrodynamic forces on the superstructure was responsible for the majority of damage to short and medium span bridges from Hurricane Katrina in 2005 (Okeil and Cai, 2008). An economic analysis of 44 bridges damaged during Hurricane Katrina performed by Padgett et al. (2008) shows a relationship between surge elevation, damage levels, and repair costs. Their subsequent analysis of 262 bridges, of which 36 were damaged, identified surge elevation as a key factor in determining damage levels from Katrina and relates it to the estimated likelihood

of damage through empirical fragility curves (Padgett et al., 2012). Both of these studies used the National Bridge Inventory (NBI) as the primary source of bridge data. Similar bridge infrastructure vulnerabilities have been witnessed at Escambia Bay, Florida in 2004 during Hurricane Ivan (Douglass et al., 2004) and in Hokkaido, Japan during the 2004 Songda Typhoon (Okada et al., 2006). Typhoon-induced extreme precipitation caused severe flooding in August 2009 damaging over 130 bridges in Southern Taiwan (Wang et al., 2014). A series of floods in 2010 and 2011 including a flood associated with category 5 cyclone Yasi caused damage to 89 bridges and culverts in Queensland, Australia, and damaged 47 bridges in Lockyer Valley Region of Queensland in a 2013 flood (Lebbe et al., 2014). More recently, severe flooding in September 2013 caused the collapse of 30 highway bridges, and damage to an additional 20 bridges in Colorado (Kim et al., 2014).

The above case history summary of bridge damage, both coastal and inland, illustrates the vulnerability of existing bridge infrastructure to extreme events. The occurrence of such severe events is expected to increase because of climate change altering precipitation intensities in many parts of the world (Melillo et al., 2014). For example, extreme rainfall events, those ranging in the 99<sup>th</sup> percentile of intensity, are happening more frequently, especially over the past three to five decades (e.g., Horton et al., 2014). The effects of Tropical Storm Irene on Vermont bridges therefore provide a uniquely large dataset, where a single hurricane-related extreme flood event caused widespread damage to over 300 bridges in a single state.

In this paper, stream power is evaluated as a measure of the hazard. Stream power is the rate of energy (i.e., power) of flowing water against the bed and banks of a river channel, and functionally controls stream dynamics and morphology. Stream power

estimates from extreme events were shown to correlate positively with the instances of stream widening in the White River watershed of Vermont (Buraas et al., 2014). Also, Gartner et al. (2015) showed that in the Fourmile Canyon of Colorado, the erosion and deposition correlates with increased power gradients and decreased power gradients, respectively. Stream power generally has been shown to correlate positively to fluvial incision (Seidl and Dietrich, 1992; Anderson, 1994), channel size, mobility and pattern changes (Magilligan, 1992; Rosenbloom and Anderson, 1994; Lecce, 1997; Knighton, 1999), and as an estimate of flood power (Brooks and Lawrence, 1999). Specific stream power (SSP) normalizes total stream power, which is the product of discharge, slope, and the specific weight of water, and normalizes it by the stream width (Bagnold, 1966). SSP allows for the expression of stream power at the unit bed area, rather than the cross-sectional area as is the case in total stream power. Magilligan (1992) and Miller (1990) showed that  $300 \text{ W/m}^2$  provides a minimum SSP threshold to separate reaches with and without large-scale geomorphic change. Stream power calculations have been conducted on multiple scales to support analysis of river systems for various objectives including risk to infrastructure, evaluation of channel stability, and assessment of instream habitats. At the finest scale, stream power has been used to conduct bridge scour analysis in erodible rock (Costa and O'Connor, 1995; FHWA 1999), and relates erodibility indices to local stream power measures. Point-location estimates have been prominent (e.g., Fonstad, 2003; Lecce, 1997; and Magilligan, 1992), with studies that sought to identify transitions in stream power along the longitudinal profile and better understand sediment storage dynamics within a basin. Longer reach-length profiles use continuous distributions of stream power to identify stream power functions through a single fluvial system (e.g.

Fonstad, 2003; Reinfeld et al., 2004; and Knighton, 1999). Geographic information systems (GIS), leveraging digital elevation models (DEM), allowed the progression from point- and reach-scale estimates of stream power to network or catchment scale modeling (Finlayson and Montgomery, 2003; Jain et al., 2006; Barker et al., 2008; and Vocal Ferencevic and Ashmore, 2012).

This paper seeks to link watershed stream power to bridge damage from Tropical Storm Irene, create a process to quantify the hazard at bridges both as a case study and for future storms, and use the hazard metric to produce probabilistic predictions of bridge vulnerability. The analysis also offers comparison between damaged bridges and bridges that were not damaged in Tropical Storm Irene. To the best of our knowledge, this is the first investigation comparing site-specific stream power to observed bridge damage at a network level.

## **5.2 Methods**

### **5.2.1 Data Collection**

To study the effects of Tropical Storm Irene on Vermont's bridge infrastructure, a comprehensive database of all available bridge records prior to Tropical Storm Irene was compiled. The collection and assembly of data identified geo-referenced information for all river and stream crossing bridges in the state, including all available inspection data and relevant photographic records. This process encompassed 4,761 state- and town-owned bridges from the Vermont Agency of Transportation (VTrans) Bridge Inventory System (BIS).

Bridge damage information from Tropical Storm Irene was sparsely recorded, and not available in a singular registry. In order to study the effects of the statewide flooding

and storm damage, a comprehensive index of bridges with associated damage was needed. Bridge damage information from the Vermont Agency of Transportation (VTrans) and the Vermont Department of Emergency Management (VDEM) was spatially joined to the VTrans Bridge Inventory System (BIS). Errors in spatial reference limiting the combination of data was corrected by matching identifying features within the databases. The BIS is a statewide database of bridge inspection records in accordance with the National Bridge Inventory (NBI) coding guide, containing all bridges, both state and town owned, with spans over 6 m. The VTrans damage records included State owned bridges damaged in Tropical Storm Irene, while the VDEM list contained town owned bridges and culverts being submitted to Federal Emergency Management Agency (FEMA) for repair funding. These lists were combined to generate a list of 153 damaged bridges. An additional 173 damaged bridges were identified through review of the VTrans online bridge inspection photograph archives, mainly drawing from post-storm inspection photographs conducted throughout the state. This process identified a total of 326 damaged bridges, which differs from 389 damaged bridges reported by the VDEM (Thomas et al. 2012). The discrepancy is thought to result from the classification of certain culverts as bridges in the higher estimate, as well as rapid and unrecorded post storm bridge repair. Bridges with spans shorter than 6 m were removed from our list of 326 damaged bridges, as they are not present in the BIS. The resulting 313 damaged bridges are included in the subsequent system-wide analysis, and all references to damaged bridges in the sequel refers to the 313. Figure 5.1a displays the location of damaged and non-damaged bridges in the state.

The stream power computations (Section 4.6) leverage a database of stream metrics developed from Rapid Geomorphic Assessments (RGA) under protocols published by the Vermont Agency of Natural Resources (VTANR). The River Management Program of VTANR has been quantitatively assessing the hydraulic stability and sensitivity of over 3,200 km of Vermont streams for the past 15 years, which feeds into the RGA database (Kline et al., 2007; Kline and Cahoon, 2010). The VTANR RGA protocols are nationally recognized and provide a measure of stream disequilibrium and stream sensitivity to indicate the likelihood of a stream responding via lateral and/or vertical adjustment to natural and/or human watershed disturbances (Somerville and Pruitt, 2004; Besaw et al., 2009). The assessments are conducted on a reach scale, designated as the length of channel considered to be consistent in slope, valley confinement, sinuosity, dominant bed material, and distinguishable from the upstream and downstream river sections in terms of average values of these channel metrics. The RGA protocols are categorized into three phases: In Phase I, stream reaches, and the subwatersheds draining to them, are delineated in ArcGIS with reference to existing topographic, photographic, and geologic information. Phase I also compiles soil and land cover characteristics, and local historical knowledge of channel and watershed modifications; Phase II comprises field survey results, and stream stability metrics performed at the reach scale; and Phase III is an in-depth assessment on a sub-reach scale, including a detailed field survey and quantitative measurements of channel dimension, pattern, profile, and sediments, used when a specific concern is identified, needing greater detail than the Phase II. In addition to providing an overall RGA (stream reach disequilibrium) score, all information collected during the RGA protocols is available in Arc-GIS, including geometry of the valley and channel reach, watershed and

floodplain characteristics, and classification of streambed materials. The stream power analysis of this study used the stream reach delineations for Vermont waters developed in RGA Phase I. All of the abovementioned data are georeferenced and available as a single file at: <http://www.uvm.edu/~mdewoolk/?Page=ResearchData.html>.

### **5.2.2 Bridge Damage Classification**

Damage to the 313 bridges affected in Tropical Storm Irene was categorized based on photographic documentation and descriptions in available reports. In cases where photographs were absent, available descriptions were used for categorizing damage into four levels: slight, moderate, extensive and complete. This damage ranking system was based on that proposed in HAZUS (Scawthorn, 2006), and later amended by Padgett et al. (2008). The ranking system descriptions were expanded to include the damage types observed in Tropical Storm Irene, particularly damage from flooded river flows as follows:

- Slight damage includes channel erosion not affecting the bridge foundation, superstructure and guardrail damage, and debris accumulation without scour present. Example bridges with slight damage is shown before and after the storm in Figures 4.2a and b, respectfully.
- Moderate damage includes scour affecting the foundation but not to a critical state, bank and approach erosion, superstructure damage but not to a critical state, and heavy channel aggradation. Example bridges with moderate damage is shown in Figures 4.2c and d.
- Extensive damage includes critical scour, with some settlement to a single foundation, but not collapse, full flanking of both approaches, and damage to the superstructure making it structurally unsafe. Example bridges with extensive damage is shown in Figures 4.2e and f.



- Complete damage includes cases where the bridge was washed away, collapsed or has significant foundation damage requiring replacement. Example bridges with complete damage is shown in Figures 4.2g and h.

Characterization of the damage level was performed independent of any knowledge of the repair costs. Of the 313 damaged bridges, 30% were categorized as having slight damage, 39% as moderate damage, 14.5% as extensive damage, and 16.5% as complete damage. Estimated repair costs were only known for 16, 35, 14 and 34 bridges with slight, moderate, extensive and complete damage, respectively. The mean estimated repair costs for these bridges were about \$46, 35, 194, and 570 per square meter of deck area.



(a)



(b)



(c)



(d)



(e)



(f)



(g)



(h)

**Figure 5.2. Bridge damage Level (VTrans, 2014) before (left panel) and after (right panels) the storm - (a) and (b) Slight Damage, Wallingford VT140-B10, (c) and (d) Moderate Damage, Bridgewater C3005-B37, (e) and (f) Extensive Damage, Cavendish C3045-B35, (g) and (h) Major Damage, Rochester VT73-B19.**

### 5.2.3 Stream Power Computation

The calculation of stream power used in this analysis occurs on a broad scale, using widely available data, rather than individual measured observations, to produce comprehensive estimates of stream power. A GIS script was developed to generate the stream power data, which automated the calculation of stream power at any desired point. Total stream power ( $\Omega$ ), also referred to as cross-sectional stream power (Fonstad, 2003) is defined as:

$$\Omega = \gamma \cdot Q \cdot s, \quad (4.1)$$

where  $\gamma$  is the specific weight of water,  $Q$  is the discharge, and  $s$  is the energy slope. SSP ( $\omega$ ) normalizes the total stream power by the width of the stream to estimate unit-bed-area stream power as:

$$\omega = \gamma \cdot Q \cdot s / b, \quad (4.2)$$

where  $b$  is the channel width. The script enables the calculation of stream power for any target point (e.g., bridge or endpoint of a stream reach) using commonly available GIS layers. The process follows those in the literature (Jain et al., 2006; Vocal Ferencevic and Ashmore, 2012; Biron et al., 2013), creating a script that leverages existing GIS tools to process the commonly available data into a stream power estimate. Channel width estimates using regression equations (Jaquith and Kline, 2001) were uniformly applied to calculate SSP for all streams.

The discharge values required for stream power were calculated using regional regression equations for flood discharge at various annual exceedance probability thresholds (Olson, 2014). The discharge used was the bankfull flow (estimated as the 2-year recurrence interval). The regression equations required the drainage area, the basin

wetland percentage and the annual rainfall average. The upstream catchment area for each individual target point was determined using both flow accumulation and direction calculations from a 1/3 arc second hydrologically-corrected DEMs of Vermont (VCGI, 2006). The wetland percentages (Homer et al., 2011) and annual rainfall totals (Daly et al., 2012) were averaged using the target point's upstream catchment area. An example illustrating the catchment area for individual bridges is provided in Figure 5.3a.

With the discharge at each target point estimated, the slope in this study was determined based on reach breaks established in the Phase I RGA database. The RGA considers each stream on a reach scale, designated as the length of channel that is considered consistent in slope, valley confinement, sinuosity, and dominant bed material, and distinguishable in some way from the upstream and downstream sections. The target slope for each bridge was selected as the slope associated with the underlying stream reach. Streamlines were extracted from the National Hydrography dataset (USGS, 2013), and the slope was determined by taking the inlet and outlet elevations of the selected reach, and dividing by the shape length (thalweg) to determine the channel slope of the target bridge. Figure 5.3b shows the determination of the slope using the reach delineations, for the same subwatershed shown in Figure 5.3a.

With the discharge and slope calculated at each target bridge and associated reach, the total stream power and SSP can be calculated according to equations 5.1 and 5.2, respectively. Total stream power and SSP for the same subwatershed are presented in Figure 5.3c and d.

In addition to the conventional SSP, which is uniformly based on a 2 yr recurrence interval discharge, an event based stream power was calculated using spatially dependent

recurrence intervals based on Tropical Storm Irene rainfall totals, called Irene Specific Stream Power (ISSP). Precipitation observed during Tropical Storm Irene throughout the state of Vermont and surrounding counties in New York and New Hampshire were used to estimate rainfall over the entire state (Springston et al., 2012). These spatial estimates were used to calculate the average recurrence interval (ARI), using a 12-hr duration storm to match the duration of Tropical Storm Irene (Kiah et al., 2013). Figure 5.1b shows the rainfall annual recurrence interval with spatially referenced damaged and non-damaged bridges on the affected sub-watersheds. Following SSP in the use of regression equations to estimate discharge, ISSP is a scaled version of SSP. ISSP uses the average rainfall ARI of the catchment area to select a scaled flow estimate, in lieu of measured stream flow estimates. The event-based ISSP provides a stream power measure scaled to the storm intensity, estimating the power present in Tropical Storm Irene. Together, SSP can be used as a measure for identifying the potential high power locations, while the event based ISSP extends upon this analysis, creating a framework of application in identifying high power in an actual storm event.

## **5.3 Results and Discussion**

### **5.3.1 Damage Distribution**

A Kruskal-Wallis one-way analysis of variance was used to compare the effectiveness of using stream power as a discriminatory feature for damaged bridges. This non-parametric equivalent of the traditional one-way ANOVA test can accommodate the observed non-Gaussian distributions of some feature residuals that limit the application of a traditional ANOVA (Kruskal and Wallis, 1952; Siegel, 1956). The set of non-damaged bridges was selected from bridges that were geographically within the subwatersheds with

damaged bridges, as seen in Figure 5.1b, creating a dataset of 313 damaged and 951 non-damaged bridges. This geographically-based selection ensures bridges are drawn from spatially-related regions, in which Tropical Storm Irene had notable impacts. A small p-value ( $p < 0.05$ ) indicates significance of the associated feature between the two observed groups used for this analysis. Both SSP (Figure 5.4) and ISSP (Figure 5.5) were significant ( $p < 0.001$ ) when testing between damaged and non-damaged bridges. Each set of figures displays the distribution of the damaged and non-damaged bridges, as well a box plot illustrating the differences between the two. The horizontal line within each box plot represents the median, the edges of the box are the 25<sup>th</sup> and 75<sup>th</sup> percentiles, and the whiskers extend to the most extreme data points not considered outliers, set at beyond 2.7 standard deviations. Outliers are plotted individually, and the asterisks indicate the mean. High values of both SSP and ISSP are correlated with bridge damage, and are a useful parameter to evaluate vulnerability of bridge damage.

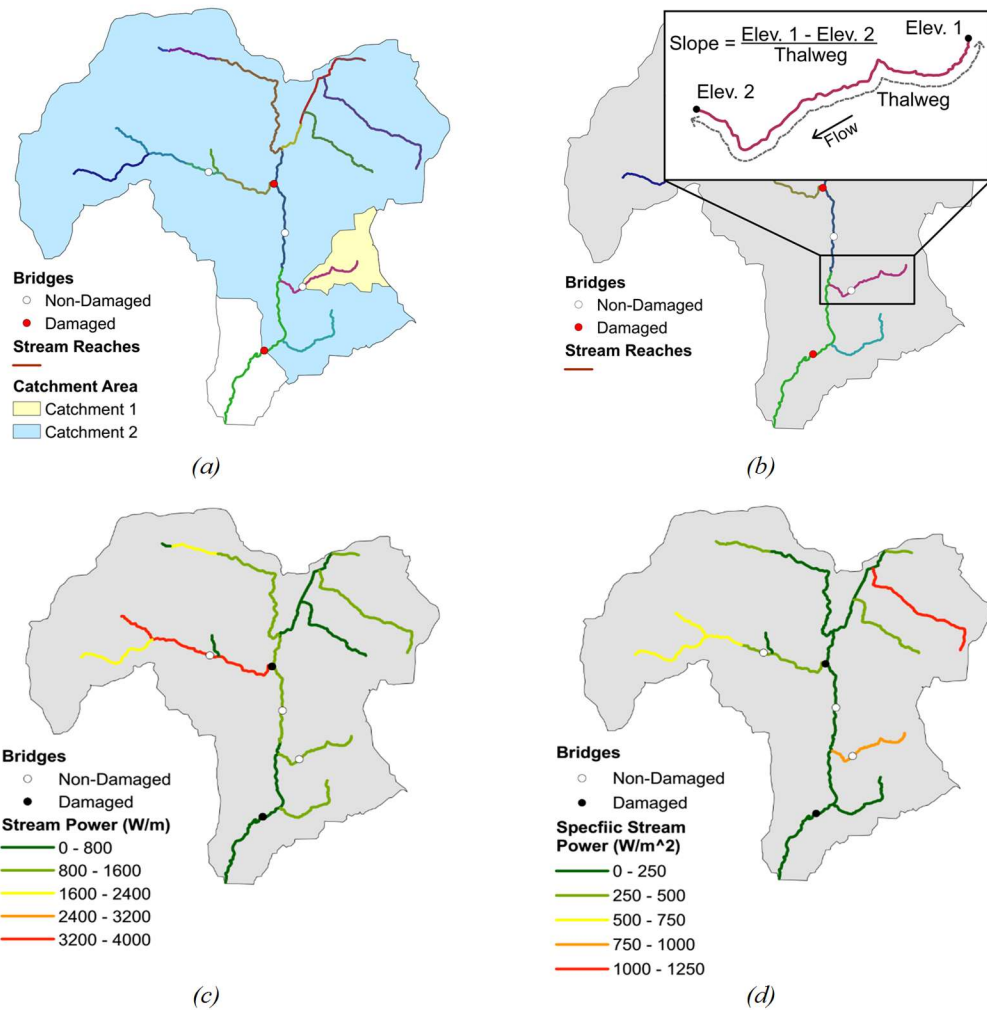


**Figure 5.3. Stream power calculation: (a) catchment delineation, (b) slope calculation, (c) stream power, (d) specific stream power**

Having determined that both SSP and ISSP are significantly correlated to bridge damage, SSP and ISSP were tested to classify between damage levels using a multivariate logistic regression. Both SSP and ISSP again were significant ( $p < 0.001$ ), this time for distinguishing between the four damage levels used, slight, moderate, extensive and complete. High values for SSP and ISSP were related to increased levels of damage in the bridges affected by Tropical Storm Irene. Since both features were found to be significant

at discriminating between damaged and non-damaged bridges, and between bridge damage levels, both may be good metrics for further probabilistic analysis.

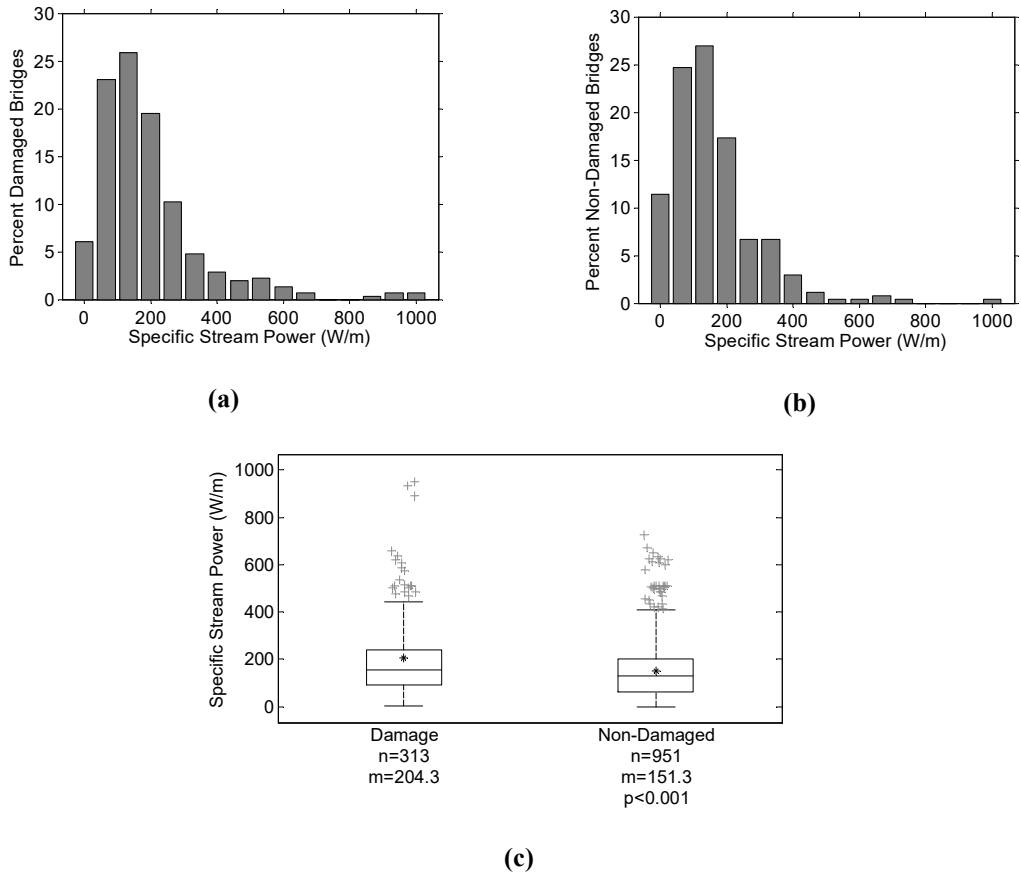


**Figure 5.4. Histogram distributions of SSP for (a) Damaged and (b) Non-Damaged bridges, and (c) Kruskal-Wallis (non-parametric) One-way Analysis of Variance on SSP**



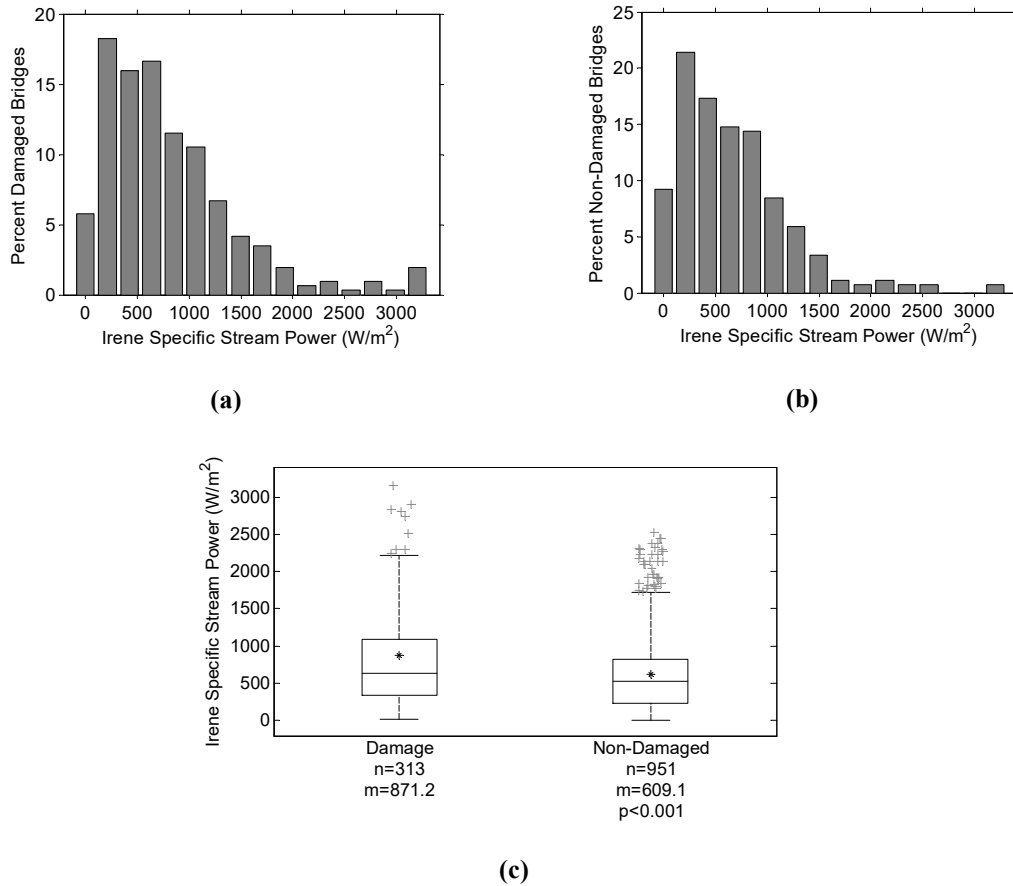


**Figure 5.5. Histogram distributions of ISSP for (a) Damaged and (b) Non-Damaged bridges, and (c) Kruskal-Wallis (non-parametric) One-way Analysis of Variance on ISSP.**

### 5.3.2 Empirical Fragility Curves

Given their significance in discriminating bridge damage, both SSP and ISSP were used to create empirical fragility curves from Tropical Storm Irene. Fragility curves have been applied to empirical bridge damage (Padgett et al., 2012), as well as comprehensively summarized in applications of water resource infrastructure (Schultz et al., 2010). Fragility curves in this study express the conditional probability of exceeding a given damage state, over the possible spectrum of steam power values. Each curve represents an individual damage level, and the probability of being damaged at or above that level. To create the

fragility curves, bridges were separated by damage level, and plotted as a histogram according to the value of the selected feature. Each set of damaged bridges is then fit with a lognormal distribution. The cumulative distribution function (CDF) of the lognormal fit to each damage level set is sampled at regular intervals to produce the conditional probability curve. The curves are then used to determine the exceedance probability curves, by combining the probability of greater damage into each of the lower damage states. The finalized fragility curves show the conditional probability of meeting or exceeding the given damage state, as a function of SSP and ISSP (Figure 5.6a and b) for the watershed bridges displayed in Figure 5.1b. The probability of damage is scaled depending on the ratio of damaged to non-damaged bridges in a given study area, with the maximum probability equivalent to the ratio of damage to non-damaged bridges being assessed. The SSP fragility curve provides a tool for determining the current hazard present at a bridge and comparing them between bridges, as a uniform flow recurrence interval was used. The ISSP curves can be used to determine the true bridge vulnerability from Tropical Storm Irene and is useful in identifying bridges with similar exposure to allow for between-bridge comparisons of structural elements or other environmental factors that may have contributed to damage. The process outlined to create SSP and ISSP can serve as a framework for predicting probability of bridge damage using any user-specified storm event.

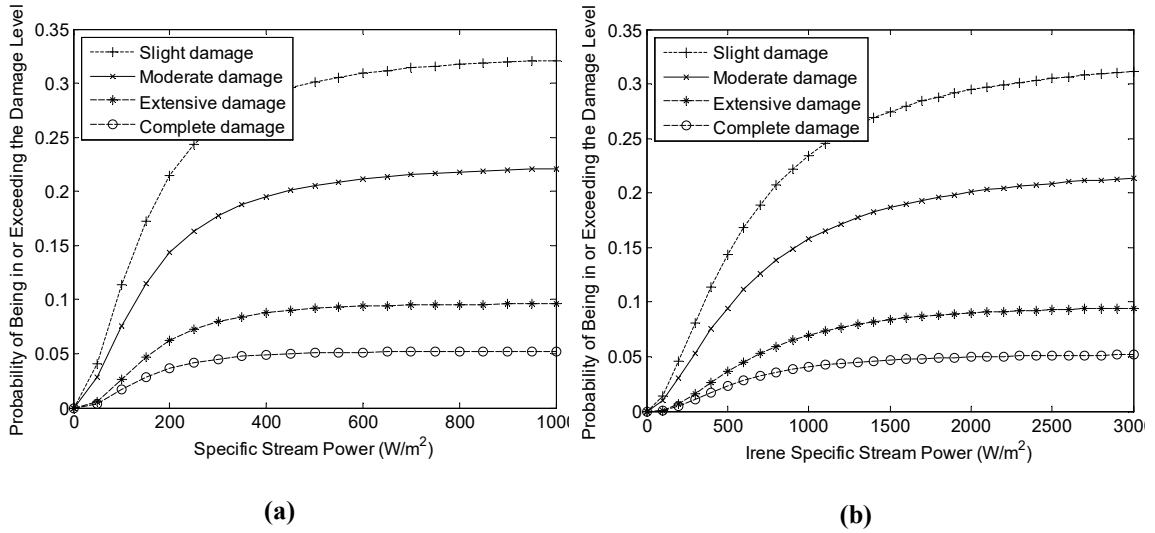


**Figure 5.6. Fragility curves of the conditional exceedance probability generated from (a) SSP and (b) ISSP for each of four bridge damage classifications**

### 5.3.3 Probability Mapping

To extend the usefulness of the SSP and ISSP fragility curve analysis, the resulting conditional exceedance probabilities may be mapped to an area, and displayed on a stream-reach network. Using the GIS script created to generate SSP and ISSP measures at bridges and applying it to all 15,261 stream reaches used in this study, a statewide map of SSP and ISSP was created. The stream power measures are used to generate conditional probabilities of damage by interpolation from the SSP and ISSP fragility curves, and scaled to represent the number of damaged to non-damaged bridges in the targeted area. The statewide probability map of ISSP (Figure 5.7), shows the overall probability of damage from Tropical Storm Irene, and shows the effects of geographic watershed differences and identifies locations of stream power differences throughout the state on a consistent measure. The maximum probability of damage in Figure 5.7 is 9.5% corresponding to 215 damaged bridges as having moderate (or greater) damage out of a total of 2,249 bridges. A

closer look at Figure 5.7 facilitates comparison of the probabilities of bridge damage between individual watersheds.

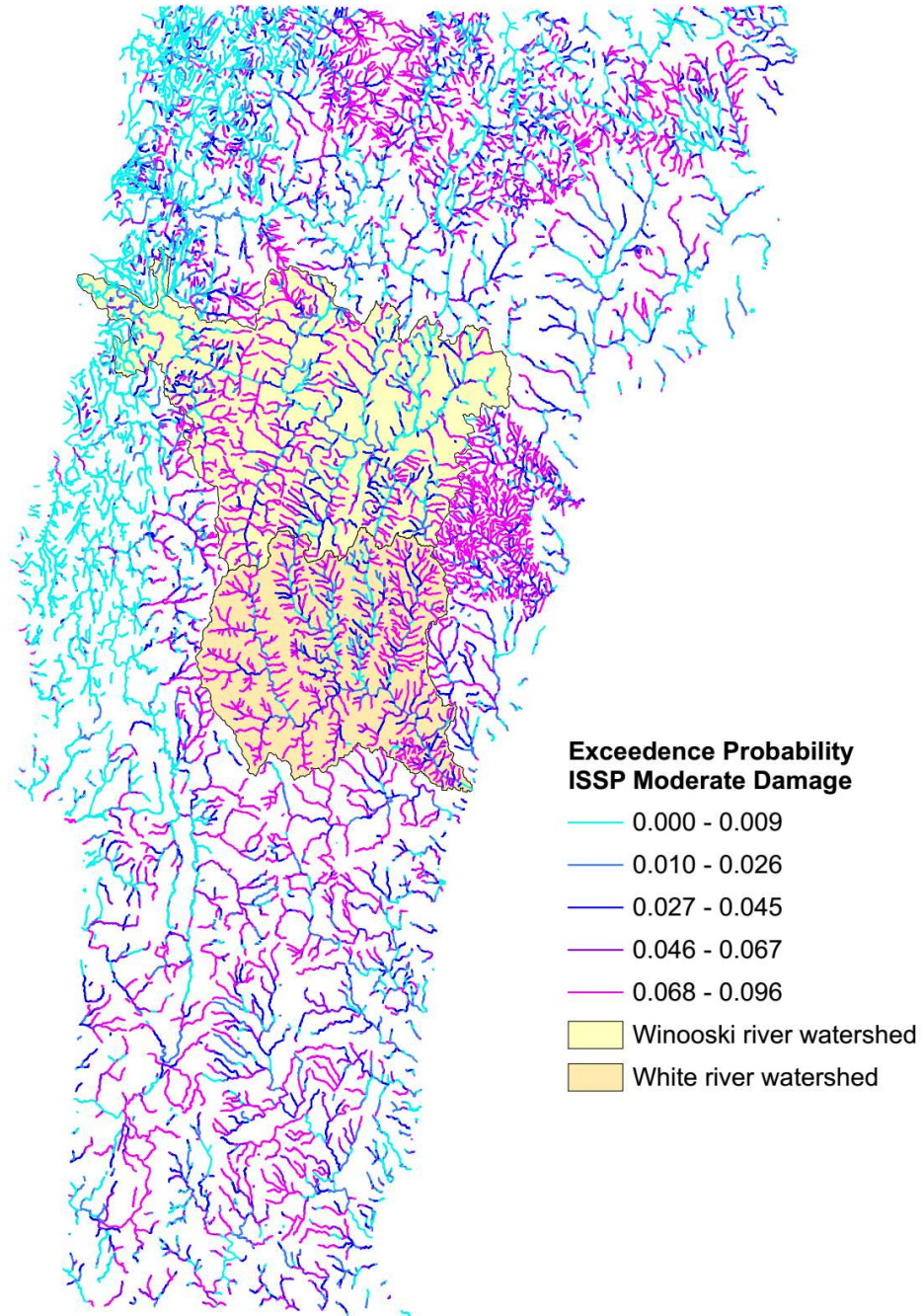


**Figure 5.7. Probability map for the state of Vermont generated from ISSP.**

For analysis focused in a single watershed, the probability of damage can be scaled to the total number of bridges in the selected watershed. For example, the probability maps (Figure 5.8a, 8b, 8c, and 8d) show the Winooski River and White River watershed, with each stream reach showing the maximum probability of damage in the Winooski watershed of 7.5 % corresponding to 23 damaged and 306 total bridges, and in the White River watershed of the 29% corresponding to 53 damaged and 180 total bridges. Because the exceedance probabilities in Figure 5.8 are calculated on the watershed scale, color references from one watershed to another are not consistent, and should not be compared. Rather, the exceedance probability can be compared in various stream reaches and sub-watersheds to others within the containing watershed, to observe differences in the spatial hazard evident from Tropical Storm Irene. The SSP probability maps (Figure 5.8a and c) help show the uniform vulnerability based on stream power differences, with areas of high probability indicating vulnerability to the bridge infrastructure in those locations. The ISSP maps (Figure 5.8b and d) illustrate the prevailing hazard from Tropical Storm Irene in those locations to bridges and likely other transportation infrastructure, showing the increased effects of high rainfall on bridge damage. We observe that some areas, which appear to have high damage probability (upper right corner of Figure 5.8c), lack any recorded bridge damage, suggesting that additional bridge and hydrogeologic characteristics not considered in this analysis (e.g., surficial geology) may be necessary to differentiate vulnerability; this will be the focus of continued work. The expected trend of higher exceedance probability of damage (thus, higher stream power measures) in the steeper headwaters and tributaries, are reduced in the flatter and broader valley floor streams, as flow progresses downstream.

Though the two pairs of maps are very similar, there are particular differences in which individual reaches are rated differently.

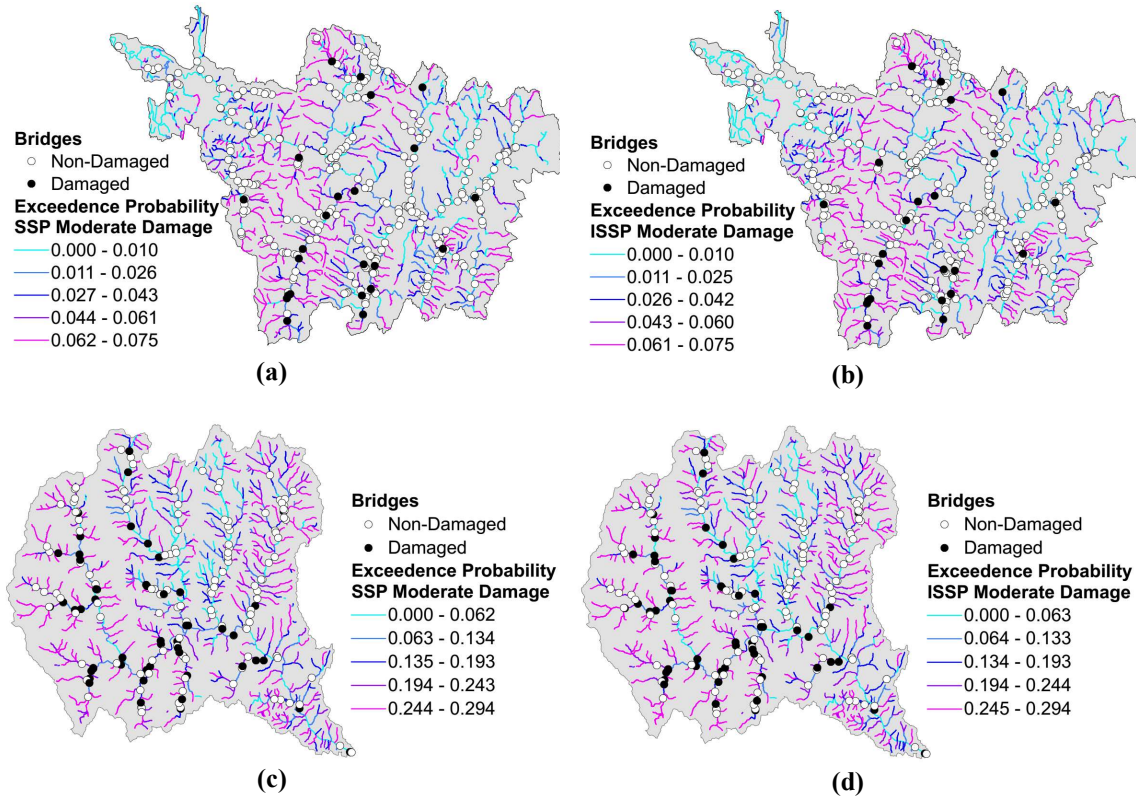


Figure 5.8. Probability Map for the White River Watershed generated from (a) and (c) SSP and (b) and (d) ISSP

## 5.4 Conclusions

This paper assimilated data and categorized the observed damage to 313 Vermont bridges from Tropical Storm Irene into four levels of severity, showed a linkage between bridge damage and stream power, and quantified and displayed the hazard statewide at the bridges and stream reaches used in this study. The application of empirical fragility curve analysis for stream power produced a probability of damage generated from the results collected from Tropical Storm Irene. With the implementation of probability mapping, the hazard to bridges from an extreme event like Tropical Storm Irene could be effectively displayed

over a broad section of stream reaches, both at select watershed and statewide scales. The following specific conclusions are drawn from this work:

- 1) A GIS script was created and implemented to generate stream power measures statewide for the studied bridges and stream reaches in Vermont, including the use of a scaled stream power value to correspond to the magnitude of the storm impact.
- 2) Specific Stream Power, and the event-based, Irene Specific Stream Power were found to be both statistically significant at discriminating between damaged and non-damaged bridges, as well as between bridge damage levels from Tropical Storm Irene.
- 3) The resulting spatial probability maps allowed for visual display of vulnerable reaches, for which bridge placement would be at increased hazard. Further application of event-based SSP probability maps could be generated using rainfall ARI in future climate simulations to produce the probability of bridge damage for a hypothetical climate scenario.

The approach presented here could be implemented in other geographic regions. The method of estimating SSP and ISSP, and the calculation and expression of bridge hazard through fragility curves and probability maps could be useful in creating a screening tool for damage prediction. The methodology, and automated scripts used allow for rapid implementation in future applications, thus not limiting this work to Vermont. The Tropical Storm Irene database used here for the 313 damaged bridges experienced rainfall recurrence intervals ranging between 10 and 500 years, indicating that this methodology could be evaluated for a wide range of design flows for any watershed beyond the borders of Vermont.

As far as we know, this is the first investigation comparing site-specific stream power to observed bridge damage at a system level, and represents a fundamental breakthrough in the prediction of flood related bridge damage.

Future studies expanding upon this work could apply the probability maps to create a risk based inventory screening tool, to aid in decision making relating to transportation infrastructure planning. The complex interactions between the inherent bridge and site vulnerability cannot solely be explained through stream power, or any single variable. Future research seeks to leverage the full database of features to identify which underlying characteristics in addition to the stream power play the most significant role in bridge damage vulnerability. Identifying these features requires the development of new feature selection techniques (i.e., genetic algorithms, learning system classifiers), which until recently were not widely available. The total cause of bridge damage also very likely includes a combined occurrence of high stresses, hydrogeologic instability, and vulnerable bridge infrastructure.



## CHAPTER 6 MULTIVARIATE FEATURE SELECTION

### 6.1 Introduction

Extreme flood events cause damage to bridges throughout the world. For example, in the United States, studies from Hurricane Katrina in 2005 indicate that uplifting and hydrodynamic forces on the superstructure caused the majority of the damage to short and medium span coastal bridges (Okeil and Cai, 2008). Subsequent analysis of 262 bridges, of which 36 were damaged, identified surge elevation as a key factor in determining damage level from Hurricane Katrina (Padgett et al., 2012). Similar bridge infrastructure vulnerabilities have been witnessed at Escambia Bay, Florida during the 2004 Hurricane Ivan (Douglass et al., 2004) and in Hokkaido, Japan during the 2004 Songda Typhoon (Okada et al., 2006). More recently, severe flooding in September 2013 caused the collapse of 30 highway bridges, and damage to an additional 20 bridges in Colorado (Kim et al., 2014).

Scour has been recognized as the primary cause of bridge failures in the United States (Kattell and Eriksson, 1998) and in other parts of the world. For example, Wardhana and Hadipriono (2003) analyzed 503 cases of bridge failures in the United States from 1989 to 2000, and found that flood and scour caused nearly 50% of all failures. Melville and Coleman (1973) report 31 case studies of scour damage to bridges in New Zealand. The HEC-18 document (Arneson et al., 2012) mentions numerous examples of scour related bridge damage and failure. During the spring floods of 1987, 17 bridges in New York and New England were damaged or destroyed by scour. The collapse of the I-90 Bridge over the Schoharie Creek near Amsterdam, NY, resulted in the loss of 10 lives and millions of dollars in bridge repair and replacement costs (FHWA, 2015). In 1985, floods in

Pennsylvania, Virginia, and West Virginia destroyed 73 bridges. A 1973 national study (FHWA, 1973) of 383 bridge failures caused by catastrophic flooding showed that 25 percent involved pier damage and 75 percent involved abutment damage, and subsequent analysis indicated local scour at bridge piers to be a problem about equal to abutment scour problems (FHWA, 1978; Arneson et al., 2012). The 1993 flood in the upper Mississippi basin caused damage to 2,400 bridge crossings (FHWA, 2015) including 23 bridge failures. Arneson et al. (2012) also report that the 1994 flooding from storm Alberto in Georgia affected over 500 state and locally owned bridges with damage attributed to scour.

Extreme flood events cause substantial geomorphic change to the stream networks. Stream migration, degradation, aggradation, and widening are all natural processes as streams seek equilibrium; however, human encroachment and development in floodways have altered the natural stream course resulting in major conflict at the intersection of floodway infrastructure and geomorphic change. Bridges in particular are vulnerable to damage, as they are a fixed node at the intersection of streams and human infrastructure, and susceptible to damage by any change in meander migration, channel width, depth, bank erosion or embankment failure. This was evident in the state of Vermont, which experienced a significant extreme flood event in August of 2011, as Tropical Storm Irene brought heavy rainfall and widespread flooding to the state. Flooding impacted 225 of the state's 251 towns, with rainfall totals of 100-200 mm (4-8 inches). Heavy rainfall at higher elevations caused flash flooding, and progressed to widespread flooding through Southern and Central Vermont. Rainfall recurrence intervals exceeded 500 years in some towns, and was in excess of 100 years in many areas. The storm damaged transportation infrastructure, as well as housing and businesses severely over wide swaths of the state. Anderson et al.

(2017a) identified 313 Vermont bridges (greater than 6m span) that were damaged in Tropical Storm Irene. The location of all long structure (greater than 6m) hydraulic bridges and their damage state (313 damaged bridges and 1936 bridges that did not have damage) are shown in Figure 6.1. Anderson et al. (2017a) assembled a comprehensive dataset of available bridge inspection and stream geomorphic assessments of Vermont hydraulic bridges that were damaged as well as not damaged.

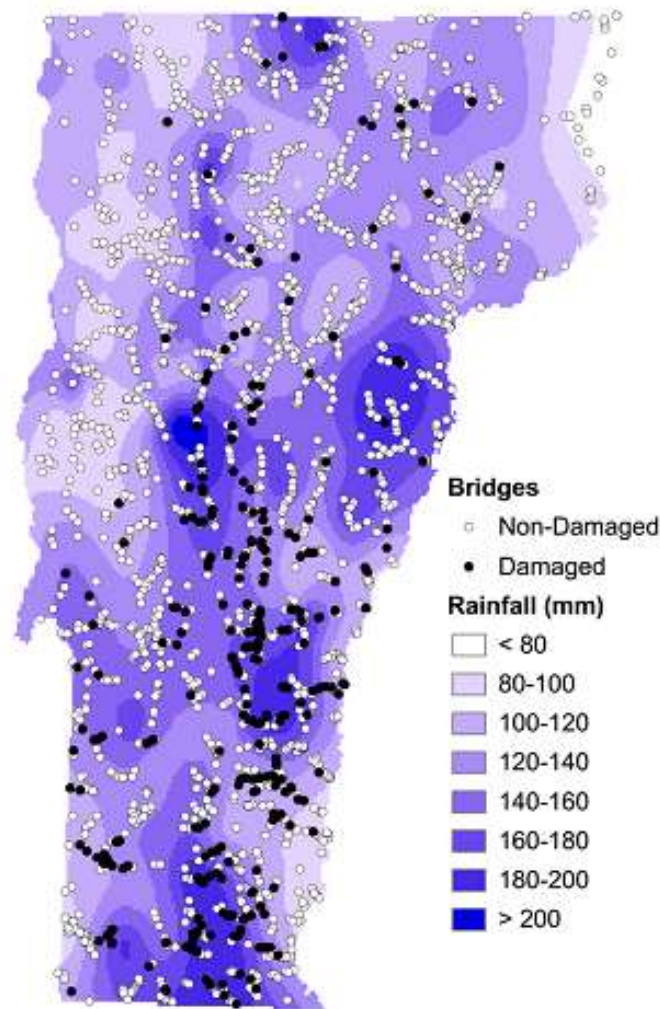


**Figure 6.1. Damaged and Non-damaged Vermont bridges in the 2011 Tropical Storm Irene, over Irene Rainfall intensity**

The study presented here adds new meaningful variables related to stream energy and watershed properties that were computed for all hydraulic bridges in Vermont and then leverages this enhanced dataset to identify structural, geomorphic, geologic and land-use features to aid in damage prediction. Multivariate feature selection was conducted on this comprehensive dataset, allowing for an impartial and exhaustive search of possible feature combinations, to generate models of available data that best predict damage. The feature combinations bring together variables from various sources, that until now have not been utilized in bridge assessments.

## **6.2 Background and Research Objectives**

The prior work of the analysis of the impacts of Tropical Storm Irene on Vermont bridges documented the number of damaged bridges, as well as the type and severity of the damage and repair costs (Anderson et al., 2017a), and therefore provides an extensive case study for the research presented here. In total, 313 bridges were identified and classified by damage type categorized as scour, channel flanking, superstructure damage, and debris blockage. Bridge damage was further categorized into four levels: slight, moderate, extensive and complete, with damage descriptions provided in Table 6.1 and examples shown in Figure 6.2. This damage ranking system was based on that proposed in HAZUS (Scawthorn, 2006), and later amended by Padgett et al. (2008). The ranking system descriptions were expanded to include the damage types observed in Tropical Storm Irene, particularly damage from flooded river flow, including scour, flanking, debris, and superstructure damage.

**Table 6.1. Description of damage categories used in analysis (Anderson et al., 2017a).**

Damage Category	Description
Slight	<i>Channel erosion that does not affect the bridge foundation, superstructure and guardrail damage and debris accumulation without scour present.</i>
Moderate	<i>Scour that affects the foundation, but not to a crucial state, bank and approach erosion, heavy aggradation and damage to the superstructure, but not to a crucial state.</i>
Extensive	<i>Crucial scour, with some settlement to a single foundation, but not to the point of collapse, full flanking of both approaches, and superstructure damage that makes it structurally unsafe.</i>
Complete	<i>Bridge washed away, collapsed, or has significant foundation damage that requires replacement.</i>



**(a) Slight Superstructure Damage**



**(b) Moderate Debris Damage**



**(c) Extensive Channel Flanking Damage**



**(d) Complete Scour Damage**

**Figure 6.2. Bridge Damage Level and Type from Tropical Storm Irene**

### **6.2.1 Data Collection and Initial Statistical Analysis**

In Anderson et al (2017a), a comprehensive dataset of bridge inspection and stream geomorphic assessments was created. In particular, the following disparate sources of data were assembled and georeferenced into GIS (Geographic Information Systems):

- (1) All records of long structure bridges (greater than 6 m in span), and the preceding years (2010) inspection from the Vermont Agency of Transportation (VAOT) Bridge Inventory System (BIS). The Vermont State bridge inspections follow the NBIS (National Bridge Inventory System) criteria (FHWA, 2015).
- (2) Estimates of post-storm damage level, damage type, and repair costs were obtained from documentation via the VAOT and the Vermont Department of Emergency Management (VDEM), and supplemented through examination of the available inspection photos for all bridges affected.
- (3) Tropical Storm Irene rainfall data were collected for Vermont, neighboring state New York and New Hampshire, and the Province of Quebec. Rainfall and recurrence interval were spatially interpolated with ordinary kriging, to provide estimates over the entire state, and allow for the determination of average rainfall and recurrence interval in each watershed.
- (4) The Vermont Agency of Natural Resources rapid geomorphic assessment (RGA) work provided a host of stream characteristics and measurements for reaches throughout the state. The RGA protocols are nationally recognized for providing a measure of stream disequilibrium and stream sensitivity indicating the likelihood of a stream responding via lateral and/or vertical adjustment to natural or human-induced watershed

disturbances (Somerville and Pruitt, 2004; Besaw et al., 2009). The RGA data characterize stream reaches, defined as river segments deemed consistent in slope, bed material and condition (Kline et al., 2007). Joining the RGA data to the bridge dataset linked the underlying stream metrics directly to the bridges located on the analyzed stream reaches, providing stream survey measurements and geomorphic characterizations to the dataset.

An analysis of variance was conducted on this dataset to differentiate between damaged and non-damaged bridges on three scales, statewide, on only the bridges within subwatersheds that contained a damaged bridge, and on a pairwise selection containing the nearest non-damaged bridge. Results showed a number of bridge inspection parameters and ratings to be significant, including channel rating and waterway adequacy. Stream geomorphic parameters, such as entrenchment, incision, straightening and width to depth ratio were also statistically significant in relation to bridge damage.

### **6.2.2 Motivation**

Bridges are critical connections in transportation network, and uniquely vulnerable in flood events, and therefore of high value in emergency response. Prioritizing infrastructure investment and emergency response during major events like Tropical Storm Irene require a broad quantitation of the vulnerability of our bridge population. A number of factors affect bridges under extreme flood events including bridge characteristics, stream characteristics, geographical features, environmental factors and land-use. We computed and included meaningful variables to characterize stream energy and watershed properties, and appended to the bridge dataset compiled by Anderson et al. (2017a). The above-mentioned dataset contains 330 such features. Finding combinations of features that may

collectively indicate why particular bridges were damaged is a severely difficult task for routine statistical techniques. Commonly, variables used in multiple regression analysis are often selected using forward selection, backward elimination, or stepwise selection. With 330 possible variables, ranging in data type (i.e., nominal, ordinal and continuous) and with varying degrees of independence, and lack thereof, variable selection using traditional methodologies is not feasible. For example, a four-effect model, using nominal logistic regression, would result in  $5 \times 10^8$  possible feature combinations. To avoid the computational challenges often associated with these large data sets, input data variables are often eliminated using expert judgement (i.e., domain experts pre-process the data and include only those variables deemed important). However, this greatly limits the power of large, comprehensive datasets.

Because numerous bridge inspection and geomorphic assessment characteristics are significant when discriminating between damaged and non-damaged bridges, here we use a novel feature selection method to identify the combination of available characteristics (i.e., features) at play in complex bridge and stream interactions. The feature selection method is an evolutionary algorithm, recently developed for the purpose of feature selection (Hanley et al., 2017, in review) in big data, and eliminate the bias associated with *a priori* expert selection processes. The result is the identification of features (i.e., combinations of bridge, stream and watershed characteristics described above) significant in the determination of bridge damage. Here, bridge damage levels classified as moderate and above were included in the positive (i.e., damaged) outcome group, while bridges identified as non-damaged or having only slight damage were used as the alternate negative (non-damaged) outcome group. This helps bias the features selection toward significant



damage, and better correlates with major erosive scour damage, excluding minor superstructure and incidental damage from flooding.

The method employed here is a nonparametric, multivariate approach to identifying the combined presence of bridge vulnerabilities, hydrogeological stressors, and increased flows from a localized flooding event (i.e., Tropical Storm Irene) to better understand why damage occurs. Our focus is to identify the set of multivariate features (i.e., characteristics within the bridge and stream interaction) most pertinent to bridge vulnerability.

### **6.3 Watershed Analysis**

An ArcGIS script was created to use a 10 m hydrologically corrected digital elevation model to iteratively delineate watersheds to the downstream end of each stream reach. Any rainfall runoff within a watershed will eventually flow to the outlet location. In total, 15,123 stream reaches were delineated to calculate their watershed area (i.e., the contributing area draining to some target location). Through the watershed analysis, the following data were generated: watershed land use characterization, watershed soil hydrologic grouping, and a reach segmented stream power assessment.

Land use is an important metric in determining watershed characterization and understanding the relationship between rainfall and streamflow. Developed land cover contribute more stormwater runoff directly to surface water bodies, increasing flooding, while natural land cover and wetlands work to buffer flooding. The National Land Cover Database provided land use classifications, and was simplified from 16 types down to five major groups for this study: developed, agriculture, open water/wetland, forest, and other.

The hydrologic soil group (HSG), established by the US Soil Conservation Service (USCS, 2009), is valuable in the determination of runoff potential. The HSG is determined

by the water transmitting soil layer with the lowest saturated hydraulic conductivity, and is categorized into four distinct groups. The HSG was sampled to find the percentage of each soil type for every stream-reach delineated watershed. Soil coverage with high runoff potential will contribute greater volumes of stormwater directly to rivers and streams, increasing occurrences of flash flooding by shortening the time to peak flow.

Stream power is the rate of energy (i.e., power) of the flowing water against the bed and banks of the river channel. Stream power functionally controls stream dynamics and morphology. Stream power estimates during extreme events show correlations to stream widening in Vermont (Buraas et al., 2014), and erosion and deposition in Colorado (Gartner et al., 2015). The calculation of stream power used in this analysis occurs on a broad scale, using widely available data, rather than individual measured observations, to produce comprehensive estimates of stream power. A GIS script was developed to generate the stream power data, which automated the calculation of stream power at any desired point, in this case at the locations of all hydraulic bridges in Vermont. Total stream power ( $\Omega$ ), also referred to as cross-sectional stream power (Fonstad, 2003) is defined as:

$$\Omega = \gamma \cdot Q \cdot s, \quad (1)$$

where  $\gamma$  is the specific weight of water,  $Q$  is the discharge, and  $s$  is the energy slope. SSP ( $\omega$ ) normalizes the total stream power by the width of the stream to estimate unit-bed-area stream power as:

$$\omega = \gamma \cdot Q \cdot s / b, \quad (2)$$

where  $b$  is the channel width. The discharge values required for stream power were calculated using regional regression equations for flood discharge at various annual exceedance probability thresholds (Olson, 2014; Olson, 2002). With the discharge at each

target reach estimated, the energy slope was determined based on reach breaks established in the RGA. Stream power, specific stream power, as well as scaled versions to represent the estimated Tropical Storm Irene intensities were calculated as detailed in Anderson et al. (2017b). These scaled versions, Irene Stream Power and Irene Specific Stream Power, represent the full power of the water that would be forced through a bridge opening. Stream power is typically modeled on the 2-year flow, as a higher flood flows would access the floodplain, and so the power within the channel is what is related to geomorphic change. Bridge intersection however often block the floodplain, forcing all flow to return to the channel, creating an intensified effect.

#### **6.4 Feature Selection Analysis**

In total, 330 features are available for every bridge in the dataset including: bridge inspection from the BIS, stream geomorphic data from the RGA, rainfall and recurrence interval, classification of the damage level and type, watershed analysis and stream power metrics. A data-driven multivariate feature selection Evolution Algorithm (EA) was performed using a newly developed evolutionary algorithm of Hanley et al., (2017, in review), to identify key features from among the 330 assembled features that correlate to the damage to Vermont bridges resulting from Tropical Storm Irene.

##### **6.4.1 Conjunctive Clause Evolutionary Algorithm Complex Interaction Identification**

The EA is specifically designed for feature selection, (i.e., identifying multivariate interactions) associated with some desired outcome,  $k$ , of interest (e.g., level of bridge damage) associated within a very large, complex dataset (Hanley et al., 2017; in review). The method searches across all multivariate combinations, where each variable, or *feature*,

may have a different data type (i.e., nominal, ordinal, continuous), each having a range of values. The only assumption inherent in the EA methodology is that ordinal and continuous features must be monotonic or unimodal. The algorithm is capable of evolving both the set of important features and the range of values using what are known as conjunctive clauses (*CC*) of the form:

$$\mathbf{CC}_k \text{ is defined as } F_i \in a_i \wedge F_j \in a_j \dots \quad (1)$$

where  $F$  represents a feature (i.e., bridge or stream characteristic) whose value lies in the range  $a_i$ ; the symbol  $\wedge$  indicates a conjunction (i.e., features are linked by the logical AND). The *CC* is interpreted as “If the  $CC_k$  is true for a given input feature vector (set of features), then the class outcome will be predicted as being associated with some user-defined outcome,  $k$  (e.g., level of bridge damage) compared to what one might expect given the global distribution of  $k$ .” The conjunctive clauses may be evaluated based on accuracy, coverage, and order. *Accuracy*, analogous to the positive predictive value (PPV), is the ratio of true positives predictions to all positives predictions (actual damage detected to all predicted damaged). *Coverage*, also called probability of detection (POD), is the ratio of true positive predictions to actual positive values (actual damage detected to total damaged). *Order* is defined as the total number of features in a given model ( $CC_k$ ).

The algorithm processes in two phases, each using an age-layered population structure (Hornby, 2006), and assesses fitness using a hypergeometric probability mass function (Kendall, 1952) that accounts for the size of the dataset, the amount of missing data, and the distribution of outcome categories. The first phase evolves an archive of conjunctive clauses (CCs) consisting of feature combinations that have a high probability

of a statistically significant association with a given outcome. The second phase evolves disjunctions of these archived CCs to create an archive of probabilistically significant clauses in disjunctive normal form (DNF). The DNF outcomes are combinations of CCs, which in turn are combinations of features.

The features identified as being important for discriminating bridge damage comprise all features archived in a 2<sup>nd</sup>-order or higher conjunctive clause during at least one of the five repetitions. Main-effect features were only selected if that feature was archived during all five repetitions.

#### **6.4.2 Multiple Logistic Regression**

Following the EA feature selection analysis, the resulting feature combinations were tested with multiple logistic regression, conducted in JMP 12. The dependent variable was bridge damage at moderate or greater level, with the feature combinations identified by the EA as the independent variables. Logistic regression models were created to include the same variables found by the EA in its features combinations. This enables direct comparison of the EA to multiple logistic regression. Each logistic regression model was then used to create probabilistic estimates for prediction.

### **6.5 Results and Discussion**

#### **6.5.1 EA and Logistic Regression**

The EA processed the bridge dataset to identify feature combinations that best correlate with observed bridge damage from Tropical Storm Irene. Damage levels classified as moderate, extensive, and complete were used as the positive state (damaged), while the two levels labeled non-damaged and slight damage comprise the negative state

(non-damaged). The EA features combinations are reported with their accuracy (PPV) and coverage (POD), two commonly used metrics for describing their quality. Coverage is the percentage of damaged bridges correctly identified, or the percent of true positives. Accuracy is the ratio of true positive results to total positive predictions (true positive and false positive). Feature combinations were identified (evolved) by the algorithm as good solutions based on fitness, as outlined in section 6.4.1. Figure 6.3 shows the accuracy and coverage of feature combinations identified using the EA for the bridge dataset, with each feature combination represented as a point on the figure. Of the 256 features combinations stored by the EA, 29 input variables are selected. Each variable within a feature combination is optimized for a range of values.

Figure 6.3 shows that selected features combinations vary by order and span a wide range of accuracies and coverages. The best solutions fall along what is known as a Pareto front, meaning they are of optimal fitness, and a move along the front does not improve the resulting fitness. An ideal feature combination has a balance to include both accuracy and coverage, predicting bridge damage correctly for a large set of the bridge population.

Four feature combinations are selected as examples (circled points in Figure 6.3) for examination here. Within Table 6.2, are the variables and ranges for each of the identified target points. A few of the features lie on the Pareto front, while others are not individually optimal solutions. The first order point, FC 5 has accuracy and coverage of 42.8 and 8.8, respectively. This feature includes waterway adequacy, which is a rating associated with the bridge's design capacity for overtopping, and shows that low ratings are related to damage. The second order feature combination, FC 31 has accuracy and coverage 44.6 and 15.3, respectively, and relates high Irene Stream Power and the low

bridge inspection channel rating to damage. The third order feature combination, FC 70 has accuracy and coverage of 29.7 and 52.6, respectively, and correlates higher elevation, and high percent of hydrologic soils B and C. The final feature combination, FC 254 is fourth order with accuracy 34.1 and coverage 34. This combination includes high rainfall, low hydrologic soil type D, lower than average open water land cover (less wetland and water bodies), and median to low confinement ratio (ratio of valley width to channel width). Each feature combination generated from the EA was also tested in logistic regression, and their results can be seen in the confusion matrices in Table 6.2 below. In the confusion matrix, the upper right hand corner is the number of True Positive, upper left is False Negative, lower left is False Positive, while lower right is True Negative.

**Table 6.2. Feature Combination Confusion Matrices, EA and Logistic Regression**

FC 5	EA		Logistic Regression	
Ord 1	Predicted		Predicted	
Actual	True	False	True	False
True	19	196	17	197
False	26	2008	17	1996

(a)

FC 31	EA		Logistic Regression	
Ord 2	Predicted		Predicted	
Actual	True	False	True	False
True	33	182	6	208
False	41	1993	9	1983

(b)

FC 70	EA		Logistic Regression	
Ord 3	Predicted		Predicted	
Actual	True	False	True	False
True	96	119	0	214
False	209	1825	0	1946

(c)

FC 254	EA		Logistic Regression	
Ord 4	Predicted		Predicted	
Actual	True	False	True	False
True	73	142	4	137
False	141	1893	8	1214

(d)

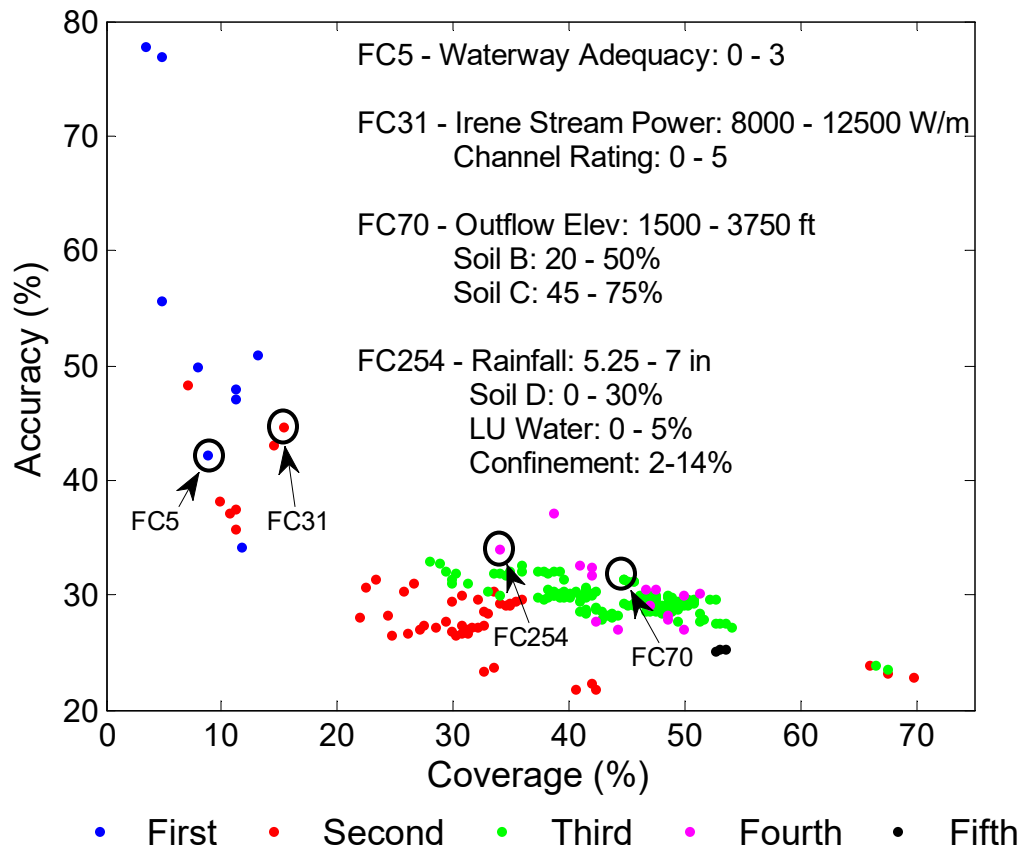


**Figure 6.3. Accuracy and Coverage for Feature Combination**

Feature combinations identified by the EA returned a significantly higher number of true positives than the logistic regression, but also return a much higher number of false positives. Overall, logistic regression models running the same feature combinations identified by the EA produced fewer true and false positive results, indicating conservative statistical predictions, which may limit its applicability to the bridge damage problem. Logistic regression assumes that observations are independent, which is not necessarily true in this problem given spatial correlations between locations. This independence issue is more difficult when variable selection is often done through either forward or backward substitution, or expert examination. With so many possible variables, and numerous



unknown interactions between variables, judgement of independence of each variable, or observation is difficult.

Several variables identified by the EA feature combinations show the value of using a computational method capable of accommodating the additional data included in the bridge damage dataset. For example, Irene Stream Power is identified as important indicator of bridge damage, showing the value of the stream power metric toward bridge vulnerability. Channel Rating and Waterway Adequacy Rating are two bridge inspection variables identified as correlating to damage, with low ratings being associated with damage prediction. High rainfall is included, which is as expected, but still important to note. Hydrologic Soil Types are showing up as key variables, with higher percentages of B and C, and lower percentages of D relating to bridge damage. Open water land use type represents the amount of available wetland or waterbodies that could act as storage to mediate the flooding. Lower percentages of open water land cover would mean a reduced storage, and increased flooding.

The predictions of damage from the EA and from the logistic regression deviate further apart as higher order models are used, as logistic regression produces similar results for the first order model, but fails to identify a meaningful number as damaged bridges in the higher order combinations. The inclusion of multiple model effects in logistic regression produces exceedingly conservative results, failing to meet the required threshold to trigger a positive prediction.

### **6.5.2 Disjunctive Normal Form Analysis**

The feature combinations identified by the EA show significant correlation to bridge damage, using only a small number of variables (select bridge, stream, and

watershed metrics). The algorithm is novel also simultaneously evolving the range of values associated with each of the selected variables, providing a threshold used to discriminate between damage states. Damaged bridges can be correlated to a number of different variables, and combinations of variables, as shown through the feature selection algorithm depending on the level of accuracy and coverage that the user deems most meaningful to the problem at hand. To add to the predictive capacity of the EA algorithm another layer of analysis was added, which would create sets of feature combinations that increase coverage while maximizing accuracy.

By creating sets of feature combinations, the Disjunctive Normal Form (DNF) algorithm is able to join independent sets of bridges from numerous feature combinations, to improve the coverage of the predictive model. Individual feature combinations that identify independent sets of bridges can be joined to improve performance. The DNF search produces results with better coverage than the individual feature combinations, while maintaining equivalent accuracy, as seen in Figure 6.4 indicated with a star. The selected set, DNF 3313 is fourth order, has accuracy and coverage of 27.6 and 68.4, respectively. The selected DNF is composed of the individual feature combinations highlighted in Figure 6.3 and Table 6.2. Predicting damaged bridges based on DNF 3313 returned 148 true positives (70% of damage), 339 false positives (17% of non-damage), 67 false negatives, and 1,695 true negatives, and an odds ratio of 11. Odds ratio is the proportion of the true outcomes, divided by the false outcomes, and is a measure of association between exposure and outcome. The odds ratio represents the odds that damage will occur given the model conditions (parameters within the ranges of the variables within the feature combinations), compared to the odds of damage without them (data outside the

selected feature combinations). DNF 3313 shows that bridges with parameters within the feature combination ranges are 11 times more likely to be damaged than those outside the group.

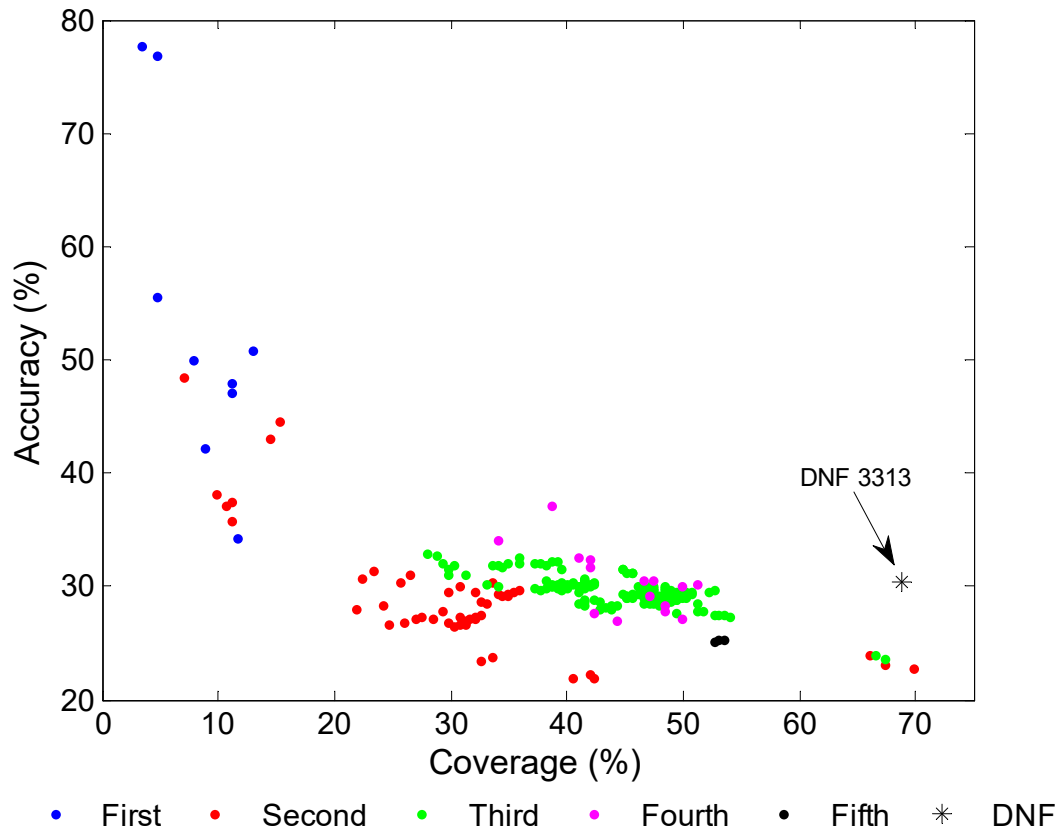


**Figure 6.4. Accuracy and Coverage for DNF and FC**

Using a group of feature combinations the DNF was able to produce a result with higher coverage with similar accuracy, allowing for the prediction of a greater number of damaged bridges. Nearly 70% of the bridges damaged at a level classified as Moderate, Extensive and Complete were successfully identified using 10 combined variables, within four feature combinations. Three variables, the Channel Rating, Waterway Adequacy Rating and Irene Stream Power were shown to be useful individually in determining bridge

damage (Anderson et al., 2017a; Anderson et al., 2017b) and have additionally been shown here to be important through multivariate feature selection. Irene Stream Power is the scaled version of stream power, meant to represent the true flood stress passing through a confined bridge, and is shown to be an important metric in damage. Channel Rating is the assessed condition of the channel and bridge riprap present during the biennial bridge inspection. Waterway Adequacy is the rating of the bridge's ability to convey its design storm, or the hydraulic overtopping flow associated with the bridge's service level. Highway bridges are designed to convey larger recurrence interval flood events without overtopping, whereas rural town bridges are often designed for lower flow events. The percentages of hydrologic soil types within each bridge's watershed drainage area, identified by including the expansive set of watershed variables found through the watershed analysis, have proven important in correlating to bridge damage. High percentages of hydrologic soil type B and C (each above the average) correlate with increased damage. Soil C is associated with increased runoffs, and could precipitate flooding. Additionally, a different feature combination included lower prevalence of Soil D, which is normally associated with higher runoff. The opposing soil types between feature combinations could indicate that there are differing and distinct relationships between certain locations with higher and lower runoff potential, with both leading to bridge damage. When the land cover type "water" is in low proportion it is shown to be more significantly related to bridge damage, as is higher elevations. Higher elevations are the source of stream headwaters, have generally higher slopes, and are more prone to flash flooding. As a result of the EA algorithm, including the selection of DNF sets, we can identify bridges with high Irene Stream Power and rainfall, poor Channel and Waterway

Adequacy ratings, higher elevation, little open water, and higher percent soil type B and C to be at greater risk for flooding damage.

### **6.5.3 Geographic Prediction**

The prediction of the bridge damage can be visualized geographically to highlight spatial relationships. Using the feature combinations associated with DNF 3313, Figure 6.5 displays the prediction of damaged bridges throughout the state of Vermont superimposed on major watersheds. The map depicts distinct geographical areas in which the bridges are predominantly predicted as damaged. The majority of the damaged bridges classified correctly were located in the central region of the state, following areas of high rainfall. The majority of the damaged bridges in the Winooski watershed were misclassified as non-damaged, while other watersheds, such as the Otter, the Connecticut-Waitsfield to White River, and Connecticut-White River to Bellows Falls had the damaged bridges predicted correctly. The White river watershed, which had a significant amount of damage, had a mix of both correct and missed damage predictions, with the missed predictions being grouped in tributary watersheds. The Mad river subwatershed received a high amount of rainfall, and experienced intense flooding, but the bridge damage was not correlated to the variables found in the DNF 3313. The differences between bridge identification in neighboring watershed is an interesting one, and suggests there are additional variables that discriminate damage between different watersheds and geographic areas. The results suggest the analysis is identifying differences on a watershed scale, while being applied at the statewide level. The EA could potentially be used to identify a different DNF solution that may be useful in damage detection in those misidentified areas.

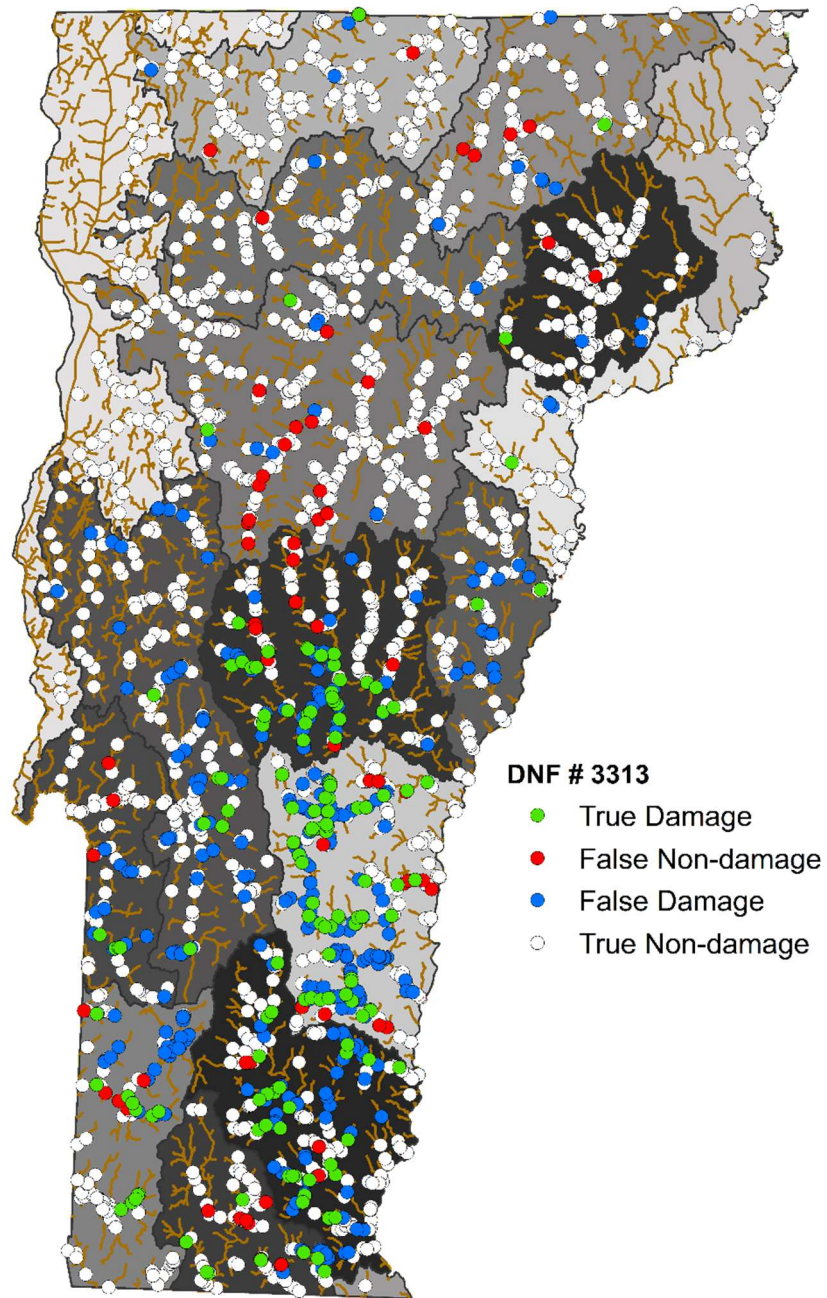


**Figure 6.5. Spatial relationship of DNF 3313 results**

## **6.6 Conclusions**

An available dataset (Anderson et al., 2017a) that incorporated a unique set of both bridge and stream characteristics, as well as documented observations of varying levels of

bridge damage from a single extreme storm event was employed. Additional analysis including watershed delineation, stream power calculation, slope determination, land cover and hydrologic soil type characterization, and rainfall interpolation were conducted on 15,123 individual stream reaches and added to the dataset. The updated dataset is available at: <http://go.uvm.edu/vtbridges-irene-data>

Features significantly correlated to and capable of discriminating damage to hydraulic bridges were identified, and combined to increase their predictive power. The feature selection was focused on more significantly damaged bridges, to allow for better correlations with major erosive scour damage, and excluding minor superstructure and incidental flooding damage. As a result, the predicted damage can be used to assess the critical needs of the transportation networks, and identifying vulnerable links during extreme flood events. Many of the collected features found to aid in the prediction were previously unavailable, and had not been applied to predict bridge damage.

The EA algorithm is capable of producing bridge damage predictions through multivariate feature selection. The EA is capable of testing a vast number of possible combinations, something that is infeasible with logistic regression, and outperforms the artificially seeded traditional logistic regression (when fed the same information).

Logistic regression is overly conservative, failing to classify affirmative results, and requires independence between samples, which is uncontrollable given the spatial correlations between bridges. The EA algorithm creates a prediction set that includes a significant number of true positive solutions, using the relatively small set of variables including: rainfall, Irene Stream Power, Waterway Adequacy Rating, Channel Rating, elevation, percentage hydrologic soil type, open water land cover, and confinement ratio.

The method allowed for the inclusion of new variables, previously unused in bridge analysis, to be applied over the full population of bridges in the state. The method is capable of handling a large amount of potential data and producing a result that improves upon the prediction of damage, compared to traditional regression analysis. Each feature combination seeks to explain bridge damage by finding correlation with a small number of features, to avoid over fitting.

The addition of the DNF search generates an enhanced set of feature combinations that improves coverage while maintaining accuracy. By leveraging this extensive dataset to classify for bridge damage, we have created a prediction of statewide bridge vulnerability under extreme flood event. The map of predicted bridge damage shows good correlation to bridges actually damaged during Tropical Storm Irene, and could aid in the identification of additional (currently undamaged) bridges at risk.

Several of the variables identified as significantly correlated with bridge damage have promise in developing risk maps of bridge damage. Irene Stream Power, scaled to a proportional flow associated with storm intensity, was often included in optimal feature combinations. Watershed hydrologic soil types were newly identified variables, and show the importance of understanding the geographically specific watershed conditions and their influence on extreme flow events. Channel Rating and Waterway Adequacy Rating, variables from the bridge inspection manual proved important, showing that prior signs of damage to the channel and the overtopping risk are likely a sign of upcoming vulnerability.

When viewed from a geographic perspective, the prediction of damage from the selected DNF appears to segment different watersheds. The difference between adjacent watersheds reveals the spatial relationship behind some of the parameters, and displays



how those differences affect the outcome, bridge damage. Other DNF solutions are likely to be better at identifying damaged bridges in those missed watersheds, and suggests the method may have applicability on a smaller scale.

The analysis conducted here collated a unique set of data (bridge assessment data, stream geomorphic, stream power, and watershed characteristics), and showed correlation between this constructed set of variables to bridge damage from Tropical Storm Irene. The knowledge gathered as a result of this study has applications beyond Vermont. Many of the variables newly added to the analysis can be created or monitored using commonly available data. The methodology, for creating watershed assessment parameters, as well as using the available EA for feature selection can be applied to any bridge dataset and may add value in assessments beyond the study of bridge damage. Bridge inspection records are commonly used in other states, and can be supplemented with additional information following the methodology used here. The EA opens up the opportunity to perform feature selection on large datasets, allowing for sets of multivariate features to be identified that are significantly correlated with levels of bridge damage while circumventing the computational challenges associated using traditional statistical analysis. With the increasing availability of sensor technology, and the emphasis on multidisciplinary approaches, the movement toward incorporating more and varying data sources continues to increase, making traditional methods even more limited.

## 6.7 Supplementary Material

The EA uses a customized version of an Age-Layered Population Structure (ALPS) (Hornby, 2006). In the first generation (and every ten generations thereafter), a novel population of clauses, each with age 1, is introduced into the first age layer. During each generation, clauses in each layer are selected to reproduce with variation introduced either through crossover (with probability  $P_x = 0.5$ ) or through mutation. If selected for crossover, a second parent is selected from the same or preceding (if one exists) age layer, using tournament selection with replacement (tournament size of 3). The EA was run for 3,000 generations using all 336 features (L) and repeated five times. Details of the parameters used in this study are provided in Tables A and B.

Feature sensitivity measures the contribution of each feature to the fitness of the conjunctive clause. In this work, the initial minimum feature sensitivity threshold is set to one, which translates to each feature improving the fitness of the conjunctive clause by at least one order of magnitude. Conjunctive clauses are archived (retained) only when they possess a fitness less than or equal to the hypergeometric PMF threshold and a minimum feature sensitivity greater than or equal to the minimum feature sensitivity threshold. For each order of archived conjunctive clauses, the minimum feature sensitivity was heuristically increased as the number of archived clauses increased.

**Table A - Parameter settings for the EA.**

<b>Parameter</b>	<b>Meaning</b>	<b>Value</b>
Param.ALna	Number of non-archived age layers	10
Param.ArchOff	Maximum number of archived clauses that will undergo either mutation or crossover	200
Param.GENn	Generations until new population is added	10
Param.MaxNumFeat	Maximum number of features in new conjunctive clause	20
Param.NonArchLMax	Maximum non-archived conjunctive clauses per age layer	20
Param.NumNewPop	Number of conjunctive clauses created in new population	20
Param.Pm	Probability that locus will be selected for mutation	1/L
Param.Pwc	Probability of wild card	0.25
Param.Px	Probability of crossover	0.50
Param.PXvals1	Probability that crossover will be at the feature value level	0.50
Param.PXvals2	Probability that a feature common to both conjunctive clauses will be crossed at the value level	0.75
Param.TotGens	Total generations	3,000
Param.TournSize	Tournament size	3
Param.WCloci	Probability that a wild card locus will be mutated	0.05

**Table B - Initial settings for the EA archive thresholds. (N is number of CC)**

<b>Threshold Parameters</b>	<b>Value</b>
Conjunctive Clause Order Layers	1-8
Hypergeometric PMF Threshold	1/N
Minimum Feature Sensitivity Threshold	1
Minimum Archived CCs per Order Layer	1,000
Maximum Archived CCs per Order Layer	1,100

## **CHAPTER 7 DAMAGE TO VERMONT'S HISTORIC BRIDGES FROM TROPICAL STORM IRENE**

### **7.1 Introduction**

Vermont's historic bridges are an important cultural, economic, and aesthetic resource. The three common historic bridge types in Vermont are timber truss bridges (mostly covered), steel truss, and masonry arch (Figure 7.1). These bridges are noticeable for the sizeable superstructure, from the network of green steel trusses, to the cedar siding of a covered bridge. These landmarks often serve as key links in transportation infrastructure as well as attract tourists, providing 19<sup>th</sup> century rural aesthetic. Bridges are deemed historic based on guidelines set by the National Historic Registry, with the intent to protect and preserve their cultural significance and value. The earliest bridges in Vermont consisted of unframed log beams resting upon timber cribbing. Advances in design led to simple trusses, most notably the king and queen post styles. With greater investment in design and the scale of the bridges, siding began to be used to protect the truss members from weathering, extending their lifespan (McCullough, 2015). Advancements in truss design lead to the implementation of the arch-truss, allowing for an increase in the clear span of the bridge.

It is believed that at least 700 covered bridges were constructed in Vermont (Conwill, 2004) beginning in the 1820's. Major flood events, like the 1927 flood, wiped out an estimated 300 timber bridges throughout the state (Thomas et al., 2013). Tropical Storm Irene in 2011 caused the loss of a number of historic bridges. Repair and remediation of these critical resources must be done with care and thought to maintain their historical significance, but at the same time, adapted to the increasing risk of extreme events. Historic

bridges are more vulnerable than a conventional bridge to the risk of high flows, as overtopping will create uplifting forces that can remove the bridge from its supports, and also increase the risk of debris strikes. In an effort to determine the vulnerability of historic bridges, the relationship to damage type and cost were assessed using the available information gathered following Tropical Storm Irene.

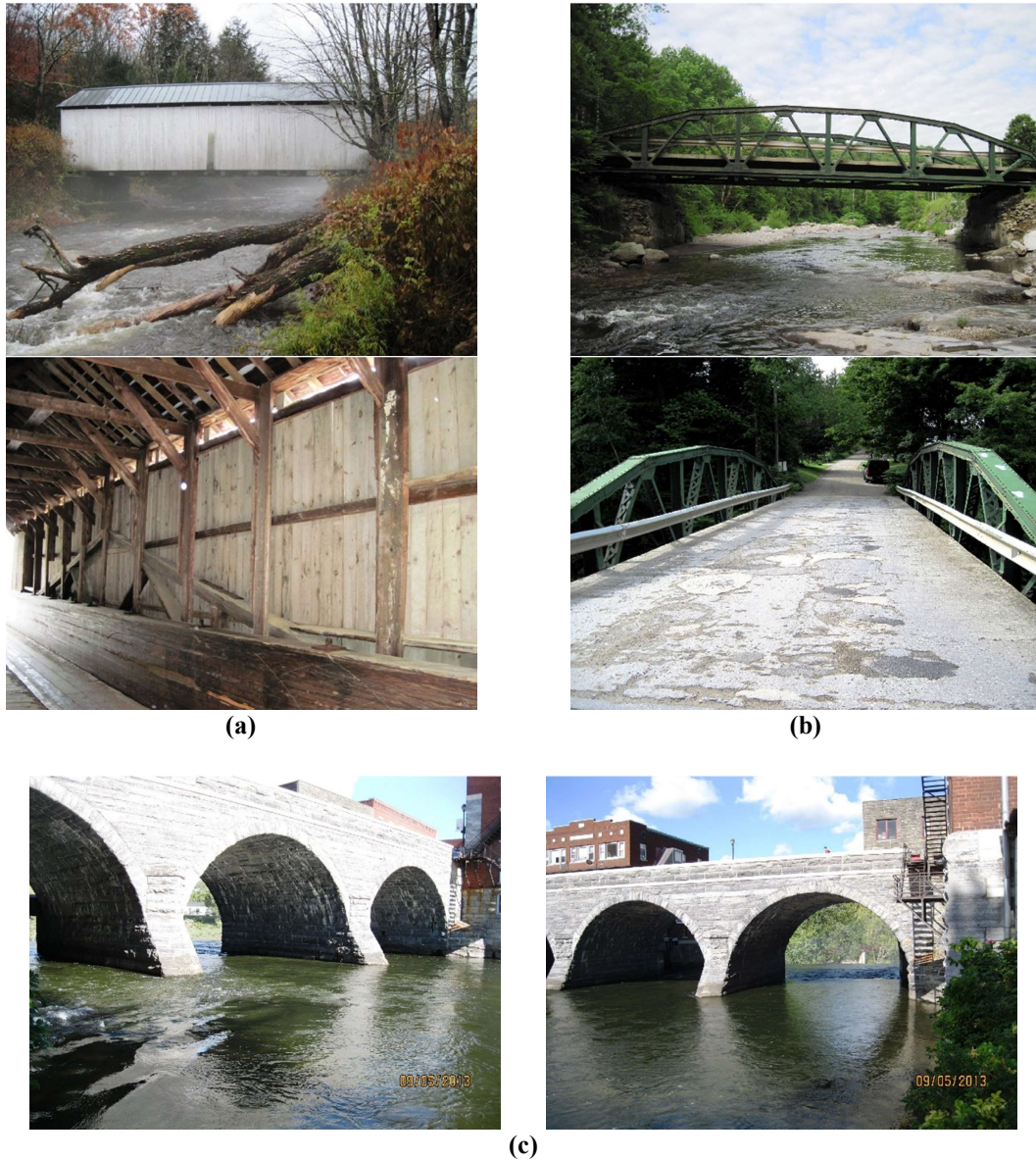


**Figure 7.1. Classic historic bridge types: (a) Kidder Hill Covered Bridge in Grafton, (b) York Hill Steel Pony Truss Bridge in Lincoln, (c) Battell Bridge in Middlebury**

A major shift occurred as a result of the flooding in 1927, 1936 and 1938, in which bridge designers and owners began to understand that large stone piers and abutments became impediments to water flow, and that in addition to carrying roads across rivers, bridges also passed streams under roads, and must be designed to allow for greater flows (VSHB, 1937). The remaining population of covered bridges were seen as a threat, acting as dams under high flows, and were vulnerable to debris/ice strikes (McCullough, 2015). Bridge design became more standardized, following national trends, which sought to improve construction efficiency, cost, and maintenance. As a result, the adaptation of steel truss bridges became widespread for larger spans, forever changing the Vermont landscape. Small span bridges were beginning to be replaced with inexpensive concrete slabs on steel beams, with plans available in 2ft increments to expedite the process.

## **7.2 Analysis**

After intensive review of the available damage records and examination of post-storm inspection photos, 26 out of the total 164 historic bridges were determined to be damaged. Bridges are categorized for damage as scour, channel flanking, superstructure, and debris, as well as for the magnitude of damage as slight, moderate, extensive, and complete. Slight damage includes channel erosion not affecting the bridge foundation, superstructure and guardrail damage, and debris accumulation without scour present. Moderate damage includes scour affecting the foundation but not to a critical state, bank and approach erosion, superstructure damage but not to a critical state, and heavy channel aggradation. Extensive damage includes critical scour, with some settlement to a single foundation, but not collapse, full flanking of both approaches, and damage to the

superstructure making it structurally unsafe. Complete damage includes cases where the bridge was washed away, collapsed or has significant foundation damage requiring replacement. Examples of damage to historic bridges can be seen in Figure 7.2.

Often times, there are multiple damage types occurring at the same bridge. Streams throughout Vermont were filled with lots of debris as a result of the widespread flooding. In the events multiple damage types were prevalent, the bridge was categorized as the greatest damage type. Often times, scour would be the most damaging, followed by flanking, superstructure, and debris. As a result, very few bridges were categorized as debris damage, even though most bridges were affected by some amount of debris accumulation. The collective list of the damaged bridges, bridge type, damage level, damage type, and cost of repair can be seen in Table 7.1. Figure 7.3 shows the distribution of bridge type by material, including the count and percentages, for all historic bridges, as well as those damaged. There is an increase number of damaged covered bridges, when compared to the distribution of the total population.

Parameters from the bridge inspection database were tested for discrimination between damaged ( $n = 26$ ) and non-damaged historic bridges. Of the variables tested, only Waterway Adequacy Rating and Channel Rating were significantly different, showing that lower ratings for those two parameters related to damage. Figure 7.4 shows the distribution of the parameters tested across the entire historic bridge population. Year built shows a spike after 1920, and corresponds to the bridges built following the 1927 flood, which destroyed hundreds of bridges. Aside from the group of low rating, the average and medians are high ratings for each parameter.





**(a) Example of slight debris damage – before and after, Montgomery C2001 B5**



**(b) Example of moderate flanking damage – before and after, Warren FAS188 B6**



**(c) Example of extensive scour damage – before and after, Woodstock C2002 B45**

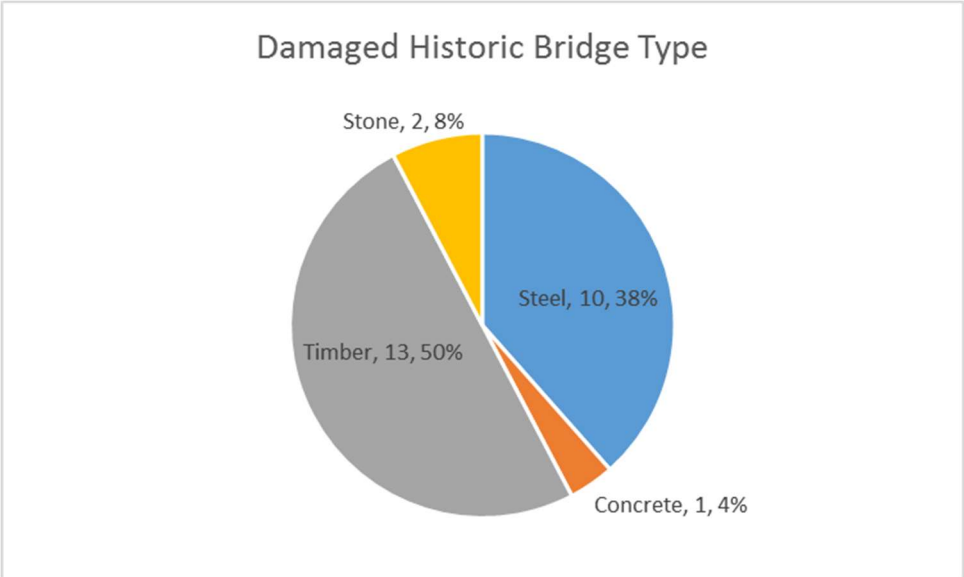
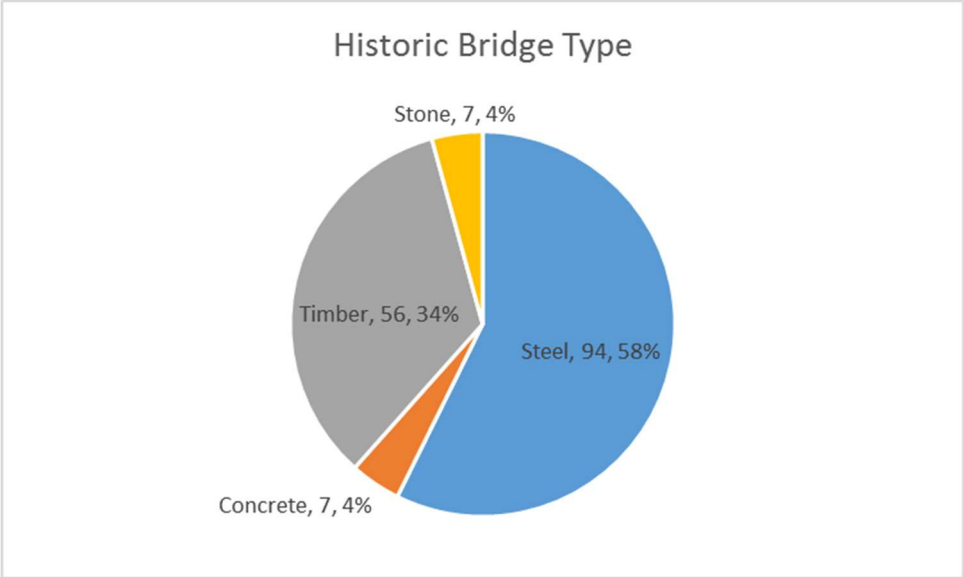


**(d) Example of complete damage – before and after, Moretown C3024 B41**

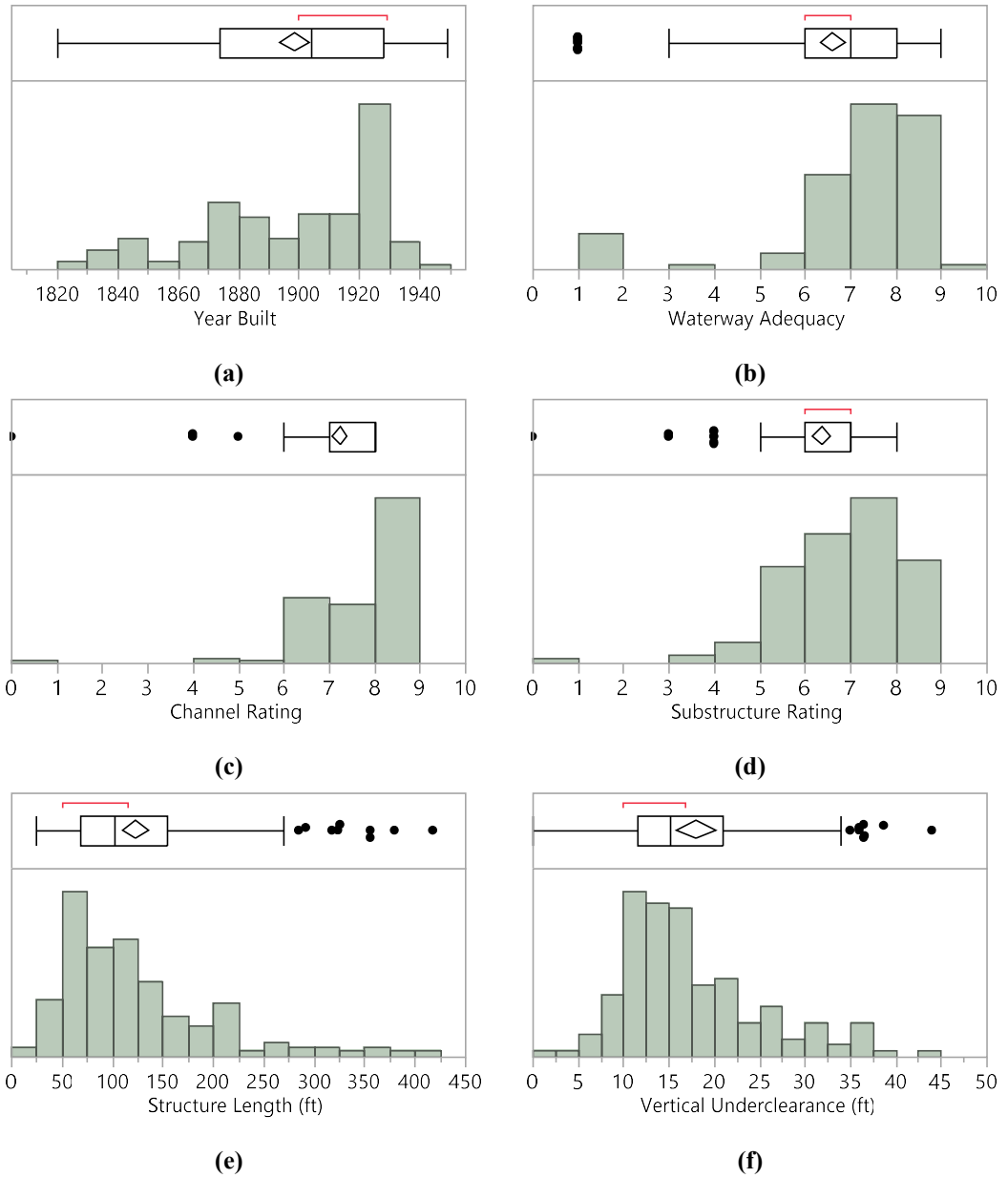
**Figure 7.2. Damage to Vermont's historic bridges**



Table 7.1. Damaged Historic Bridges						
Town	Bridge	Bridge Type	Damage Level	Damage Type	Initial Est. Cost	Revised Cost
Woodstock	Lincoln Covered	Pratt Truss	Extensive	Scour	34,872	34,872
Woodstock	Woodstock Warren Truss	Steel Truss	Slight	Superstructure	853,606	
Woodstock	Taftsville Covered	King Post	Complete	Scour	835,359	2,500,000
W. Windsor	Mill Brook Covered	Timber Arch	Complete	Scour	291,716	229,166
Warren	Warren Covered	Queen Post	Moderate	Flanking		
Waitsfield	Great Eddy Covered	Burr Truss	Moderate	Superstructure	13,085	38,423
Thetford	Union Village Covered	Multi Kingpost	Slight	Superstructure		14,000
Sunderland	Chiselville	Town Lattice	Moderate	Scour		
Shrewsbury	Brown Covered	Town Lattice	Moderate	Flanking	95,919	
Royalton	Bridge Street	Steel Thru Truss	Extensive	Flanking		87,649
Rockingham	Lower Bartonville Rd	Town Lattice	Complete	Scour	1,076,427	2,688,526
Rockingham	Worrall Covered	Town Lattice	Moderate	Flanking		18,000
Poulnsey	South Street	Steel Thru Truss	Moderate	Scour		
Northfield	Covered Bridge 3	Queen Post	Slight	Scour	18,155	
Moretown	Bridge Road	Steel Pony Truss	Complete	Scour	1,045,200	1,188,697
Montgomery	Fuller Covered	Town Lattice	Slight	Debris	8,700	
Ludlow	Black River	Steel Pony Truss	Slight	Superstructure	9,781	
Guilford	Green River Covered	Town Lattice	Moderate	Scour	37,337	
Grafton	Kidder Hill Covered	King Post	Slight	Superstructure	3,062	
Brattleboro	Whetstone Brook	Stone Arch	Complete	Scour	320,008	
Brandon	Neshobe River	Two Span Stone	Moderate	Scour		
Bethel	Gilead Brook	Steel Deck Truss	Moderate	Scour		
Bethel	River Street	Steel Thru Truss	Extensive	Scour		
Bethel	Peavine Truss	Steel Thru Truss	Slight	Superstructure	29,320	923,000
Barre	South Main Street	Two Span Stone	Slight	Scour		
Arlington	Arlington Green Covered	Town Lattice	Moderate	Superstructure	58,969	



**Figure 7.3. Historic bridge type, between population and damaged group**



**Figure 7.4. Distributions of historic bridge features**

### 7.3 Conclusions

Historic bridges throughout Vermont are culturally important, and are in need of remediation to ensure their continued survival. Major storm events like the flood of 1927 and Tropical Storm Irene in 2011 have major impacts on the historic covered and truss

bridges in Vermont. Repairs and remediation on historic structures is constrained by the types of replacements and designs to ensure the historical significance is preserved, and is often more expensive as a result.

Of Vermont's 164 historic bridges, 26 were damaged in Tropical Storm Irene. The majority of damage was either scour or superstructure damage. Damage occurred more frequently to timber covered bridges, than the steel truss bridges, likely as a result of overtopping debris collisions. Costs range widely based on the level of damage experienced, with the highest reported cost of 2.68 million U.S. dollars for full replacement of the Lower Bartonville Rd Covered Bridge.

## **CHAPTER 8 CONCLUSIONS AND RECOMMENDATIONS**

Bridges are critical connections in our transportation system, and their vulnerability to bridge scour, and other hydraulic damage is difficult to predict making their design resilient a difficult task. The likelihood of bridge damage in the event of a flood event can be thought of as a weakness in the system. The streamflow intensity of the flood event occurs independently of the bridge, and acts as a stressor on the system. The intersection of the bridge infrastructure weaknesses and stream stressors is a complex interaction, resulting in varying levels of damage, and from the uniformed prospective look random. Hypotheses regarding damage seen at individual bridges can be made, but when resources are limited and recovery must start immediately following an event, the observations will not aid in treatment of the system as a whole. The modeling of a transportation system of scale requires a measurement of the hazard presented to its most vulnerable connections. Without some measure of risk, allocation of resources for prevention, rehabilitation, and emergency management is uncertain.

The research presented here used over 300 damaged Vermont bridges during the 2011 Tropical Storm Irene as the case study. Individual bridge, stream geomorphic and watershed variables tested show benefit in performing vulnerability screening for bridge damage. The dataset created increases the knowledge available on bridge scour, and allows for the identification of the underlying complex relationships between bridges, streams and the landscape.

### **8.1 Work Performed**

The following work was first accomplished in support of the analysis presented in this thesis:

- (1) A comprehensive dataset of bridge inspection and stream geomorphic assessments was created. The following disparate sources of available data were first assembled and georeferenced into GIS (Geographic Information Systems):
  - (i) All records of long structure bridges (greater than 6 m in span), and the preceding years (2010) inspection from the Vermont Agency of Transportation (VAOT) Bridge Inventory System (BIS);
  - (ii) Estimates of post-storm damage level, damage type, and repair costs obtained from documentation via the VAOT and the Vermont Department of Emergency Management (VDEM), and supplemented through our own examination of the available inspection photos for all bridges affected;
  - (iii) Tropical Storm Irene rainfall data collected for Vermont, neighboring states New York and New Hampshire, and the Province of Quebec; the rainfall and recurrence interval were spatially interpolated with ordinary kriging; and
  - (iv) The Vermont Agency of Natural Resources (VTANR) rapid geomorphic assessment (RGA) data consisting of a host of stream characteristics and measurements for reaches throughout the state.
- (2) The above database was further augmented with additional following variables that were computed as part of this work:
  - (v) A GIS script was developed to generate stream power measures statewide at each of the 15,123 stream reaches (as specified in the VTANR RGA data) and at each of the 2,249 hydraulic bridge locations in Vermont. The Stream Power, Specific Stream Power, and the event-based, Irene Specific Stream Power were computed at each of the locations.

- (vi) Additional GIS scripts were developed to compute watershed delineation, slope determination, watershed land use characterization, and hydrologic soil type characterization on 15,123 individual stream reaches and at each of the 2,249 hydraulic bridge locations in Vermont.
- (3) Characterization of the level and type of damage of over 300 bridges was performed independent of any knowledge of the repair costs. The damage type was classified into four categories: scour, channel flanking, superstructure, and debris. The damage state was classified into four categories as well: slight, moderate, extensive, and complete.
- (4) Initial statistical analysis included a Kruskal-Wallis one-way analysis of variance (ANOVA) using variables from the above-mentioned data items (i) through (iv) and comparison was made between the bridges that were damaged versus those that did not experience damage. Identified significant variables from the ANOVA were then tested for correlation to damage state with a multivariate logistic regression.
- (5) A more focused statistical analysis comparing bridges that were damaged versus those that did not experience damage was conducted using stream power metrics – stream power, specific stream power and Irene specific stream power.
- (6) To leverage the assembled database using data (i) through (vi), and capture the full scope of the assembled resources, feature selection on multiple variables was conducted using a newly developed Conjunctive Clause Evolutionary Algorithm (EA) by Hanley et al., (2017, in review).
- (7) The data on Vermont’s historic bridges damaged in the storm were extracted from the above database and analyzed to examine the damage type and extent and cost of repair of these bridges.

## 8.2 Overall Conclusions

The following conclusions are drawn from our analyses:

- Of the 313 damaged bridges, 55% were steel beam, 34% were concrete slab or beam, and the remaining 11% were historical steel or wood truss superstructures. Single span bridges made up the vast majority, 82%, of bridges damaged, with 12% double span, and the few remaining including 3 and 4 span structures.
- About 55.6% of the damaged bridges had scour damage, 29.7% had channel flanking, 8.3% had debris damage, and the remaining 6.3% had superstructure damage. Scour damage resulted in the highest estimated cost to repair, followed by channel flanking, and then superstructure damage.
- Damage due to flanking had an estimated average repair cost of \$70,000 per bridge, and that the average cost of flanking-induced repair was \$55 per square meter of deck area. In comparison, scour damage was estimated to cost \$290,000 on average to repair per bridge with an average repair cost of \$401 per square meter of deck area. The estimated cost of repair for superstructure damage was about \$24 per square meter of deck area.
- Of the damaged bridges, 30% were categorized as having slight damage, 39% as moderate damage, 14.5% as extensive damage, and 16.5% as complete damage. Damage level correlated well with the estimated cost of repair and the cost of repair per deck area.
- The bridge rating assessment characteristics were all strongly correlated to damage. Channel rating and waterway adequacy rating had strong discriminating power between bridge damage levels.



- The analysis indicated that stream geomorphic data have the potential in supplementing and enhancing the bridge rating systems, and may aid in identifying hydraulic vulnerability. Ratios such as entrenchment, incision, width to depth and straightening showed significance at the watershed scale, and indicated that relative measures of a stream's geomorphic condition (disequilibrium) are more important than specific measurements.
- Specific Stream Power, and the event-based, Irene Specific Stream Power were both statistically significant at discriminating between damaged and non-damaged bridges, as well as between bridge damage levels. The resulting spatial probability maps allowed for visual display of vulnerable reaches, for which bridge placement would be at increased hazard.
- With 330 possible variables in the assembled database, ranging in data type (i.e., nominal, ordinal and continuous) and with varying degrees of independence, and lack thereof, variable selection using traditional methodologies is not feasible. For example, a four-effect model, using nominal logistic regression, would result in  $5 \times 10^8$  possible feature combinations. To avoid the computational challenges often associated with these large data sets, input data variables are often eliminated using expert judgment (i.e., domain experts pre-process the data and include only those variables deemed important). However, this greatly limits the power of large, comprehensive datasets. The Conjunctive Clause Evolution Algorithm employed in this work was found to be capable of producing bridge damage predictions through multivariate feature selection. The EA was able to test the vast number of possible combinations, something that is infeasible with logistic regression, and outperformed the artificially

seeded traditional logistic regression (when fed the same information identified through EA analysis).

- The EA algorithm created a prediction set that included a significant number of true positive solutions, using the relatively small set of variables including: rainfall, Irene Stream Power, Waterway Adequacy Rating, Channel Rating, elevation, percentage hydrologic soil type, open water land cover, and confinement ratio. The features combinations found by the EA were capable of correctly predicting 70% of damaged bridges, with an odds ratio indicating that damage is 11 times more likely to occur in the predicted set than the remaining bridges.
- The resulting damage prediction can be represented graphically to allow for observations of spatial patterns. Analysis can be done on varying scales, to determine local variations from the statewide results, and to provide a focused prediction that would be more applicable to stakeholders.
- Historic bridges are at risk of damage from extreme flood events, and particularly susceptible to overtopping flow with debris impact. Timber covered bridges were affected the most by the flooding, and are in need of remediation to remain an enduring cultural resource.

### **8.3 Intellectual Merit/Contributions of the Research**

This research made the following contributions to the state-of-the-art:

- The collection and georeferencing of hundreds of damaged and non-damaged hydraulic bridges during a single extreme hurricane-related storm event, in combination with their inspection records, associated stream geomorphic assessments,

stream power, watershed delineations, land use and hydrologic soil group characteristics, and damage evaluation create a unique and significantly useful data set. To the best of our knowledge, such a database is not available in the literature. This data set is made available in a spreadsheet format and can be downloaded from: <http://go.uvm.edu/vtbridges-irene-data>.

- To the best of our knowledge, this is the first study that links hydrologic stream networks with performance of bridges. As geomorphic data become more widely available, the framework presented here could be applied elsewhere.
- This is the first investigation comparing site-specific stream power to observed bridge damage at a network level and represents a fundamental breakthrough in the evaluation of flood-related bridge damage.
- The analysis identified individual features of the bridge and stream that correlate with underlying damage vulnerability, through comparisons at the stream reach and watershed scales, and outlines a framework to leverage these features to aid in the prediction of bridge vulnerability. Empirical fragility curves were created to depict the exceedance probability for a given damage level against the channel and waterway adequacy ratings, creating insights that can aid in evaluating bridges' vulnerability to extreme events.
- The Evolutionary Algorithm of Hanley et al. (2017, in review) was shown as an effective big data analysis tool for feature selection. The EA is capable of testing a vast number of possible combinations, something that is infeasible with logistic regression, and outperforms the artificially seeded traditional logistic regression (when fed the same information). Logistic regression is overly conservative, failing to

classify affirmative results, and requires independence between samples, which is uncontrollable given the spatial correlations between bridges.

#### **8.4 Broader Impacts of the Research**

The research used Vermont bridges damaged in the Tropical Storm Irene as the case study. Yet, the approaches presented here could be implemented in other geographic regions. The method of estimating SSP and ISSP, and the calculation and expression of bridge hazard through fragility curves and probability maps could be useful in creating a screening tool for damage prediction. The methodology, and automated scripts used allow for rapid implementation in future applications, thus not limiting this work to Vermont.

The Tropical Storm Irene database used here for the 313 damaged bridges experienced rainfall recurrence intervals ranging between 10 and 500 years, indicating that this methodology could be evaluated for a wide range of design flows for any watershed beyond the borders of Vermont.

Further application of event-based SSP (specific stream power) probability maps could be generated using rainfall ARI (average recurrence interval) in future climate simulations to produce the probability of bridge damage for a hypothetical climate scenario.

The knowledge gathered as a result of this study has applications beyond Vermont. Many of the variables newly added to the analysis can be created or monitored using commonly available data. The methodology, for creating watershed assessment parameters, as well as the using the available EA for feature selection can be applied to any bridge dataset and may add value in assessments beyond the study of bridge damage. Bridge inspection records are commonly used in other states, and can be supplemented

with additional information following the methodology used here. The EA opens up the opportunity to perform feature selection on large datasets, allowing for sets of multivariate features to be identified that are significantly correlated with levels of bridge damage while circumventing the computational challenges associated using traditional statistical analysis.

## **8.5 Recommendations for Future Work**

The resulting damage prediction based on Evolutionary Algorithm included in this thesis can be represented graphically to allow for observations of spatial patterns. Analysis can be done on varying scales, to determine local variations from the statewide results, and to provide a focused prediction that would be more applicable to stakeholders. A future study could apply the methodology presented on a smaller scale to determine if a localized approach would provide new information on the determination of bridge vulnerability. A tighter focus may remove features that correlate with geographic differences, and present features previously excluded.

Many of the parameters created through the watershed analysis were found to be useful in the bridge damage prediction. The documentation of the watershed delineation for each stream reach in Vermont is a useful resource for future work, and provides a useful tool in evaluating watershed properties upstream of study areas.

Stream geomorphic assessment variables, particularly the ratios relating to the confinement, entrenchment and incision are valuable metrics for stream stability, and thus potentially critical to preventing bridge scour. A modified version of the geomorphic assessment could be designed to gather these measurements for bridge projects, including

the upstream, bridge section, and downstream reach. A reasonable solution could be to conduct these as part of an updated bridge inspection.

Watershed stream power, as well as specific stream power, are shown to be useful in bridge damage prediction. A review of both stream power metrics could be included in future bridge design, as well as when assessing existing bridges. By representing the hazard in relation to the stream network, it allows for a statewide prediction of damage that can be useful for a number of planning purposes beyond bridges.

Historic bridges are in need of remediation to survive future flooding events. Because their superstructures are susceptible to damage from overtopping flows, they can be upgraded for improved hydraulic conveyance. When available they could be raised to provide additional freeboard. In instances where they cannot be risen, approach spans or relief culverts may be considered, to remove some floodplain impediments, and improve floodplain conveyance.

## CHAPTER 9 COMPREHENSIVE BIBLIOGRAPHY

- Anderson, I., Rizzo, D. M., Huston, D. R., and Dewoolkar, M. M. (2017a). "Analysis of bridge and stream conditions of over 300 Vermont bridges damaged in Tropical Storm Irene" *Structure and Infrastructure Engineering*, <http://dx.doi.org/10.1080/15732479.2017.1285329>.
- Anderson, I., Rizzo, D. M., Huston, D. R., and Dewoolkar, M. M. (2017b). "Stream Power Application for Bridge-Damage Probability Mapping Based on Empirical Evidence from Tropical Storm Irene." *Journal of Bridge Engineering*, [http://dx.doi.org/10.1061/\(ASCE\)BE.1943-5592.0001022](http://dx.doi.org/10.1061/(ASCE)BE.1943-5592.0001022).
- Anderson, R. S. (1994). "Evolution of the Santa Cruz Mountains, California, through tectonic growth and geomorphic decay". *Journal of Geophysical Research: Solid Earth*, 99(B10), 20161-20179.
- Arneson, L. A., Zevenbergen, L. W., Lagasse, P. F., and Clopper, P. E. (2012). "Evaluating scour at bridges." (No. FHWA-HIF-12-003).
- Bagnold, R. A. (1966). "An approach to the sediment transport problem from general physics." *U.S. Geol. Surv. Prof. Paper*, 422, 37.
- Barker, D. M., Lawler, D. M., Knight, D. W., Morris, D. G., Davies, H. N., and Stewart, E. J. (2009). "Longitudinal distributions of river flood power: the combined automated flood, elevation and stream power (CAFES) methodology." *Earth Surface Processes and Landforms*, 34(2), 280-290.
- Besaw, L. E., Rizzo, D. M., Kline, M., Underwood, K. L., Doris, J. J., Morrissey, L. A., and Pelletier, K. (2009). "Stream classification using hierarchical artificial neural networks: A fluvial hazard management tool." *J. of Hydrology*, 373(1), 34-43.
- Betts, A. K. (2011). "Climate change in Vermont." *Vermont Agency of Natural Resources* <http://www.anr.state.vt.us/anr/climatechange/Pubs/VTCCAdaptClimateChangeVTBetts.pdf> Accessed on July, 25, 2014.
- Biron, P. M., Chone, G., Buffin-Belanger, T., Demers, S., and Olsen, T. (2013). "Improvement of streams hydro-geomorphological assessment using LiDAR DEMs." *Earth Surf. Processes Landforms*, 38(15), 1808–1821.
- Briaud, L., Ting, K., Chen, C., Gudavalli, R., Perugu, S., Wei, G. (1999). "SRICOS: prediction of scour rate in cohesive soils at bridge piers," *J. Geotech. Geoenviron. Eng.*, 125(4), 237246.
- Brooks, G. R., and Lawrence, D. E. (1999). "The drainage of the Lake Ha! Ha! reservoir and downstream geomorphic impacts along Ha! Ha! River, Saguenay area, Quebec, Canada." *Geomorphology*, 28(1), 141-167.

- Buraas, E. M., Renshaw, C. E., Magilligan, F. J., and Dade, W. B. (2014). "Impact of reach geometry on stream channel sensitivity to extreme floods." *Earth Surface Processes and Landforms*, 39(13), 1778-1789.
- Chang, F. and Davis, S. (1999). "Maryland SHA procedure for estimating scour at bridge abutments, Part II - Clear Water Scour." ASCE Compendium, Stream Stability and Scour at Highway Bridges, Richardson and Lagasse (eds.), Reston, VA., 1999, pp. 412-416
- Chang, F., and Davis, S. (1998). "Maryland SHA Procedure for Estimating Scour at Bridge Abutments Part 2-Clear Water Scour. In Stream Stability and Scour at Highway Bridges: Compendium of Stream Stability and Scour Papers Presented at Conferences Sponsored by the Water Resources Engineering (Hydraulics) Division of the American Society of Civil Engineers" (pp. 398-398). ASCE.
- Conwill, J. D. (2004). *Vermont Covered Bridges*. Arcadia Publishing.
- Cook, W., Barr, P. J., and Halling, M. W. (2013). "Bridge failure rate." *Journal of Performance of Constructed Facilities*, 29(3), 04014080.
- Costa J. E., O'Connor J. E. (1995). "Geomorphically effective floods." *Natural and Anthropogenic Influences in Fluvial Geomorphology, Geophysical Monograph* 89: 45-56. DOI: 10.1029/GM089p0045
- Daly, C., Doggett, M., Gibson, W., and Smith, J. (2012). PRISM Climate Group Oregon State University.
- Douglass, S. L., Hughes, S., Rogers, S., and Chen, Q. (2004). "The impact of Hurricane Ivan on the coastal roads of Florida and Alabama: a preliminary report." Rep. to Coastal Transportation Engineering Research and Education Center, Univ. of South Alabama, Mobile, Ala.
- ESRI (2011). "ArcGIS Desktop: Release 10." Redlands, CA: Environmental Systems Research Institute.
- Ettema, R., Melville, B. W., and Constantinescu, G. (2011). "Evaluation of bridge scour research: Pier scour processes and predictions." Washington, DC: Transportation Research Board of the National Academies.
- Ettema, R., Nakato, T., and Muste, M. (2010). "Estimation of Scour Depth at Bridge Abutments," NCHRP Project 24-20, Draft Final Report, Transportation Research Board, National Academy of Science, Washington, D.C. (Ettema, R., T. Nakato, and M. Muste).
- FHWA (1973). "A Statistical Summary of the Cause and Cost of Bridge Failures," Federal Highway Administration, U.S. Department of Transportation, Washington, D.C. (Chang, F.F.M.).



- FHWA (2015). "Recording and coding guide for the structure inventory and appraisal of the nation's bridges." Federal Highway Administration Report No. FHWA-PD-96-01, U.S. Department of Transportation, Washington, D.C.
- FHWA (1999). "Predicting Scour in Weak Rock of the Oregon Coast Range," Report No. FHWA-OR-RD-00-04, Washington, D.C., October (Dickenson, S.E. and M.W. Baillie).
- FHWA (1978). "Countermeasures for hydraulic problems at bridges." Vol. 1 and 2, FHWA/RD-78-162 and 163. Washington, DC: Federal Highway Administration, US Department of Transportation. (Brice, J.C. and J.C. Blodgett).
- FHWA (1995). "Recording and coding guide for the structure inventory and appraisal of the nation's bridges." FHWA-PD-96-001, U.S. Dept. of Transportation, Washington, D.C.
- Finlayson, D. P., and Montgomery, D. R. (2003). "Modeling large-scale fluvial erosion in geographic information systems." *Geomorphology*, 53(1), 147-164.
- Fonstad MA. (2003). "Spatial variation in the power of mountain streams in the Sangre de Cristo Mountains, New Mexico." *Geomorphology* 55: 75–96.
- Froehlich, D.C. (1989). "Abutment Scour Prediction," Presentation, Transportation Research Board, Washington, D.C. (Froehlich, D.C.).
- Frumhoff, P. C., McCarthy, J. J., Melillo, J. M., Moser, S. C., and Wuebbles, D. J. (2007). "Confronting climate change in the US Northeast. A report of the northeast climate impacts assessment." Union of Concerned Scientists, Cambridge, Massachusetts.
- Gartner, J. D., Dade, W. B., Renshaw, C. E., Magilligan, F. J., and Buraas, E. M. (2015). "Gradients in stream power influence lateral and downstream sediment flux in floods." *Geology*, 43(11), 983-986.
- Gee, K.W. (2008). "Action: Technical Guidance for Bridges over Waterways with Unknown Foundations." Federal Highway Administration, Washington, D.C., <http://www.fhwa.dot.gov/engineering/hydraulics/policymemo/20080109.cfm>. Accessed June 2014
- Hanley, J. P., Rizzo D. M., Buzas J. S., and Eppstein M. J. (2017). "A Tandem Evolutionary Algorithm for Identifying Optimal Association Rules from Complex Data." *Evolutionary Computation*, under review.
- Homer, C.G., Dewitz, J.A., Yang, L., Jin, S., Danielson, P., Xian, G., Coulston, J., Herold, N.D., Wickham, J.D., and Megown, K. (2015). "Completion of the 2011 National Land Cover Database for the conterminous United States-Representing a

decade of land cover change information.” *Photogrammetric Engineering and Remote Sensing*, v. 81, no. 5, p. 345-354

- Hornby, G.S., Lohn, J.D., Linden, D.S. (2011). “Computer-automated evolution of an x-band antenna for Nasa’s space technology 5 mission.” *Evolut Comput* 19(1):1–23.
- Horton, R., Yohe, G., Easterling, W., Kates, R., Ruth, M., Sussman, E., Whelchel, A., Wolfe, D., and Lipschultz, F. (2014). “Ch. 16: Northeast, climate change impacts in the United States.” *The Third National Climate Assessment*, edited by J. M. Melillo, T. C. Richmond, and G. W. Yohe, pp. 371–395, U.S. Global Change Research Program, Washington, D. C., doi:10.7930/J0SF2T3P.
- Jain, V., Preston, N., Fryirs, K., and Brierley, G. (2006). “Comparative assessment of three approaches for deriving stream power plots along long profiles in the upper Hunter River catchment, New South Wales, Australia.” *Geomorphology*, 74(1), 297-317.
- Jaquith, S., and Kline, M., (2001). “Vermont regional hydraulic geometry Curves.” River Management Program of the Vermont Department of Environmental Conservation, Waterbury, Vermont.
- Kattell, J., and Eriksson, M. (1998). “Bridge scour evaluation: Screening, analysis, and countermeasures” (No. 9877 1207–SDTDC). San Dimas, CA: USDA Forest Service.
- Kendall, M. G. (1952). “The Advanced Theory of Statistics”. 5th ed. Vol. 1. New York, New York: Hafner Publishing Company.
- Kiah, R.G., Jarvis, J.D., Hegemann, R.F., Hilgendorf, G.S., and Ward, S.L. (2013). “Hydrologic conditions in New Hampshire and Vermont, water year 2011.” U.S. Geological Survey Open- File Report, 2013–1135, 36 p., <<http://pubs.usgs.gov/of/2013/1135>> (Accessed June 2014)
- Kim, Y. J., Marshall, W., and Pal, I. (2014). “Assessment of infrastructure devastated by extreme floods: a case study from Colorado.” USA. In *Proceedings of the ICE-Civil Engineering* (Vol. 167, No. 4, pp. 186-191). Thomas Telford.
- Kline M., Alexander C., and Pytlik S. (2007). “Vermont stream geomorphic assessment protocol handbooks.” Resources VAoN (ed). Waterbury, Vermont.
- Kline, M., and Cahoon, B. (2010). “Protecting River Corridors in Vermont.” *Journal of the American Water Resources Association*, 46(2), 227-236.
- Knighton, A.D. (1999). “Downstream variation in stream power.” *Geomorphology* 29, 293 – 306.

- Kruskal, W. H., and Wallis, W. A. (1952). "Use of ranks in one-criterion variance analysis." *Journal of the American Statistical Association*, 47(260), 583-621
- Laursen, E.M. (1960). "Scour at Bridge Crossings." *Journal Hydraulic Division*, American Society of Civil Engineers, Vol. 86, No. HY 2. 11.4
- Laursen, E.M. (1963). "An Analysis of Relief Bridge Scour." *Journal Hydraulic Division*, American Society of Civil Engineers, Vol. 89, No. HY3.
- Laursen, E.M. (1980). "Predicting Scour at Bridge Piers and Abutments." General Report No. 3, Arizona Department of Transportation, Phoenix, AZ.
- Lebbe, M. F. K., Lokuge, W., Setunge, S., and Zhang, K. (2014). "Failure mechanisms of bridge infrastructure in an extreme flood event." Proc., 1st Int. Conf. on Infrastructure Failures and Consequences (ICIFC2014), RMIT, Melbourne, Australia.
- Lecce, S.A., (1997). "Nonlinear downstream changes in stream power on Wisconsin's Blue River." *Annals of the Association of American Geographers* 78 (3), 471 – 486.
- Liu, H. K., Chang, F. M., and Skinner, M. M. (1961). "Effect of bridge construction on scour and backwater." CER 60 HKL 22, Colorado State Univ., Civil Engrg. Section, Ft. Collins, Colo.
- Magilligan, F.J. (1992). "Thresholds and the spatial variability of flood power during extreme floods." *Geomorphology* 5, 373 – 390.
- McCullough, R. (2005). *Crossings: A History of Vermont Bridges*. Vermont Historical Society in partnership with the Vermont Agency of Transportation.
- Melillo, J. M., Richmond, T.C., and Yohe, G. W. (Eds.) (2014), "Climate Change Impacts in the United States: The Third National Climate Assessment". U.S. Global Change Research Program, 841 pp. Doi: 10.7930/J0Z31WJ2.
- Melville, B. W., and Coleman, S. E. (1973). "Bridge Scour." *Water Resources Publications*, LLC.
- Melville, B.W. (1992). "Local Scour at Bridge Abutments." *Journal of Hydraulic Engineering*, American Society of Civil Engineers, Hydraulic Division, Vol. 118, No. 4.
- Miller, A. J. (1990). "Flood hydrology and geomorphic effectiveness in the central Appalachians." *Earth Surface Processes and Landforms*, 15(2), 119-134.

- MSHA (2010). "Manual for Hydrologic and Hydraulic Design." Maryland State Highway Administration, Baltimore, MD Report available at [www.gishydro.umd.edu](http://www.gishydro.umd.edu).
- Mueller, D.S., and Wagner C.R. (2005). "Field Observations and Evaluations of Streambed Scour at Bridges." Report FHWA-RD-03-052, Federal Highway Administration.
- National Weather Service (2011). "Preliminary Hurricane/Tropical Storm Irene weather summary for the North Country." National Weather Service Forecast Office, Burlington VT, <<http://www.erh.noaa.gov/btv/events/Irene2011/>> (Accessed July 2014).
- Okada, S., Mitamura, H., Ishikawa, H., and Hokkaido, S. R. (2006). "The collapse mechanism and the temporary restoration of Omori Bridge damaged by the storm surge of Typhoon No. 18 in 2004." *Technical Memorandum of Public Works Research Institute*, 40(9), 185-192.
- Okeil, A. M., and Cai, C. S. (2008). "Survey of Short-and Medium-Span Bridge Damage Induced by Hurricane Katrina." *Journal of Bridge Engineering*, 13(4), 377-387.
- Olson S (2014). "Estimation of flood discharges at selected annual exceedance probabilities for unregulated, rural streams in Vermont, with a section on Vermont regional skew regression, by Veilleux, a.g. Scientific Investigations Report 5078." US Geologic Survey.
- Olson S (2002). "Flow-frequency characteristics of Vermont streams." *Water- Resources investigations report 02-4238*, USGS.
- Padgett, J. E., Spiller, A., and Arnold, C. (2012). "Statistical analysis of coastal bridge vulnerability based on empirical evidence from Hurricane Katrina." *Structure and infrastructure engineering*, 8(6), 595-605.
- Padgett, J., DesRoches, R., Nielson, B., Yashinsky, M., Kwon, O. S., Burdette, N., and Tavera, E. (2008). "Bridge damage and repair costs from Hurricane Katrina." *Journal of Bridge Engineering*, 13(1), 6-14.
- Reinfelds, I., Cohen, T., Batten, P., and Brierley, G. (2004). "Assessment of downstream trends in channel gradient, total and specific stream power: A GIS approach." *Geomorphology*, 60(3-4), 403-416.
- Richardson, E. V., and Davis, S. R. (2001). "Evaluating scour at bridges." Hydraulic Engineering Circular No. 18 (HEC-18), Rep. No. FHWA NHI 01-001, Federal Highway Administration, Washington, D.C.

- Rosenbloom, N. A., and Anderson, R. S. (1994). "Hillslope and channel evolution in a marine terraced landscape, Santa Cruz, California." *Journal of Geophysical Research: Solid Earth*, 99(B7), 14013-14029.
- Scawthorn, C., Flores, P., Blais, N., Seligson, H., Tate, E., Chang, S., Mifflin, E., Thomas, W., Murphy, J., Jones, C., and Lawrence, M. (2006). "HAZUS-MH Flood Loss Estimation Methodology. II. Damage and Loss Assessment." *Nat. Hazards Rev.*, 10.1061/(ASCE)1527-6988(2006)7:2(72), 72-81.
- Schultz, M. T., Gouldby, B. P., Simm, J. D., and Wibowo, J. L. (2010). "Beyond the factor of safety: Developing fragility curves to characterize system reliability." *Geotechnical and Structures Laboratory, Engineer Research and Development Center, Vicksburg, MS.*
- Seidl, M. A., and Dietrich, W. E. (1992). "The Problem of Channel Erosion into Bedrock." *CATENA SUPPLEMENT*, 23, 101-124.
- Sheppard, D. M., Demir, H., and Melville, B. W. (2011). "Scour at wide piers and long skewed piers (Vol. 682)." *Transportation Research Board.*
- Siegel, S. (1956). "Nonparametric statistics for the behavioral sciences." *International Student Edition-McGraw-Hill Series in Psychology*, Tokyo: McGraw-Hill Kogakusha.
- Somerville, D.E. and B.A. Pruitt. (2004). "Physical Stream Assessment: A Review of Selected Protocols for Use in the Clean Water Act Section 404 Program." Prepared for the U.S. Environmental Protection Agency, Office of Wetlands, Oceans, and Watersheds, Wetlands Division (Order No. 3W-0503- NATX). Washington, D.C. 213 pp. Document No. EPA 843-S-12-002.
- Springston, G. E., Underwood, K.L., Robinson, K., and Swanberg, N. (2012). "Tropical Storm Irene and the White River Watershed of Vermont: flood magnitude and geomorphic impacts in guidebook to field trips in western New Hampshire and adjacent Vermont and Massachusetts." 104th meeting of the New England Intercollegiate Geological Conference edited by P. Thompson and T. Thompson, University of New Hampshire and T. Allen, Keene State College (330 pages).
- Stager, C., and Thill, M. K. (2010). "Climate change in the Champlain Basin: What natural resource managers can expect and do." *Nature Conservancy, Adirondack Chapter.*
- State of Vermont (2012). "State of Vermont Tropical Storm Irene after action report/improvement plan final draft." p. 242  
<[https://gmunitedway.files.wordpress.com/2012/04/ts-irene-aar-ip-2012\\_0409\\_final.pdf](https://gmunitedway.files.wordpress.com/2012/04/ts-irene-aar-ip-2012_0409_final.pdf)> (Accessed July 14, 2015)

- Straub, L. G. (1934). "Effect of channel-contraction works upon regimen of movable bed-streams." *Eos, Transactions American Geophysical Union*, 15(2), 454-463.
- Sturm, T. W. (2006). "Scour around bankline and setback abutments in compound channels." *Journal of Hydraulic Engineering*, 132(1), 21-32.
- Thomas, P., Jones, T., Azizi, S.C., (2013). "Jousting with bridges." FEMA's Historic Preservation Section, Joint Field Office, Essex Junction, VT.
- U. S. Geological Survey (2011). "High flows in New Hampshire and Vermont from Tropical Storm Irene estimated." U.S. Geological Survey, <[http://nh.water.usgs.gov/WhatsNew/Irene\\_aug2011.htm](http://nh.water.usgs.gov/WhatsNew/Irene_aug2011.htm)> (Accessed July 15, 2014)
- U.S. Geological Survey and U.S. Department of Agriculture, Natural Resources Conservation Service, (2013). "Federal Standards and Procedures for the National Watershed Boundary Dataset (WBD)" *Techniques and Methods 11-A3*, p. 63, <<http://pubs.usgs.gov/tm/11/a3/>> (Accessed January 13, 2016).
- U.S. Geological Survey, (2013). "National hydrography dataset, high resolution: U.S. Geological Survey, The National Map, National Hydrography Dataset," available at <http://nhd.usgs.gov/> (accessed October 18, 2013).
- U.S. Soil Conservation Service., (2009). "National engineering handbook." Hydrology, section 7. U.S. Department of Agriculture, Washington, DC (2009)
- VCGI (2006). "Vermont Hydrologically Corrected Digital Elevation Model (VTHYDRODEM)." Vermont Center for Geographic Information, Burlington, VT.  
<[http://www.vcgi.org/dataware/search\\_tools/moreinfo.cfm?catalog\\_id=1andlayer\\_id=28andlayer\\_name=ElevationDEM\\_VTHYDRODEM](http://www.vcgi.org/dataware/search_tools/moreinfo.cfm?catalog_id=1andlayer_id=28andlayer_name=ElevationDEM_VTHYDRODEM)> (Accessed June 2014)
- Vermont Agency of Transportation (2014). "Engineering Image Archives." Vermont Agency of Transportation, <<http://vtransmap01.aot.state.vt.us/rp/dpr/Diphotowebstore//dpr.asp>> (Accessed June 2014).
- Vermont State Highway Board, (1937). Ninth Biennial Report (1937-38), 28
- Vocal Ferencevic, M., and Ashmore, P. (2012). "Creating and evaluating digital elevation model-based stream-power map as a stream assessment tool." *River Research and Applications*, 28(9), 1394-1416.
- Wang, H., Hsieh, S.-C., Lin, C., and Wang C.-Y. (2014). "Forensic diagnosis on flood-induced bridge failure. I. Determination of the possible causes of failure," *Journal of Performance of Constructed Facilities*, 28(1), 76-84.

Wardhana, K., and Hadipriono, F. C. (2003). "Analysis of recent bridge failures in the United States," *Journal of Performance of Constructed Facilities*, 17(3), 144-150.